

**Human Steroid Sulfatase:  
Inhibitor Studies and Photoaffinity Labeling**

by

Chau-Minh Phan

A thesis

presented to the University of Waterloo

in fulfillment of the

thesis requirement for the degree of

Master of Science

in

Chemistry

Waterloo, Ontario, Canada, 2010

© Chau-Minh Phan 2010

## **Author's Declaration**

I hereby declare that I am the sole author of this thesis. This is a true copy of the thesis, including any required final revisions, as accepted by my examiners.

I understand that my thesis may be made electronically available to the public.

## Abstract

Steroid sulfatase (STS) is considered to be one of the key enzymes contributing to the development of breast cancer. It catalyzes the hydrolysis of inactive sulfated steroids such as estrone sulfate (ES) to inorganic sulfate active steroids such as estrone (E1), a precursor to estradiol (E2), a key stimulator for breast cancer development. Inhibitors of STS are currently being pursued in both academia and industry as potential drugs for treating breast cancer.

A series of 4-substituted estrone and estradiol derivatives were examined as inhibitors of STS. Inhibition of STS with 4-FE1, an irreversible inhibitor of STS previously studied in the Taylor group, can be enhanced by introducing a hydrophobic benzyl group at the 17-position of 4-FE1. As with 4-FE1, the inhibition was concentration and time-dependent. Only 14% of the activity could be recovered after extensive dialysis. Introducing substituents at the 2-position of 4-formyl estrogen derivatives resulted in loss of concentration and time-dependent inhibition and a considerable decrease in inhibitor affinity. Studies with estrogen derivatives substituted at the 4-position with groups other than a formyl revealed that a relatively good reversible inhibitor can be obtained simply by introducing an electron withdrawing group at this position. These types of inhibitors are non-competitive inhibitors suggesting an alternative steroid binding site.

A series of estrone derivatives were examined as photoaffinity labels of STS. 4-azidoestrone sulfate and 4-azidoestrone phosphate exhibited properties that are suitable for photoaffinity labeling studies with STS. These labels may be useful for ascertaining pathways of substrate entry into the STS active site. 16-diazoestrone phosphate was not a photoaffinity label of STS. 2- and 4-azido estrone and 16-diazoestrone all acted as photoaffinity labels of STS. These compounds may be useful for ascertaining pathways of product release from the STS active site.

## **Acknowledgements**

I am greatly indebted to my supervisor, Dr. Scott Taylor, whose encouragement, guidance and support from the initial to the final level enabled me to develop an understanding of the subject.

Lastly, I offer my regards and thanks to my committee members, Dr. Joseph Guillemette and Dr. Thorsten Dieckmann, and all of those who supported me in any respect during the completion of the project.

## Table of Contents

List of Tables	viii
List of Figures	ix
List of Schemes	xv
List of Abbreviations	xvi

### Chapter 1 – Steroid Sulfatase: Function, Structure, Inhibitors, and Substrate Inhibition

1.1	Introduction	
1.1.1	Estrogen Dependent Breast cancer	1
1.1.2	Estrogen Biosynthesis	2
1.1.3	Aromatase	2
1.1.4	17 $\beta$ -Hydroxysteroid Dehydrogenase	3
1.1.5	Estrone sulfotransferase	4
1.1.6	Steroid Sulfatase	4
1.2	Steroid Sulfatase	
1.2.1	STS Expression and Location	5
1.2.2	Crystal Structure of STS	6
1.2.3	Substrate Movement	7
1.2.4	Post-Translational Modification of Aryl Sulfatases	9
1.2.5	Proposed mechanism for Aryl Sulfatases	10
1.2.6	STS Specific for Sulfate-Esters	12
1.3	STS Inhibitors	
1.3.1	Reversible Inhibitors	13
1.3.2	Irreversible Inhibitors	16
1.4	Substrate Inhibition	
1.4.1	4-DFMES unique irreversible inhibitor	19
1.4.2	Substrate Inhibition	21
1.4.3	Evidence for Substrate Inhibition in STS	23
1.5	Research Objectives	23

### Chapter 2 – Purification and Assaying of Steroid Sulfatase

2.1	Introduction	24
2.2	Results and Discussion	
2.2.1	Placental Purification of STS	25
2.2.2	2-Nitroestrone sulfate as a potential chromogenic substrate for STS	27
2.3	Conclusions and Future Work	35
2.4	Experimental	

2.4.1	Materials	36
2.4.2	STS purification	36
2.4.3	STS activity in purification	38
2.4.4	Protein determination	38
2.4.5	Spectral data	38
2.4.6	HPLC studies	39

## Chapter 3 – 4-Substituted Estrogens as Reversible and Irreversible Inhibitors of STS

3.1	Introduction	40
3.2	Results and Discussion	
3.2.1	Inhibition of STS with 17- $\alpha$ -benzyl-4-formyl estradiol	41
3.2.2	Reversible Inhibition of STS with 4-substituted estrogen derivatives	46
3.3	Conclusions and Future Work	52
3.4	Experimental	
3.4.1	Materials	53
3.4.2	IC <sub>50</sub> determinations	53
3.4.3	K <sub>i</sub> determination	54
3.4.4	Determination of time and concentration dependent inhibition of STS with <b>3.4</b>	54
3.4.5	Time and concentration-dependent inhibition of STS in the presence of estrone phosphate (EP) (protection experiments)	55
3.4.6	Dialysis Experiment	55

## Chapter 4 – Photoaffinity Labeling to Reveal Mode of Substrate and Product Transport in STS

4.1	Introduction	
4.1.1	Photoaffinity labeling	56
4.1.2	Photaffinity Probes	57
4.2	Results and Discussion	
4.2.1	Studies with compounds 4.1 and 4.2	59
4.2.2	Studies with compounds 4.3-4.5	71
4.2.3	Deglycosylation of STS	84
4.3	Conclusions and Future Work	84
4.4	Experimental	
4.4.1	Materials	85
4.4.2	Effect of 350nm light on STS activity	85
4.4.3	Spectrophotometric studies with compounds <b>4.1-4.8</b>	86
4.4.4	Photoaffinity labeling procedure	86
4.4.5	HPLC Studies with <b>4.1</b> and <b>4.2</b>	87
4.4.6	IC <sub>50</sub> and K <sub>i</sub> determinations	88

4.4.7	Deglycosylation of STS	88
-------	------------------------	----

<b>REFERENCES</b>	89
-------------------	----

## **APPENDICES**

<b>Appendix A. IC<sub>50</sub> plots for compounds 3.3, 3.7-3.9, 3.11, 3.16-3.24, E1 and E2 and replots of the data in figures 3.10-3.12.</b>	96
---	----

<b>Appendix B. IC<sub>50</sub> plots for compounds 4.1-4.5, 4.8 and EP and replots of the data in figures 4.12, 4.13, 4.26, 4.27, 4.29</b>	106
--	-----

## List of Tables

### Chapter 1 – Steroid Sulfatase: Function, Structure, Inhibitors, and Substrate Inhibition

Table 1.1. Estrone-3-sulfate mimics as reversible inhibitors of STS .....14

Table 1.2. 17-substituted analogs as reversible inhibitors of STS .....14

### Chapter 2 – Purification and Assaying of Steroid Sulfatase

Table 2.1. Spectra of 2-NE1 at various pH. Concentrations of 2-NE1 .....30

Table 2.2 Spectra of 2-NES at pH 8.....33

### Chapter 3 – 4-Substituted Estrogens as Reversible and Irreversible Inhibitors of STS

Table 3.1. Inhibition of STS with 2-substituted 4-FE1 Derivatives.....46

Table 3.2. Inhibition of STS with 4-substituted estrogen derivatives. ....47

Table 3.3.  $K_i$ 's for compounds 3.19, 3.20 and 3.24 .....51

### Chapter 4 – Photoaffinity Labeling to Reveal Mode of Substrate and Product Transport in STS

Table 4.1. Summary of results with compounds 4.1-4.8.....83



## List of Figures

### Chapter 1 – Steroid Sulfatase: Function, Structure, Inhibitors, and Substrate Inhibition

<b>Figure 1.1</b> Biosynthesis of estradiol from dehydroepiandrosterone .....	2
<b>Figure 1.2.</b> STS crystal structure revealing the tertiary mushroom-shape structure .....	6
<b>Figure 1.3.</b> Structure depicting the electrostatic potential of STS and its association with the RER. ....	7
<b>Figure 1.4.</b> Structure of STS showing the three flexible loops in red which may allow substrates to enter and leave the active site .....	8
<b>Figure 1.5.</b> The post-translational modification found in all aryl sulfatases.....	10
<b>Figure 1.6.</b> The active site of steroid sulfatase showing a sulfated formylglycine hydrate residue .....	11
<b>Figure 1.7.</b> Vanadate, sulfite, and sulfate as initial inhibitors of STS .....	13
<b>Figure 1.8.</b> General structures for madurahydroxylacetone thiosemicarbazones, aryl piperazines and arylsulfonylureas. ....	15
<b>Figure 1.9.</b> Structures of two potent STS inhibitors: EMATE and 667 COUMATE.....	17
<b>Figure 1.10.</b> Time- and concentration-dependent inactivation of STS with 4-DFMES at concentrations 10 $\mu$ M or less.....	20
<b>Figure 1.11.</b> Time- and concentration-dependent inactivation of STS with 4-DFMES at concentrations of 10 $\mu$ M and greater .....	20
<b>Figure 1.12.</b> The kinetics associated with substrate inhibition are slightly different than that of normal Michaelis-Menten kinetics .....	21

### Chapter 2 – Purification and Assaying of Steroid Sulfatase

<b>Figure 2.1.</b> Elution profile of STS activity by DEAE chromatography .....	26
<b>Figure 2.2.</b> Elution profile of STS activity by anti-STS immunoaffinity chromatography .....	26
<b>Figure 2.3.</b> SDS PAGE of purified STS. The gel was stained in Fermentas PageBlue	

Protein staining solution. ....	27
<b>Figure 2.4.</b> Structures of <i>p</i> -nitrophenyl phosphate and 2-nitrophenol .....	28
<b>Figure 2.5.</b> Replots of 2-NE1 spectra at pH 12 .....	31
<b>Figure 2.6.</b> Replots of 2-NE1 spectra at pH 1.5 .....	31
<b>Figure 2.7.</b> Replots of 2-NE1 spectra at pH 7.5 .....	32
<b>Figure 2.8.</b> Replots of 2-NE1 spectra at pH 8.0 .....	32
<b>Figure 2.9.</b> Replots of 2-NES spectra at pH 8.0 .....	33
<b>Figure 2.10.</b> HPLC chromatograms for reaction of STS with 2-NES measured at 281 nm .....	34
<b>Figure 2.11.</b> HPLC chromatograms for reaction of STS with 2-NES measured at 299 nm .....	35

### **Chapter 3 – 4-Substituted Estrogens as Reversible and Irreversible Inhibitors of STS**

<b>Figure 3.1.</b> Structures of 4- ( <b>1.29</b> ) and 2-formyl estrone ( <b>3.1</b> ) and estra-1,3,5(10)-triene-17-one-3-carbaldehyde ( <b>3.2</b> ) .....	40
<b>Figure 3.2.</b> Structures of compounds <b>3.3-3.4</b> .....	41
<b>Figure 3.3.</b> Time- and concentration-dependent inhibition of STS with compound <b>3.4</b> .....	42
<b>Figure 3.4.</b> Time- and concentration-dependent inhibition of STS with <b>4-FE1</b> .....	43
<b>Figure 3.5.</b> Dialysis experiment with 1 $\mu$ M <b>3.4</b> .....	43
<b>Figure 3.6.</b> Time- and concentration-dependent inhibition of STS with 500 nM <b>3.4</b> in the presence varying amounts of EP .....	44
<b>Figure 3.7.</b> Structure of compound <b>3.5</b> .....	44
<b>Figure 3.8.</b> Determination of time and concentration dependent inhibition of STS with compound <b>3.5</b> .....	45
<b>Figure 3.9.</b> Lineweaver-Burk plot for competitive (A), non-competitive (B), and mixed inhibition (C) .....	49
<b>Figure 3.10.</b> Lineweaver-Burk plot for <b>3.19</b> .....	50

<b>Figure 3.11.</b> Lineweaver-Burk plot for <b>3.20</b> .....	50
<b>Figure 3.12.</b> Lineweaver-Burk plot for <b>3.24</b> .....	51
<b>Figure 3.13.</b> Structure of BOG.....	52
<b>Figure 3.14.</b> Crystal structure of STS showing the location of bound BOG .....	52

## **Chapter 4 – Photoaffinity Labeling to Reveal Mode of Substrate and Product Transport in STS**

<b>Figure 4.1.</b> The photolabelled ligand is covalently linked by UV irradiation to the binding site on the enzyme .....	57
<b>Figure 4.2.</b> Proposed PAL's for STS. ....	58
<b>Figure 4.3.</b> Effect of irradiation at 300 or 350 nm on the activity of STS. ....	59
<b>Figure 4.4.</b> Absorbance spectra of a 30 $\mu$ M solution of <b>4.1</b> .....	60
<b>Figure 4.5.</b> Absorbance spectra of a 30 $\mu$ M solution of <b>4.2</b> .....	61
<b>Figure 4.6.</b> Absorbance spectra of 50 $\mu$ M ES.....	61
<b>Figure 4.7.</b> Products ( <b>4.6</b> and <b>4.7</b> ) resulting from the STS-catalyzed hydrolysis of <b>4.1</b> , and <b>4.2</b> .....	62
<b>Figure 4.8.</b> Absorbance spectra of a 50 $\mu$ M solution of <b>4.6</b> .....	63
<b>Figure 4.9.</b> Absorbance spectra of a 50 $\mu$ M solution of <b>4.7</b> .....	63
<b>Figure 4.10.</b> HPLC chromatograms for 50 $\mu$ M <b>4.1</b> or <b>4.2</b> incubation with STS monitored at 255 nm .....	64
<b>Figure 4.11.</b> HPLC chromatograms for 50 $\mu$ M <b>4.1</b> AND <b>4.2</b> incubation with STS monitored at 299 nm .....	65
<b>Figure 4.12.</b> Lineweaver-Burk plot for <b>4.2</b> .....	66
<b>Figure 4.13.</b> Lineweaver-Burk plot for <b>4.1</b> . ....	66
<b>Figure 4.14.</b> Percent STS activity recovered versus time with incubation of photoaffinity label.....	67

<b>Figure 4.15.</b> Percent STS activity remaining versus time in the absence of <b>4.1</b> with no irradiation and upon irradiation at 350 nm in the presence of varying concentrations of <b>4.1</b> .....	68
<b>Figure 4.16.</b> Percent STS activity remaining versus time in the absence of <b>4.1</b> with no irradiation and upon irradiation at 350 nm in the presence of varying concentrations of <b>4.2</b> .....	69
<b>Figure 4.17.</b> Percent STS activity remaining versus time in the absence of <b>4.1</b> and <b>4.2</b> with no irradiation and upon irradiation at 350 nm in the presence of 50 $\mu$ M of <b>4.1</b> or <b>4.2</b> .....	69
<b>Figure 4.18.</b> Percent STS activity remaining versus time in the absence of <b>4.6</b> and <b>4.7</b> with no irradiation and upon irradiation at 350 nm in the presence of 50 $\mu$ M of <b>4.6</b> or <b>4.7</b> .....	71
<b>Figure 4.19.</b> Structure of compound <b>4.8</b> .....	72
<b>Figure 4.20.</b> Absorbance spectra of a 50 $\mu$ M solution of <b>4.3</b> .....	72
<b>Figure 4.21.</b> Absorbance spectra of a 50 $\mu$ M solution of <b>4.4</b> .....	73
<b>Figure 4.22.</b> Absorbance spectra of a 200 $\mu$ M solution of <b>4.5</b> .....	73
<b>Figure 4.23.</b> Absorbance spectra of 50 $\mu$ M EP .....	74
<b>Figure 4.24.</b> Absorbance spectra of a 50 $\mu$ M solution of <b>4.8</b> .....	75
<b>Figure 4.25.</b> Percent STS activity recovered versus time upon a 1/10 dilution of a solution of STS containing no inhibitor , 50 $\mu$ M <b>4.8</b> , 50 $\mu$ M <b>4.3</b> , 50 $\mu$ M <b>4.5</b> , or 50 $\mu$ M <b>4.4</b> into a solution of 4-MUS .....	76
<b>Figure 4.26.</b> Lineweaver-Burk plot for <b>4.5</b> . .....	77
<b>Figure 4.27.</b> Lineweaver-Burk plot for <b>4.3</b> .....	77
<b>Figure 4.28.</b> Effect of 4-MUS concentration on the recovery of STS activity after incubating STS with 10 $\mu$ M EP and 10 $\mu$ M <b>4.6</b> .....	78
<b>Figure 4.29.</b> Lineweaver-Burk plot for compound <b>4.4</b> . .....	78
<b>Figure 4.30.</b> Percent STS activity remaining versus time in the absence of <b>4.5</b> with no irradiation and upon irradiation at 350 nm in the presence of 50 $\mu$ M of <b>4.5</b> .....	79
<b>Figure 4.31.</b> Percent STS activity remaining versus time in the absence of <b>4.8</b> with no irradiation and upon irradiation at 350 nm in the presence of 50 $\mu$ M of <b>4.8</b> .....	80
<b>Figure 4.32.</b> Percent STS activity remaining versus time in the absence of <b>4.3</b> with	

no irradiation and upon irradiation at 350 nm in the presence of 50  $\mu$ M of **4.3** .....81

**Figure 4.33.** Percent STS activity remaining versus time in the absence of **4.4** with no irradiation and upon irradiation at 350 nm in the presence of 50  $\mu$ M of **4.4** .....82

**Figure 4.33.** Percent STS activity remaining versus time in the absence of **4.4** with no irradiation and upon irradiation at 350 nm in the presence of 50  $\mu$ M of **4.4** and varying concentrations of EP .....82

**Figure 4.35.** SDS PAGE of purified STS. ....84

## **Appendix A. IC<sub>50</sub> plots for compounds 3.3, 3.7-3.9, 3.11, 3.16-3.24, E1 and E2**

**Figure A.1** IC<sub>50</sub> for compounds **3.3** .....96

**Figure A.2** IC<sub>50</sub> for compounds **3.7** .....96

**Figure A.3** IC<sub>50</sub> for compounds **3.8** .....97

**Figure A.4** IC<sub>50</sub> for compounds **3.9** .....97

**Figure A.5** IC<sub>50</sub> for compounds **3.11** .....98

**Figure A.6** IC<sub>50</sub> for compounds **3.16** .....98

**Figure A.7** IC<sub>50</sub> for compounds **3.17** .....99

**Figure A.8** IC<sub>50</sub> for compounds **3.18** .....99

**Figure A.9** IC<sub>50</sub> for compounds **3.19** .....100

**Figure A.10** IC<sub>50</sub> for compounds **3.20** .....100

**Figure A.11** IC<sub>50</sub> for compounds **3.21** .....101

**Figure A.12** IC<sub>50</sub> for compounds **3.22** .....101

**Figure A.13** IC<sub>50</sub> for compounds **3.23** .....102

**Figure A.14** IC<sub>50</sub> for compounds **3.24** .....102

**Figure A.15** IC<sub>50</sub> for compounds **E1** .....103

**Figure A.16** IC<sub>50</sub> for compounds **E2** .....103

<b>Figure A.17</b> Replot of the data from <b>Figure 3.10</b> to determine $K_i$ of inhibitor <b>3.19</b> .....	104
<b>Figure A.18</b> Replot of the data from <b>Figure 3.11</b> to determine $K_i$ of inhibitor <b>3.20</b> .....	104
<b>Figure A.19</b> Replot of the data from <b>Figure 3.12</b> to determine $K_i$ of inhibitor <b>3.24</b> .....	105

## **Appendix B. Supplementary Figures for Compounds 4.1-4.5. 4.8. EP**

<b>Figure B.1</b> $IC_{50}$ for compounds <b>4.1</b> .....	106
<b>Figure B.2</b> $IC_{50}$ for compounds <b>4.2</b> .....	106
<b>Figure B.3</b> $IC_{50}$ for compounds <b>4.3</b> .....	107
<b>Figure B.4</b> $IC_{50}$ for compounds <b>4.4</b> .....	107
<b>Figure B.5</b> $IC_{50}$ for compounds <b>4.5</b> .....	108
<b>Figure B.6</b> $IC_{50}$ for compounds <b>4.8</b> .....	108
<b>Figure B.7</b> $IC_{50}$ for compounds <b>EP</b> .....	109
<b>Figure B.8</b> Replot of the data from <b>Figure 4.13</b> to determine $K_i$ of inhibitor <b>4.1</b> .....	109
<b>Figure B.9</b> Replot of the data from <b>Figure 4.12</b> to determine $\alpha K_i$ of inhibitor <b>4.2</b> .....	110
<b>Figure B.10</b> Replot of the data from <b>Figure 4.12</b> to determine $K_i$ of inhibitor <b>4.2</b> .....	110
<b>Figure B.11</b> Replot of the data from <b>Figure 4.26</b> to determine $K_i$ of inhibitor <b>4.5</b> .....	111
<b>Figure B.12</b> Replot of the data from <b>Figure 4.27</b> to determine $K_i$ of inhibitor <b>4.3</b> .....	111
<b>Figure B.13</b> Replot of the data from <b>Figure 4.29</b> to determine $\alpha K_i$ of inhibitor <b>4.4</b> .....	112
<b>Figure B.14</b> Replot of the data from <b>Figure 4.29</b> to determine $K_i$ of inhibitor <b>4.4</b> .....	112

## List of Schemes

### **Chapter 1 – Steroid Sulfatase: Function, Structure, Inhibitors, and Substrate Inhibition**

- Scheme 1.** Proposed general mechanism for arylsulfatases based on ARSA .....11
- Scheme 1.2.** Possible mechanism for the inhibition of STS by aryl sulfamates .....17
- Scheme 1.3.** Mechanism for the inhibition of STS with 4-DFMES.....19

### **Chapter 2 – Purification and Assaying of Steroid Sulfatase**

- Scheme 2.1.** The 4-methylumbelliferyl sulfate (4-MUS) assay for STS .....27
- Scheme 2.2.** Reaction of STS with 2-NES.....29

### **Chapter 4 – Photoaffinity Labeling to Reveal Mode of Substrate and Product Transport in STS**

- Scheme 4.1.** General mechanism for photoaffinity labeling of proteins with aryl azides.....58

## List of Abbreviations

<b>Abbreviation</b>	<b>Full Name</b>
2-NE1	2-nitrestrone
2-NES	2-nitroestrone sulfate
4-DFMES	4-difluoromethylestrone sulfate
4-MUS	4-methylumbelliferyl sulfate
17 $\beta$ -HSDs	17 $\beta$ -Hydroxysteroid dehydrogenases
AE	Androstenedione
AI	Aromatase Inhibitors
ARSA	Arylsulfatase A
ARSB	Arylsulfatase B
BOG	$\beta$ - <i>n</i> -octyl-D-glucopyranoside
E1	Estrone
E2	Estradiol
EP	Estrone Phosphate
ER	Estrone Receptor
ERit	Endoplasmic Reticulum
ES	Estrone sulfate
EST	Estrone sulfotransferase
FGly	Formylglycine
HPLC	High Performance Liquid Chromatography
mRNA	Messenger RNA
MSD	Multiple sulfatase deficiency
MU	4-methylumbelliferone
NADH	Nicotinamide adenine dinucleotide
NADPH	Nicotinamide adenine dinucleotide phosphate
PAL	Photoaffinity Labeling
PNPS	p-nitrophenyl sulfate
RBC	Red Blood Cell
RER	Rough Endoplasmic Reticulum
STS	Steroid Sulfatase
T	Testosterone



# **Chapter 1 – Steroid Sulfatase: Function, Structure, Inhibitors, and Substrate Inhibition**

## **1.1 Introduction**

### **1.1.1 Estrogen Dependent Breast cancer**

Despite recent advances in medical breakthroughs, breast cancer still remains one of the most prevalent forms of cancer in women, claiming over forty thousand lives a year in the United States alone (Briest and Stearn, 2009). Approximately 30-50% of breast cancers depend on the bioavailability of active estrogens, in particular estradiol (E2) for development. In normal cells, E2 is a key regulator in processes involving bone formation, fat metabolism, heart health, menstrual cycle, and breast growth. However, E2 when not under physiological check, can over stimulate enzymes and proteins involved in nucleic acid synthesis, as well as activating oncogenes leading to cancer development (Clemons and Goss, 2001).

It has been well established that blocking E2 from interacting with its receptor results in the inhibition of cancer cell growth (Pasqualini et al., 1992). For decades, this finding has been exploited by the drugs such as tamoxifen, an antagonist of the estrogen receptor (ER), to treat estrogen dependent breast cancers. While tamoxifen and its derivatives remains the gold standard for the endocrine treatment of breast cancers, their efficacy and safety varies greatly between individuals (Briest and Stearn, 2009). Consequently, alternative treatment options have been explored in the past decade. This led to an increase interest in the key enzymes responsible for estrogen biosynthesis as potential therapeutic targets for breast cancer (Pasqualini et al., 1992).

### 1.1.2 Estrogen Biosynthesis

The inhibition of estrogen biosynthesis to block the cancerization effect of estrogen provides a rational alternative to tamoxifen. E2 binds the estrogen receptor, forming a complex which enters the nucleus and regulates gene transcription. Consequently, enzymes synthesizing E2 precursors are prime candidates for inhibition. These enzymes include aromatase, 17- $\beta$  hydroxysteroid dehydrogenases, estrone sulfotransferase, and steroid sulfatase (**Figure 1.1**) (Pasqualini et al., 1992).

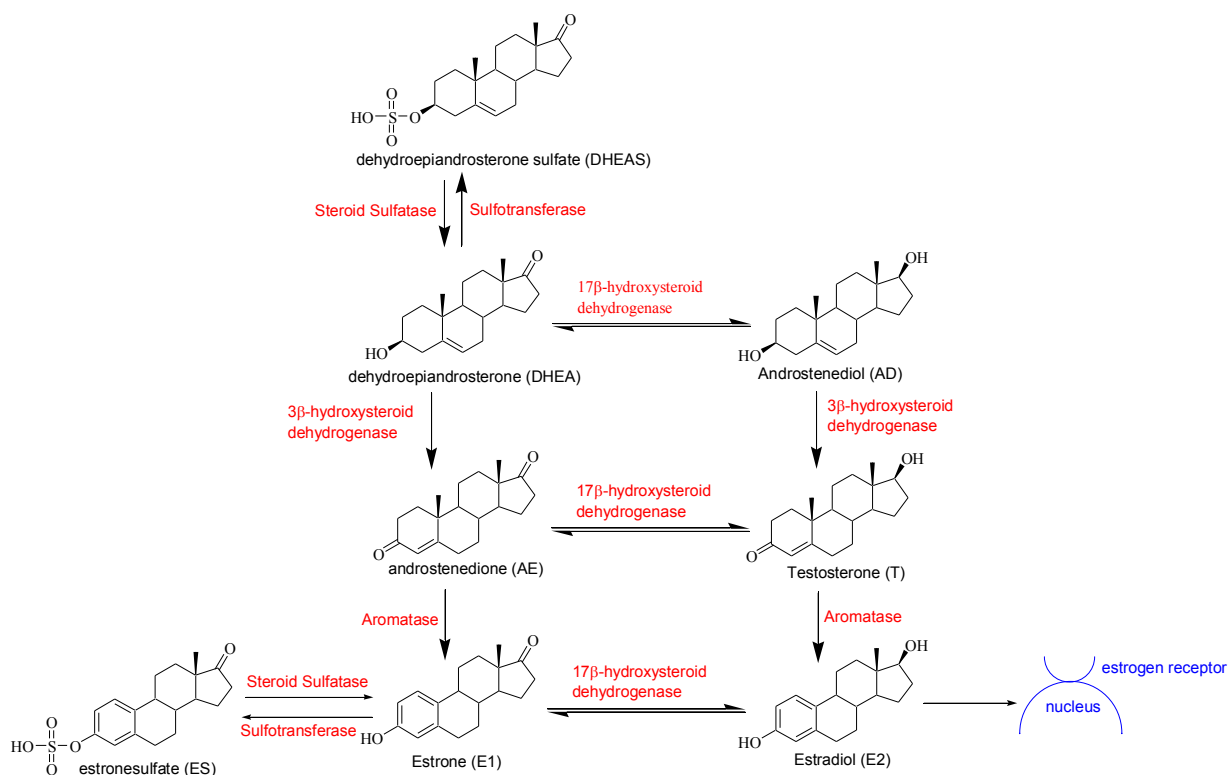


**Figure 1.1** Biosynthesis of estradiol from dehydroepiandrosterone (Clemons and Goss, 2001; Pasqualini et al., 1992; Suzuki et al., 2009).

### 1.1.3 Aromatase

Aromatase is responsible for the aromatization of the androgens androstenedione (AE) and testosterone (T) into E1 and E2 respectively, a key step in estrogen biosynthesis (Clemons and Goss, 2001). Without aromatase, virtually no estrogen can be biosynthesized. In post

menopausal women, aromatase becomes the primary source for serum estrogen. It has been reported that the levels of aromatase mRNA levels in tumour tissues increase with progressing clinical stages of breast cancer (Suzuki et al., 2009). While this does not necessarily translate directly into increased aromatase activity, it does provide evidence for the importance of aromatase in the development of breast cancers. It is not surprising that this enzyme has unprecedented popularity as a therapeutic target.

Aromatase inhibitors (AIs) such as anastrozole and letrozole are effective inhibitors for estrogen dependent breast cancers. In fact, some studies report higher efficacy with AI treatment than with tamoxifen (Gnant et al., 2009). Unfortunately, despite the effectiveness of AI treatment, some women still experience cancer progression and reoccurrence when under treatment with AI and tamoxifen (Foster et al., 2008). So while aromatase is a very good target for breast cancer, it is clear that other therapeutic targets also need to be explored.

#### **1.1.4 17 $\beta$ -Hydroxysteroid Dehydrogenase**

17 $\beta$ -Hydroxysteroid dehydrogenases (17 $\beta$ -HSDs) catalyze the reduction of the 17-ketone moiety on several steroids to their corresponding alcohol derivative utilizing NADH or NADPH as cofactors. 17 $\beta$ -HSDs is known to exist as several isoforms, but only 17 $\beta$ -HSD1 and 17 $\beta$ -HSD2 are known to catalyze the final step of estrogen synthesis, the interconversion of E1 and E2. Both isoforms favour the forward conversion from E1 to E2 by 240 fold more than the backward conversion from E2 to E1. Since 17 $\beta$ -HSDs are key regulators of E2 concentrations in gonadal and peripheral tissues, they are an attractive target for breast cancer therapeutics. However, the similarities between the various isoforms of 17 $\beta$ -HSDs present an obvious problem in designing specific inhibitors targeting only 17 $\beta$ -HSD1 and 17 $\beta$ -HSD2 (Jin et al., 1999).

### **1.1.5 Estrone sulfotransferase**

Estrone sulfotransferase (EST) is responsible for sulfating E1 into estrone sulfate (ES). It is widely accepted that sulfated steroids are biologically inactive, and serve mainly as a reservoir for their activated counterparts. ES is accepted as the most important source of E1, and consequently E2. Stimulating the activity of EST would hence decrease the serum concentrations of E1 and E2, both of which are crucial for cancer development (Clemons and Goss, 2001; Suzuki et al., 2003). There has been considerable evidence showing that levels of EST mRNA and ES are elevated in progressing clinical stages of cancer, suggesting that EST plays a key role in regulating the progression of breast cancers (Suzuki et al., 2003; Suzuki et al., 2009). However, EST lacks popularity amongst other enzyme targets, partly due to the fact that designing drugs to stimulate the activity of EST would be incredibly difficult.

### **1.1.6 Steroid Sulfatase**

Steroid sulfatase (STS), one of fifteen known human sulfatases, catalyzes the desulfation reaction of sulfated steroids, such as DHEAS into DHEA, and more importantly ES into E1 (Hanon et al., 2004). ES has several fold better solubility and half life than its non-sulfated counterpart. This allows ES to act as steroid storage pool, with concentrations of ES reaching up to ten times E1 in tissues (Hankinson et al., 1995; Utsumi et al., 2000). Due partly to this rich substrate pool, STS can produce up to ten times more E1 than aromatase in both normal and cancerous tissues (Foster et al., 2008). In fact, studies suggests that the estrogen formed in breast tumours is the result of STS activity and not aromatase (Santner et al., 1984; Masamura et al., 1996). Much like other key estrogen biosynthesis enzymes, STS mRNA also increases with progressing clinical stages of cancers. For the most part, higher STS mRNA expression results in poorer prognosis and recovery, suggesting STS' pivotal role in breast tumours (Suzuki et al.,

2009). These convincing lines of evidence suggest that STS could be an excellent therapeutic breast cancer target.

## **1.2 Steroid sulfatase**

### **1.2.1 STS Expression and Location**

Human steroid sulfatase (E.C.3.1.6.2) is found ubiquitously in virtually all mammalian tissues, but localized primarily in skin, fallopian tubes, testis, ovary, adrenal glands, brain, fetal lung, endometrium, aorta, kidney, bone, placenta, and breasts (Miki et al., 2002; Foster et al., 2008). STS is expressed as a 63-73kDA monomeric protein consisting of 583 amino acid residues. The variation in molecular weight is due to the variation in glycosylation states at four possible N-glycosylation sites on the enzyme (Stein et al., 1989). Mutation studies at two of the glycosylation sites, Asn47 (N47Q) and Asn259 (N259Q), resulted in a significantly decline in STS activity (Stengel et al., 2008), suggesting the glycosylation states have a critical impact on the overall tertiary structure of STS.

Unlike the other two aryl sulfatases, STS is an integral membrane protein found in the rough endoplasmic reticulum, but can also be found in trace amounts in the Golgi, cell surfaces, multivesicular endosomes and lysosomes (Stein et al., 1989). Its property as a membrane bound enzyme made it initially difficult to obtain a crystal structure, as well as to work with. Fortunately, in 2003 Ghosh et al. were able to resolve the crystal structure of STS at a 2.60 Å resolution (**Figure 1.2**) (Hernandez-Guzman et al., 2003).

## 1.2.2 Crystal Structure of STS

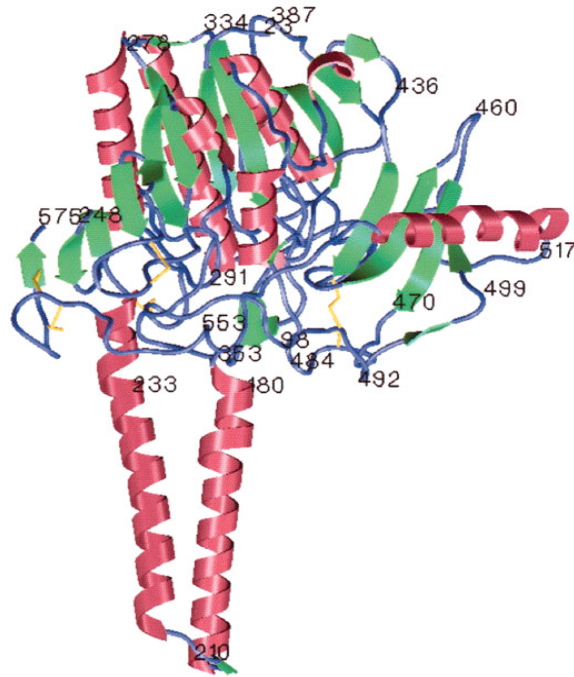


**Figure 1.2.** STS crystal structure revealing the tertiary mushroom-shape structure (Hernandez-Guzman et al., 2003)

STS assumes an overall tertiary shape resembling the shape of a mushroom, consisting of a polar globular domain and a hydrophobic stem domain. It is suggested that the enzyme anchors into the endoplasmic reticulum (ERit) membrane via the stem or transmembrane domain, consisting of two antiparallel hydrophobic  $\alpha$ -helices (helices 8 and 9). In addition to these two helices, there are two other hydrophobic regions on the globular polar domain that is thought to also interact or bind to the ERit membrane (Hernandez-Guzman et al., 2003). The polar domain contains several disulfide bonds that would be reduced in the cytoplasmic environment; so it has been suggested that it faces the lumen of the ERit. The four possible glycosylation sites on STS are also present on the polar domain (Hernandez-Guzman et al., 2003).

The active site lies in a cavity situated at the base of the polar domain, just at the top of the two hydrophobic  $\alpha$ -helices. Not surprisingly, the structure of the polar functional domain is similar to the other two soluble human aryl sulfatases, arylsulfatase A (ARSA) and arylsulfatase B (ARSB). The location of the active site, which is inside a cavity within STS, has raised several speculations on how the substrate may enter or leave the active site (Hernandez-Guzman et al., 2003).

### 1.2.3 Substrate Movement

The two antiparallel hydrophobic  $\alpha$ -helices, consisting of 25-30 amino acid residues, forms a tunnel 40 Å long that could potentially allow the sulfated substrate to pass from the cytosol directly into the active site (**Figure 1.3**). The tunnel is comprised mainly of aromatic and hydrophobic residues, which could aid the movement of the hydrophobic steroid backbone into the active site. Alternatively, the tunnel could also serve as an exit for the product (Hernandez-Guzman et al., 2003).

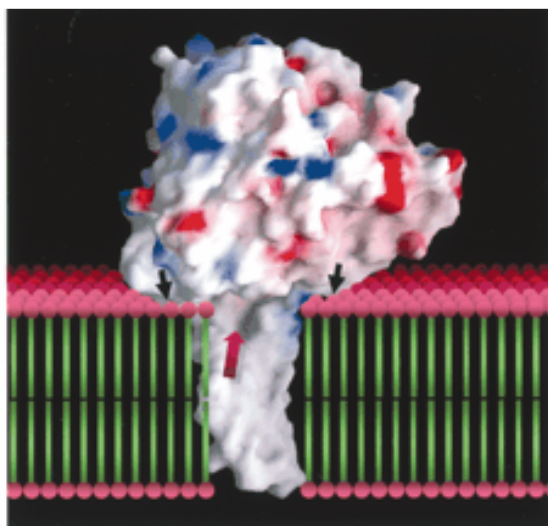


**Figure 1.3.** Structure depicting the electrostatic potential of STS and its association with the RER. The black arrows indicate regions of STS-membrane interactions. The red arrow shows a potential tunnel pathway that could allow substrate to enter or product to leave the active site (Hernandez-Guzman et al., 2003)

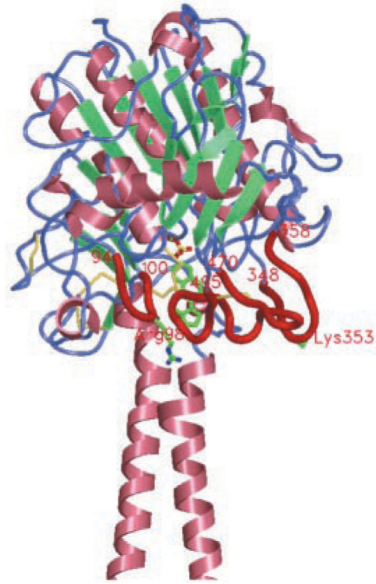


**Figure 1.4.** Structure of STS showing the three flexible loops in red which may allow substrates to enter and leave the active site (Hernandez-Guzman et al., 2003)

An alternative mode of entry to the active site is for the substrate to enter from the lumen side via three flexible loops surrounding the active site (**Figure 1.4**). In order for this to occur, the sulfated substrate first be transported through the ERit membrane via a specific transporter into the lumen of the ERit. The three flexible loops are situated at the top of the two  $\alpha$ -helices. The first loop, also known as the “front swing door” is formed by residues Thr470 to Thr495 and is located directly in front of the active site. The second loop, called the “right swing door”, is formed from Glu348 to Gly358, and is located just to the right of the first loop. The second loop is proposed to have possible interactions with the ERit. The third loop or the “left swing door” is located to the left of the first loop, and consists of res94-100. Amongst the residues constituting to the third loop, of particular importance is Arg98 and Thr99 which may have possible interaction with the 17-hydroxyl or ketone group on the steroid (Hernandez-Guzman et al., 2003). The second loop, from Glu348 to Gly358, forms the right swing door, and may have association with the endoplasmic reticulum surface. The third loop is found between



residues Ala94 and Gly100, which includes Arg98 and Thr99, forms the left swing door to the active site. Arg98 and Thr99 have been thought to interact with the 17-hydroxyl or ketone group of the steroid. The same mode of entry of the substrate could also serve as the mode of exit for the hydrolyzed product. In this case, the hydrolyzed hydrophobic product could be released into the lumen or into the membrane of the ER through one of the swing doors (Hernandez-Guzman et al., 2003).

While the most energetically favourable route for substrate entry would likely be via the tunnel, and product release exit via one of the flexible loops, there is no evidence to suggest this is the case. These uncertainties shrouding the transport mechanisms within STS could present difficulties when designing inhibitors for the enzyme.

#### **1.2.4 Post-Translational Modification of Aryl Sulfatases**

All aryl sulfatases, including STS, become active only after undergoing an essential post-translational modification (**Figure 1.5**). In eukaryotes, a conserved cysteine residue is converted into a formylglycine by the formyl glycine modifying enzyme. A similar reaction occurs within prokaryotes with the exception that either a conserved serine or cysteine is converted (Schmidt et al, 1995). The formyl group resulting from this reaction becomes hydrated and forms an  $\alpha$ -formyl glycine (FGly) hydrate, the active catalytic residue of STS. The inability to undergo this post translational modification results in multiple sulfatase deficiency (MSD), a lysosomal storage disorder, which is characterized by a significant decrease in activity of all sulfatases (Schmidt et al., 1995).

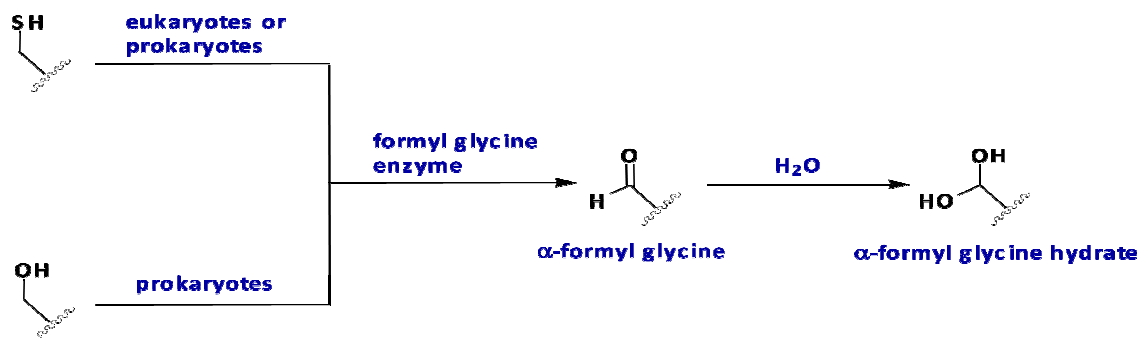
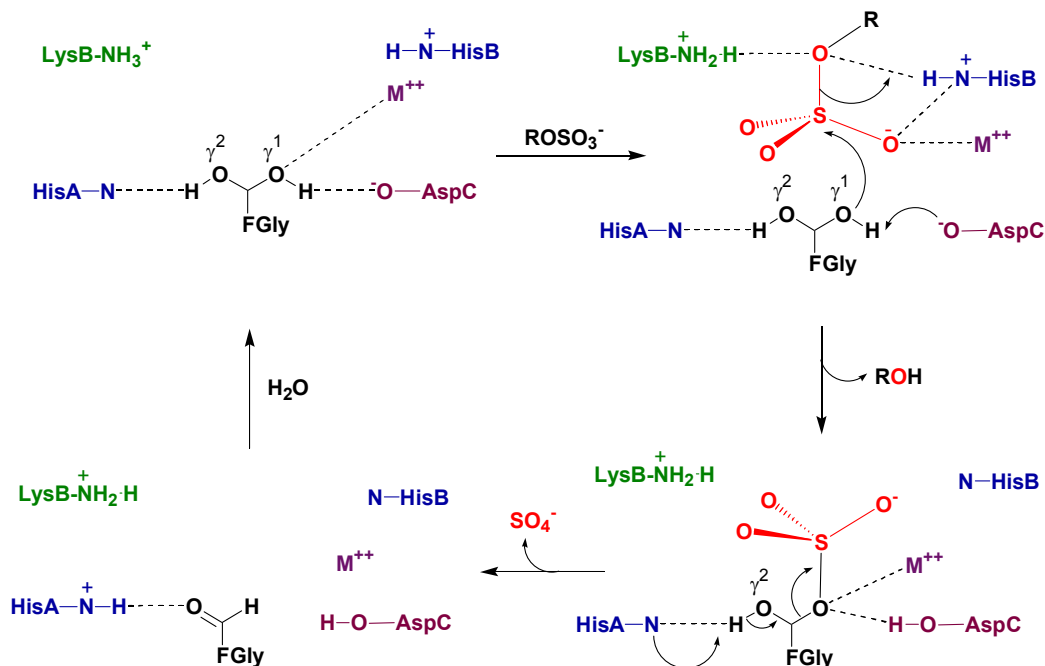


**Figure 1.5.** The post-translational modification found in all aryl sulfatases (Schmidt et al., 1995).

### 1.2.5 Proposed mechanism for Aryl Sulfatases

The functional domain of STS shows considerable similarity to ARSA and ARSB. Nine out of the ten residues that are believed to be important for catalysis in ARSA are found in the active site of STS and ARSB (Bond et al., 1997; Lukatela et al., 1998). Hence, it has been suggested that the catalytic mechanism for STS, and likely all other ARS, are similar to that proposed for ARSA.

Von Figura and coworkers proposed a general mechanism ARS's based on the crystal structure of ARSA and kinetic studies involving ARSA and other common ARS's. The important steps are highlighted in **Scheme 1**. The first step of the mechanism involves the activation of one of the oxygens on the formylglycine hydrate by an aspartate residue acting as a general base. The oxygen performs a nucleophilic attack on the sulphur atom of the substrate, which consequently releases the desulfated product as well as forming a sulfated hydrate intermediate. A histidine residue acting as a general acid aids the displacement of the desulfated product. The sulfated hydrate then undergoes a general-base catalyzed elimination reaction to release inorganic sulfate and forming formylglycine, which is then rehydrated to regenerate the initial formylglycine hydrate. A Mg<sup>++</sup> in ARSA, or a Ca<sup>++</sup> in ARSB and STS, in addition to a positively charged lysine aid in stabilization of the substrate during catalysis (Boltes et al., 2001).



**Scheme 1.** Proposed general mechanism for arylsulfatases based on ARSA (Boltes et al., 2001)

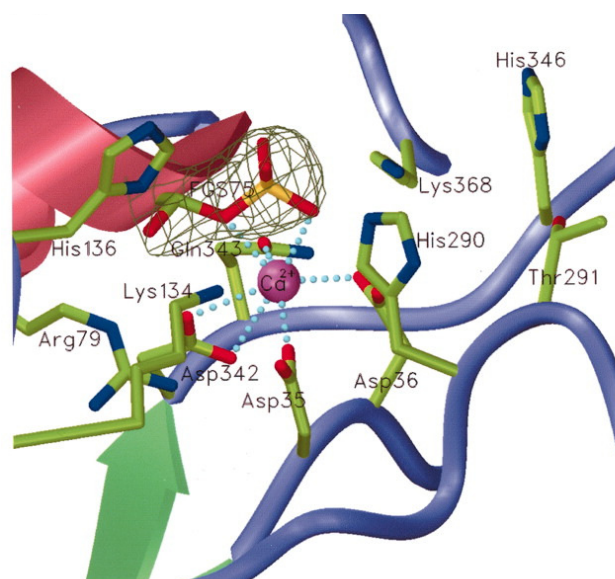


**Figure 1.6.** The active site of steroid sulfatase showing a sulfated formylglycine hydrate residue. The sulphur atom is shown in yellow (Hernandez-Guzman et al., 2003).

The first step in the mechanism proposed for ARSA depicts the hydrate as being unsulfated consistent with the crystal structure of ASA showing the formyl glycine hydrate to be

unsulfated (Boltes et al., 2001). However, ARSB and STS crystallize with the hydrate sulfated (for example see **Figure 1.6**). It is thought that the sulfated hydrate is the resting state of the enzyme, or the first step of the mechanism for STS and ARSB. If this is indeed the case, then the initial proposed mechanism for ARSA need to be revised for ARSB and STS. It could simply be that the binding of the substrate to these enzymes somehow induces a conformational change that results in the desulfation of the hydrate and initiates the first step of the reaction cycle. Another possibility is that STS and ARSB might simply just crystallize better with the hydrate sulfated in the crystallization conditions, which does have sulfate present (Hernandez-Guzman et al., 2003).

### **1.2.6 STS is specific for sulfate esters**

According to recent crystallographic studies, arylsulfatases show structural similarity to alkaline phosphatases, which catalyze the hydrolysis of phosphate esters. The possible evolutionary linkage between these two distinct families of enzymes might suggest that they could also partially hydrolyze each other's substrate. After all, phosphate-esters and sulfate esters differ only by one atom and, depending on pH, a single negative charge. A purified alkaline phosphatase from *E. coli* was found to catalyze the hydrolysis of *p*-nitrophenyl sulfate (PNPS) (O'Brien and Herschlag, 1998). While the catalytic efficiency was much lower as expected than compared to its phosphate substrate, the rate was nonetheless higher than compared to non-enzymatic hydrolysis by a water molecule (O'Brien and Herschlag, 1998). The presence of sulfatase activity in alkaline phosphatase prompted the question of whether arylsulfatases, such as STS, could also have phosphatase activity. A substrate analogue of ES, estrone phosphate (EP) was the rational candidate to test this question. Indeed, STS could not differentiate between the two compounds in terms of binding. In fact, the binding of monoanion

of EP ( $K_i=0.17\mu\text{M}$ , pH 6.0) was significantly better than the natural substrate ES ( $K_i =1.5\mu\text{M}$  pH 6.0), but no explanation is available to as why this is this case. However, the inhibitory potential of EP decreased with increasing pH, at pH 7.0 the  $K_i$  of EP is at  $0.4\mu\text{M}$  compared to that of ES at  $0.9\mu\text{M}$  (Li et al., 1995; Anderson et al., 1995). The dianion of EP did not bind as well as ES; this could be simply because the natural substrate is a monoanion. However, STS could differentiate between ES and EP in terms of catalysis, and only specifically hydrolyzed the sulfated ester (Anderson et al., 1995). The reasons to as why STS can only hydrolyze sulfate esters and not also phosphate esters are still unclear.

### 1.3 STS Inhibitors

#### 1.3.1 Reversible inhibitors

There have been few reversible inhibitors of STS reported. The first were vanadate and sulfite which showed decent micromolar potency (Dibbelt and Kuss, 1991) (**Figure 1.7**). Sulfate itself however is not a good inhibitor, suggesting that the hydrolysis of the sulfate ester bond proceeds via a trigonal pyramidal transition state, of which sulfate doesn't readily assume.

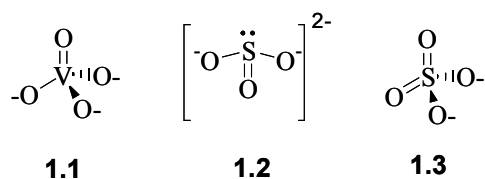
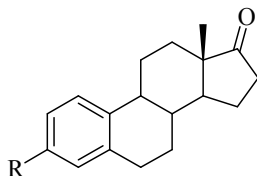


**Figure 1.7.** Vanadate, sulfite, and sulfate as initial inhibitors of STS

Not surprisingly, the first designs of reversible inhibitors of STS were substrate analogs of ES by replacement of the 3-O-sulfate ester. Many of them, as listed in **Table 1.1**, were not very effective inhibitors, with the exception of the phosphate replacement such as that found in EP, which showed promising inhibition with  $K_i$  in the submicromolar range at pH's less than 7 (Li et al., 1995). Other potent substrate analog inhibitors include  $17\alpha$ -phenyl and benzyl substituted estradiol derivatives exhibiting  $K_i$  in the low nanomolar range as shown in **Table 1.2**

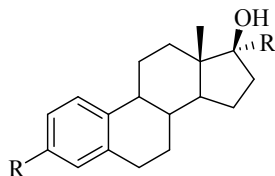
(Poirier and Boivin, 1998; Boivin et al., 2000). Increase in potency was also observed with the introduction of alkyl chains at the 17-position of estradiol up to octyl length (Boivin et al., 2000). It is likely that the increased inhibition of these compounds is due to their hydrophobic interaction with the hydrophobic transmembrane helices.

**Table 1.1.** Estrone-3-sulfate mimics as reversible inhibitors of STS



Compound	R group	Inhibition	Reference
1.4	SO <sub>2</sub> Cl	92% at 300μM	Li et al., 1993
1.5	SO <sub>3</sub> <sup>-</sup> K <sup>+</sup>	40% at 300μM	Li et al., 1993
1.6	SO <sub>2</sub> NH <sub>2</sub>	45% at 300μM	Li et al., 1993
1.7	SO <sub>2</sub> F	44% at 300μM	Li et al., 1993
1.8	SO <sub>2</sub> CH <sub>3</sub>	36% at 300μM	Li et al., 1993
1.9	NHSO <sub>2</sub> CH <sub>3</sub>	IC <sub>50</sub> = 10.20 μM	Selcer et al., 1996
1.10	NHCOCF <sub>3</sub>	IC <sub>50</sub> = 8.7 μM	Selcer et al., 1996
1.11	CH <sub>2</sub> SO <sub>3</sub> <sup>-</sup>	K <sub>i</sub> = 140 μM	Li et al., 1995
1.12	OP <sub>3</sub> <sup>2-</sup>	K <sub>i</sub> = 0.4 μM	Li et al., 1995

**Table 1.2.** 17-substituted analogs as reversible inhibitors of STS (Poirier and Boivin, 1998; Boivin et al., 2000)



Compound	R group	IC <sub>50</sub> (nM)
1.13	(CH <sub>2</sub> ) <sub>2</sub> CH <sub>3</sub>	5640
1.14	(CH <sub>2</sub> ) <sub>3</sub> CH <sub>3</sub>	3490

<b>1.15</b>	(CH <sub>2</sub> ) <sub>4</sub> CH <sub>3</sub>	1980
<b>1.16</b>	(CH <sub>2</sub> ) <sub>5</sub> CH <sub>3</sub>	930
<b>1.17</b>	(CH <sub>2</sub> ) <sub>6</sub> CH <sub>3</sub>	780
<b>1.18</b>	(CH <sub>2</sub> ) <sub>7</sub> CH <sub>3</sub>	440
<b>1.19</b>	(CH <sub>2</sub> ) <sub>7</sub> CH <sub>3</sub>	1000
<b>1.20</b>	CH <sub>2</sub> Ph-3'-Br	24
<b>1.21</b>	CH <sub>2</sub> Ph-4'-t-Bu	28

In addition to substrate analogue inhibitors, there are 3 classes of very potent non-steroidal STS inhibitors worth mentioning: madurahydroxyacetone thiosemicarbazones, aryl piperazines and arylsulfonylureas. The general structures for these compounds are shown in **Figure 1.8**. Compound **1.22**, a madurahydroxyacetone thiosemicarbazones derivative, has an IC<sub>50</sub> of 460nM and K<sub>i</sub> of 350nM with purified STS (Jutten et al., 2002). Two potent piperazine derivatives include compound **1.23** and **1.24**, which have IC<sub>50</sub>s of 47 and 78 nM respectively (Hejaz et al., 2004). An arylsulfonylurea derivative, compound **1.25**, was shown to be a competitive inhibitor of STS with K<sub>i</sub> of 890 nM.

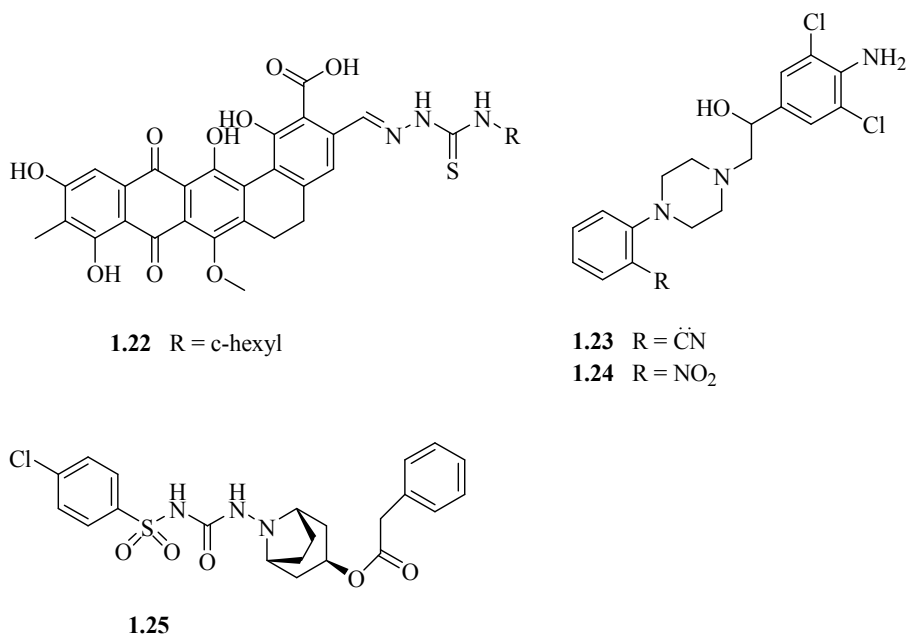


**Figure 1.8.** General structures for madurahydroxyacetone thiosemicarbazones, aryl piperazines and arylsulfonylureas.

### 1.3.2 Irreversible inhibitors

The majority of inhibitors developed for STS are irreversible inhibitors and the majority of these irreversible inhibitors are aryl sulfamates ( $\text{ArO-SO}_2\text{NH}_2$ ). The literature on this class of inhibitors is vast and so only key examples will be discussed. Two original inhibitors of this class are EMATE and 667 COUMATE (STX64), shown in **Figure 1.9** (Bojarova and Williams, 2009). EMATE was one of the first potent inhibitor for STS with  $\text{IC}_{50}$  value of 100 nM and  $\text{K}_i$  of 670 nM with STS in placental microsomes (Purohit et al., 1995). There have been several mechanisms suggested for the inhibition of STS by aryl sulfamates (**Schemes 1.2 A-D**). The first mechanism A suggests that the sulfamate inhibitor first forms a Schiff base with the active site residue. The intermediate complex is then hydrolyzed to release the phenolic product while the sulfamate moiety remains and inhibits the enzyme (Woo et al., 2000). However, non hydrolysable *N*-sulfamate and *S*-sulfamates did not exhibit irreversible inhibition, suggesting that the hydrolysis of the  $\text{ArO-S}$  bond is essential for inhibition to occur (Bojarova et al, 2008). Bojarova et al. suggested a second mechanism B beginning with a  $\text{S}_{\text{N}}2$  attack by the hydrated FGly on the sulfur atom, which consequently displaces the steroid portion of the inhibitor. The reformation of the FGly generates a free sulfamate, which then can react by the mechanism proposed in A. However, incubation of STS with sulfamic acid did not result in inhibition. A third mechanism C involves an active site base catalyzed reaction, releasing the product and forming  $\text{HNSO}_2$ .  $\text{HNSO}_2$  is a highly reactive electrophile which can react both specifically and non-specifically with proximal nucleophiles. This mechanism is highly supported as multiple labeling of STS by aryl sulfamates is observed. (Bojarova et al, 2008). A fourth possible mechanism D involves a nucleophilic attack on the sulfur atom of the inhibitor by



a nucleophile other than the FGly hydrate. This reaction forms a covalent adduct with the active site nucleophile and displaces the phenolic product. However, N,N-dialkyl sulfamates which react solely by S<sub>N</sub>2 mechanism are not inhibitors of STS early reference . One explanation to account for this observation is the sterics of N,N-dialkyl sulfamates could prevent the S<sub>N</sub>2 attack from occurring (Bojarova et al., 2008).

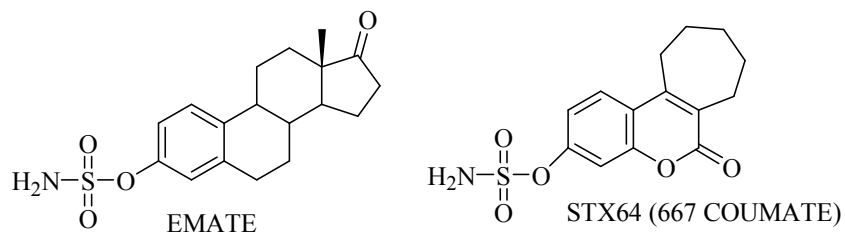
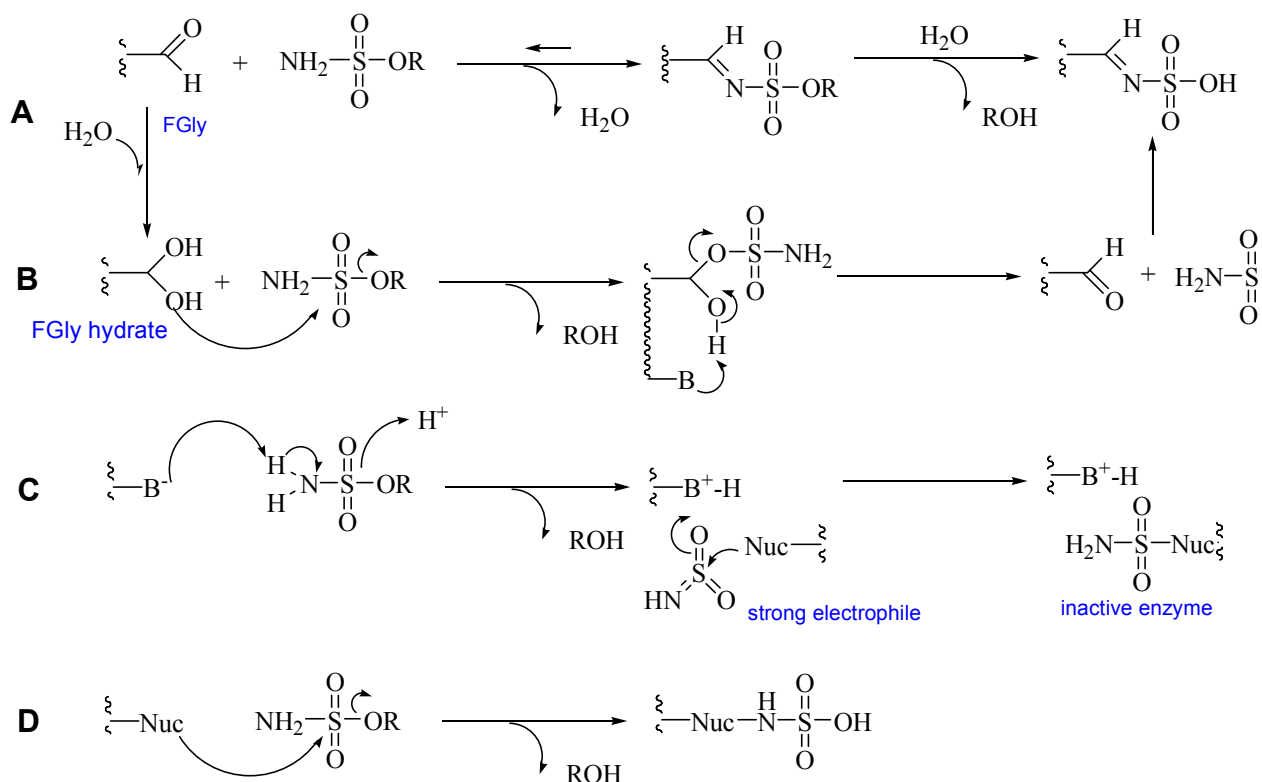


**Figure 1.9.** Structures of two potent STS inhibitors: EMATE and 667 COUMATE (Bojarova and Williams, 2009)



**Scheme 1.2.** Possible mechanism for the inhibition of STS by aryl sulfamates (Bojarova et al., 2008).

However, the hydrolysis of EMATE by STS yields E1, which is highly undesirable for a cancer inhibitor. In fact, oral administration of EMATE in rats results in higher observed estrogenic activity than oral administration of E1 (Elger et al., 1995). Studies later report that this enhanced activity is due to the sulfamates ability to bind to red blood cells (RBCs), consequently allowing them to bypass first pass metabolism in the liver (Elger et al., 2001). To overcome this problem, the estrogenic backbone was replaced with a coumarin core. The result was STX64, also known as 667 COUMATE, a potent non-estrogenic inhibitor of STS (Ahmed et al., 2001). In 2005 STX64 passed Phase I clinical trials, but unfortunately no further clinical studies have been reported with this or any other sulfamate based STS inhibitors (Stanway et al., 2007).

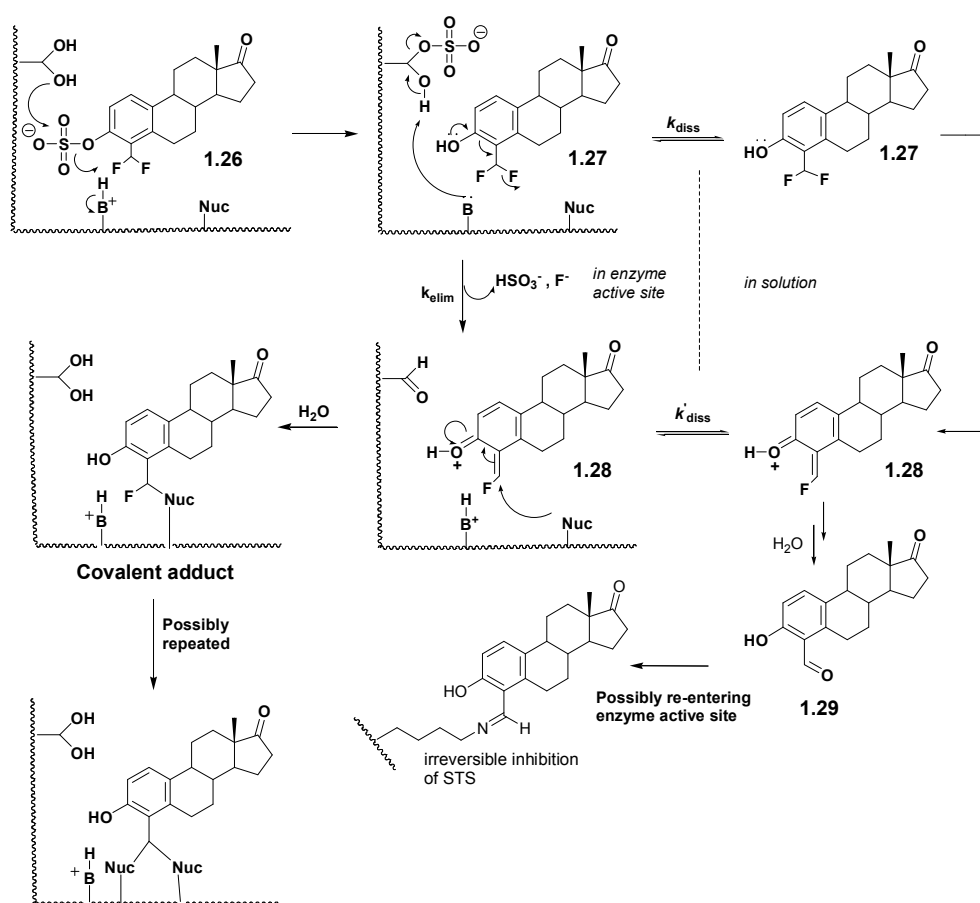
Two reasons for the sulfamate's incomplete success are partly due to their instability and non-selectivity. Sulfamate based inhibitors decompose in solution into their corresponding phenols (Nussbaumer and Billich, 2004). In addition, they are also very potent competitive inhibitors of carbonic anhydrase (CA), commonly found in RBCs, with  $IC_{50}$  at 25nM (Ho et al., 2003). CAs catalyze the interconversion between  $CO_2$  to bicarbonate ions, and serves as an important regulator of respiration, pH,  $CO_2$  homeostasis, and electrolyte secretion. Due to potential side effects associated with sulfamate based inhibitors, other classes of inhibitors for STS are currently being explored (Nussbaumer and Billich, 2004)

## **1.4 Substrate Inhibition**

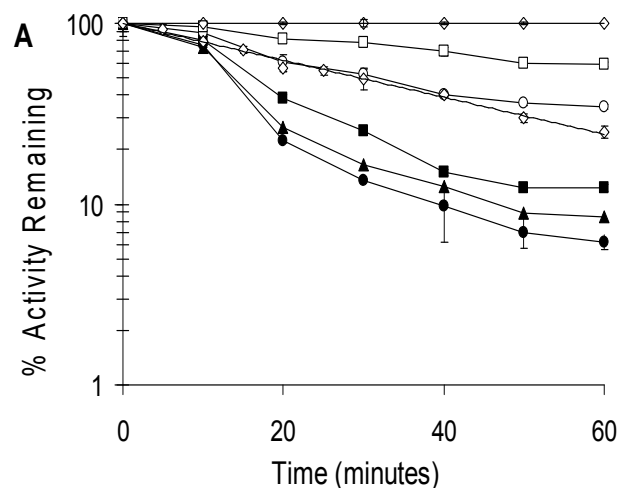
### **1.4.1 4-DFMES unique irreversible inhibitor**

During the course of our studies on the development of irreversible inhibitors of STS, we developed 4-difluoromethylestrone sulfate (**1.26**) as a suicide inhibitor for STS (Ahmed et al.,

2009). The mode of inhibition of **1.26** is unique in that it exhibits multiple pathways for irreversible STS inhibition (**Scheme 1.3**). The compound undergoes hydrolysis by the enzyme to produce inorganic sulfate and 4-difluoromethylestrone (**1.27**). **1.27** then undergoes a spontaneous elimination of HF to produce quinone methide species **1.28**. This species can react with active site residues causing irreversible STS inhibition or it can diffuse out of the active site where it reacts with water to eventually give 4-formyl estrone (**1.29**). **1.29** then enters the active site and can also irreversibly inhibit STS. How **1.29** irreversibly inhibits STS is not known, however, it is likely that it is forming a Schiff base with an active site lysine or arginine residue.



**Scheme 1.3.** Mechanism for the inhibition of STS with 4-DFMES



2

**Figure 1.10.** Time- and concentration-dependent inactivation of STS with 4-DFMES at concentrations 10  $\mu\text{M}$  or less: 0  $\mu\text{M}$  ( $\diamond$ ); 1  $\mu\text{M}$  ( $\square$ ); 2.5  $\mu\text{M}$  ( $\circ$ ); 5  $\mu\text{M}$  ( $\blacksquare$ ); 7.5  $\mu\text{M}$  ( $\blacktriangle$ ); 10  $\mu\text{M}$  ( $\bullet$ ) (Ahmed et al., 2009).

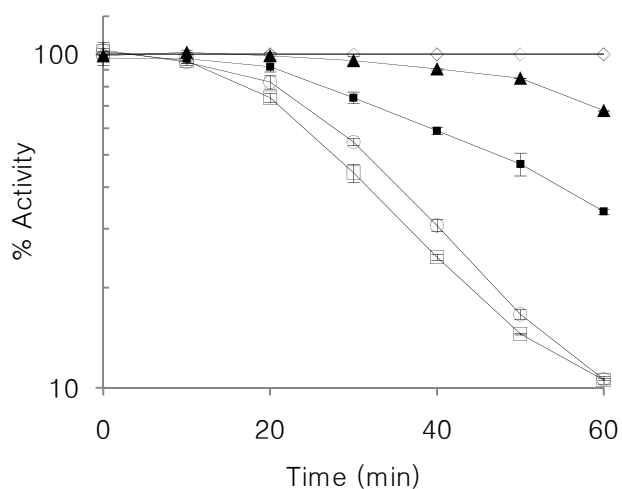


**Figure 1.11.** Time- and concentration-dependent inactivation of STS with 4-DFMES at concentrations of 10  $\mu\text{M}$  and greater: 0  $\mu\text{M}$  ( $\diamond$ ); 10  $\mu\text{M}$  ( $\square$ ); 20  $\mu\text{M}$  ( $\circ$ ); 40  $\mu\text{M}$  ( $\blacksquare$ ); 80  $\mu\text{M}$  ( $\blacktriangle$ ) (Chau, Ahmed and Taylor, unpublished results).

As expected of most suicide inhibitors, the rate of inhibition of STS with 4-DFMES increases with increasing inhibitor concentrations (**Figure 1.10**). Strangely enough, at concentrations greater than 10  $\mu\text{M}$ , the rate of inhibition begins to decrease (**Figure 1.11**). There are two possible explanations for this. One is that at higher 4-DFMES concentrations it takes longer for 4-FE1 to accumulate and compete with 4-DFMES for the active site. The other

possible explanation is that there is substrate inhibition taking place as it has been reported that at substrate concentrations greater than 10  $\mu\text{M}$ , STS begins to experience substrate inhibition (Prost et al., 1984; Dibbelt et al., 1994)

### 1.4.2 Substrate Inhibition

Enzyme kinetics for most part follow the Michaelis-Menten curve such that as substrate concentration increases, the rate of catalysis also increases until it begins to plateau nearing a threshold  $V_{\text{max}}$ . In some enzymes however, reaching a particular threshold concentration of substrate causes the rate to decrease; a phenomenon known as substrate inhibition (shown in **Figure 1.12**). This phenomenon presents potential problems in data interpretation and extrapolation of enzyme kinetics, but at the same time can be exploited for inhibitor design (Lin et al., 2001).

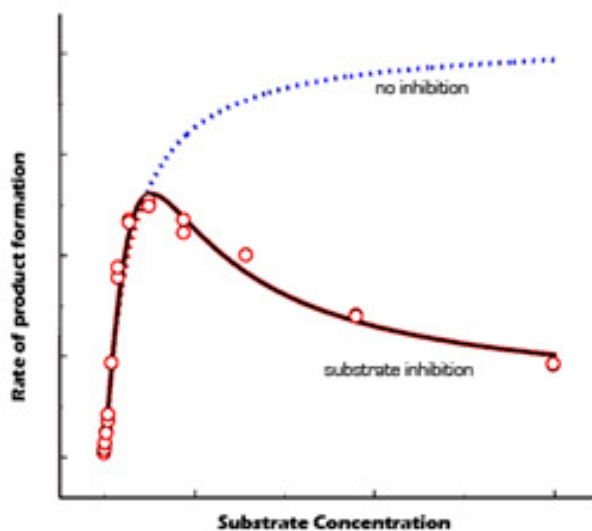


**Figure 1.12.** The kinetics associated with substrate inhibition are slightly different than that of normal Michaelis-Menten kinetics (Lin et al., 2001).

The phenomenon is not entirely uncommon as several different classes of enzymes exhibit substrate inhibition to some extent. For example, some cytochrome P450 enzymes, responsible for catalyzing numerous endogenous substrates and xenobiotic, experience a reduction in activity from 39% up to 97% as a result of substrate inhibition (Lin et al., 2001). An important sulfotransferase enzyme, SULT1A1, which is involved in the sulfate conjugation of numerous endogenous compounds is also substrate inhibited by its xenobiotic substrates (Gamage et al., 2003). Another example of an enzyme subject to substrate inhibition is adenosine 5'-phosphosulfate (APS) kinase, which catalyzes APS to 3'-phosphoadenosine 5'-phosphosulfate (PAPS) (Sekulic et al., 2007).

### **1.4.3 Substrate Inhibition in STS**

The kinetics observed with 4-DFMES suggest that STS may indeed be substrate inhibited. In 1984, Prost et al. showed that concentrations of ES above approximately 7  $\mu\text{M}$  resulted in substrate inhibition in STS (Prost et al., 1984). This same phenomenon was also later reported by Dibbelt et al. in 1994 who stated that STS is inhibited by its substrates such as ES ( $K_m = 2\text{-}4 \mu\text{M}$ ) at concentrations greater than 10  $\mu\text{M}$  (Dibbelt et al., 1994) though no data was presented to support Dibbelt claim. However, 4-methylumbelliferyl sulfate (4-MUS), a compound that is commonly used to assay STS activity, does not exhibit substrate inhibition. One argument to account for this exception is the structure of 4-MUS is very different than that of the natural substrate ES. Hence, it may behave and bind differently than ES as suggested by its  $K_m$  at 180  $\mu\text{M}$  (Ahmed, 2009) which is substantially higher than that of ES. Since Dibbelt et al., no studies have been done to validate the existence of this phenomenon or investigate the mechanism by which substrate inhibition within STS could occur. In any case, the possibility of

substrate inhibition suggests additional binding sites which could potentially be utilized for future inhibitor design. Inextricably linked to the phenomenon of substrate inhibition in STS is the question of how STS substrates enter and leave the active site. However, as discussed above, it is not known exactly how STS substrates and products enter and leave the active site

## **1.5 Research Objectives**

The possibility that STS is subject to substrate inhibition suggests that it has multiple substrate binding sites. The uncovering of non-active site binding sites for substrates and ligands could lead to the development of novel inhibitors that utilize these alternative sites. The global objective of the work described in this thesis is to learn more about the presence of alternative substrate/ligand binding sites in STS. In *Chapter 2*, we discuss the purification of STS and examine whether 2-nitroestrone sulfate can be used as chromogenic substrates for STS. Such a chromogenic assay could potentially be used to readily study substrate inhibition in STS and would be a convenient alternative to the cumbersome radioassays used by Prost et al., and Dibbelt et al employing tritiated substrates. In *Chapter 3*, we examine the inhibition of STS with various 4-substituted estrogen derivatives anticipating that these studies may indirectly reveal the existence of a secondary binding site. Finally in *Chapter 4*, we determine whether a series of azido and diazo ES and EP derivatives can act as photoaffinity labels of STS. Photoaffinity labels of STS could have potential for studying pathways of substrate entry and product release in STS.

## Chapter 2 – Purification and Assaying of Steroid Sulfatase

### 2.1 Introduction

In order to assay STS accurately a pure form of the enzyme is required. Impurities such as contaminating enzymes can yield unreliable results. In addition, in some cases it is useful to know the exact concentration of STS such as in photoaffinity labeling studies. There are only a few cases where researchers have used purified STS in their studies (Li et al., 1995; Dibbelt et al., 1994; Nussbaumer et al. 2002; Selcer et al., 1997). While there have been efforts in the past to overexpress STS in *E.coli*, so far only limited success has been reported using 293-EBNA cells from human embryonic kidney cells (Stengel et al., 2008). Hence, pure STS has traditionally been obtained by purifying it from human placenta, which is a good source of the enzyme. Human placenta is readily available and no specialized equipment is required for STS extraction and purification. There is a considerable number of published procedures on the purification of STS from human placenta, although the purification results in regards to enzymatic properties varies greatly amongst them (van der Loos et al., 1983; Noel et al., 1983; Burns et al., 1983; Dibbelt et al., 1986; Vaccaro et al., 1987; Shakaran et al., 1991; Suzuki et al., 1992; Purohit et al., 1998; Hernandez-Guzmen et al., 2003). Despite their differences, the initial steps in the process share common elements. The first step always involves homogenization of the placenta followed by centrifugation of the homogenate which yields crude STS in the microsomal fraction. The second process is the solubilization of the enzyme in the microsomal fraction using a detergent, such as Triton X-100. The third involves the use of an anion exchange column to separate STS from other aryl sulfatases. After this step, a wide variety of chromatographic media and techniques have been used to obtain the pure enzyme. The objective of the work described in this chapter is to purify STS using a procedure developed by researchers



at Novartis and modified in the Taylor group (Ahmed et al., 2005). In addition we examine an alternative approach to assaying STS using a chromogenic substrate based on a natural steroidal substrate.

## **2.2 Results and Discussion**

### **2.2.1 Placental Purification of STS**

STS was extracted from human placental based on procedures provided by (Hernandez-Guzman et al., 2001) and purified using the procedure developed at Novartis and in the Taylor group (Ahmed et al., 2005). Briefly, fresh placenta was homogenized and the resulting homogenate centrifuged to obtain the microsomal fractions which contained STS. The fractions were solubilized in buffer containing Triton X-100, applied to a DEAE ion exchange column, and then eluted using a salt gradient. Those fractions with STS activity, as determined by the 4-MUS assay (as discussed in section 2.2.2 below) were pooled and dialyzed into buffer containing 20 mM HEPES 1% Triton X-100 pH 7.4. This sample was then applied to an immunoaffinity column containing a covalently bound anti-STS antibody that binds specifically to STS. The column was washed with buffer to remove any residual protein that may bind non-specifically. Buffer containing 50mM citric acid, 140mM NaCl, 0.01% Triton X-100 at pH 2.7 is used to elute STS from the column, and fractions containing STS are pooled, dialyzed into 20 mM Tris-HCl buffer, pH 7.0 containing 0.1% Triton X-100, and stored at -80 °C. This procedure yields STS in high purity; two bands on the SDS page correspond to the two main glycosylation states of the enzyme (Figure 2.3). The molecular mass of purified STS is approximately 63 kDA (Hernandez-Guzman et al., 2003; Stein et al., 1989; Sugawara et al., 2006). The protein concentration was determined using a DC Protein Assay kit from BioRad Laboratories. The

specific activity of purified STS varied between purifications, from 0.5 to 1.25  $\mu\text{mol}$  4-MUS/min/mg enzyme.

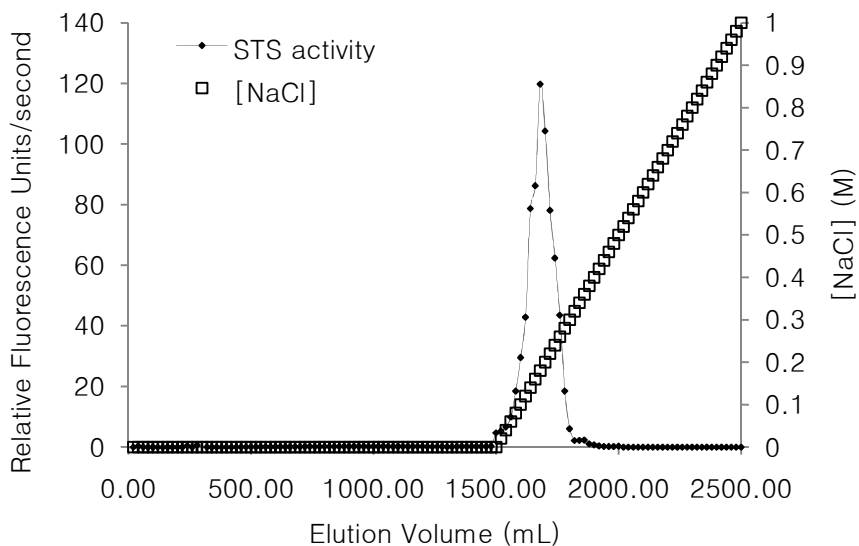


**Figure 2.1.** Elution profile of STS activity by DEAE chromatography

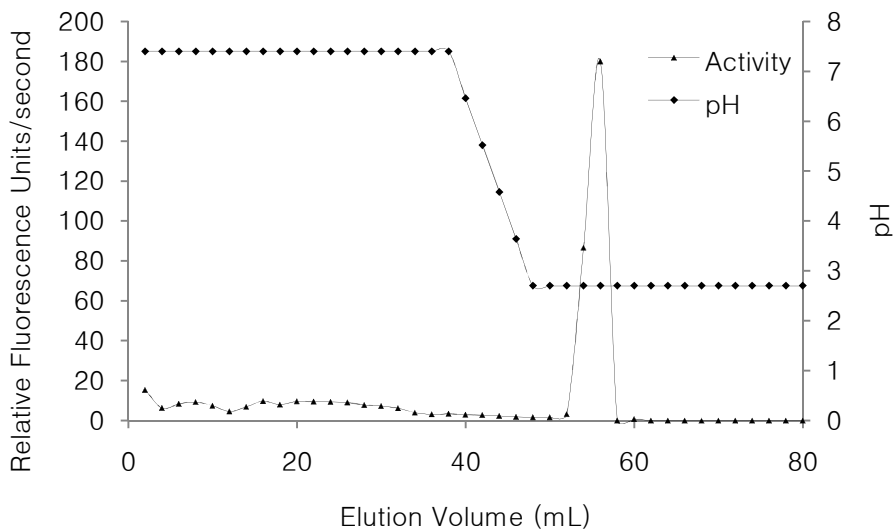


**Figure 2.2.** Elution profile of STS activity by anti-STS immunoaffinity chromatography

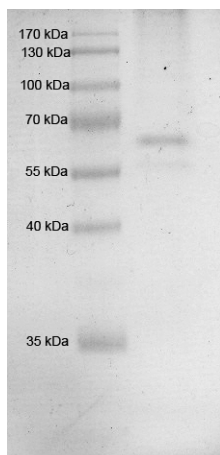
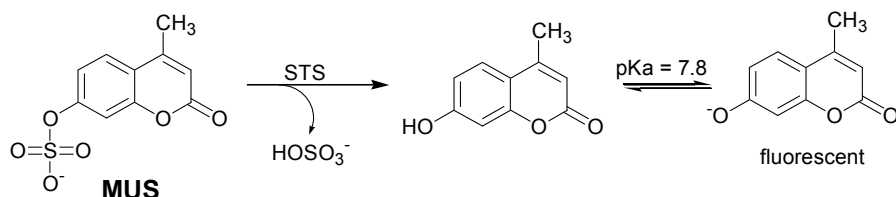


**Figure 2.3.** SDS PAGE of purified STS. The gel was stained in Fermentas PageBlue Protein staining solution. Lane 1 contains Fermentas PageRuler™ Prestained Protein Ladder. Lane 2 contains purified STS.

### 2.2.2 2-Nitroestrone sulfate as a potential chromogenic substrate for STS

STS is commonly assayed using the synthetic substrate 4-methylumbelliferyl sulfate (4-MUS) between pH 7.0-8.0 (Scheme 1). 4-MUS is hydrolyzed by STS to give 4-methylumbelliferone (MU), which in its ionized form, is fluorescent and can be measured by fluorescence spectroscopy by excitation at 360 nm and emission detection at 460nm.



**Scheme 2.1.** The 4-methylumbelliferyl sulfate (4-MUS) assay for STS.

As stated in Chapter 1, 4-MUS does not exhibit any apparent form of substrate inhibition, and one argument is because it does not resemble the natural substrate. They exhibit significantly differences in  $K_m$ 's: The  $K_m$  for 4-MUS is 180  $\mu\text{M}$  while that for ES is about 2-4  $\mu\text{M}$  (Ahmed, 2009). For this reason, we believe that it is essential to use steroidal substrates which are structurally similar to ES, in order to study substrate inhibition in STS. Unfortunately, the only method developed so far to assay STS using steroidal substrate involves the use of

radiolabelled steroidal substrates, such as tritiated estrone sulfate, combined with scintillation counting. These types of assays were used by Prost et al., and Dibbelt et al. to report substrate inhibition in STS (Dibbelt et al., 1994; Prost et al., 1984). However, they are very expensive, time consuming and tedious to perform.

One possible solution to assaying STS using steroidal substrates without resulting to radioassays is to use chromogenic steroidal substrates, and then using absorbance spectrophotometry to assay STS activity. Nitrated compounds are commonly used to assay various enzymes by spectrophotometry, such as *p*-nitrophenylphosphate in assaying phosphatase activity (Tabatabai and Bremner, 1969) and 2-nitrophenol in assaying nitrophenol oxygenase in *Pseudomonas putida* B2, which converts 2-nitrophenol to catechol (Folsom, 1997).

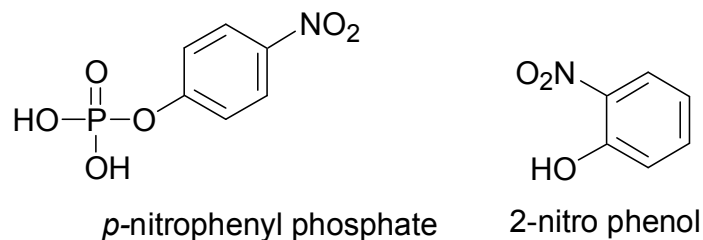
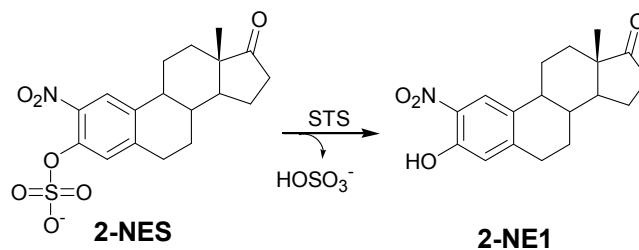


**Figure 2.4.** Structures of *p*-nitrophenyl phosphate and 2-nitrophenol (Folsom, 1997; Tabatabai and Bremner, 1969).

From our previous studies, we noted that STS is able to accommodate small groups at the 2-position of the A-ring (Ahmed et al., 2009). This suggests to us that 2-nitroestrone sulfate (2-NES) (Scheme 2) might act as a substrate for STS. If 2-NES is a substrate for STS the S-O bond on 2-NES will be hydrolyzed to produce 2-nitroestrone (2-NE1, Scheme 2) and so it might be possible to follow the reaction by monitoring the production of 2-NE1.



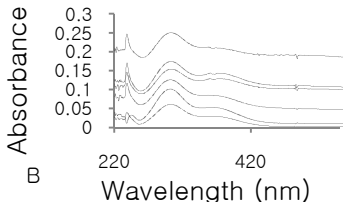
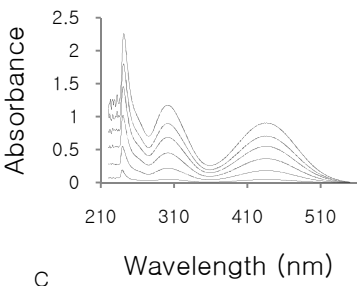
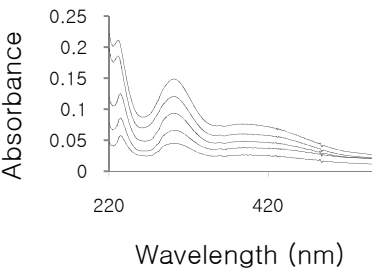
**Scheme 2.2.** Reaction of STS with 2-NES.

### 2.2.2 Determination of the extinction coefficient of 2-NE1 and 2-NES

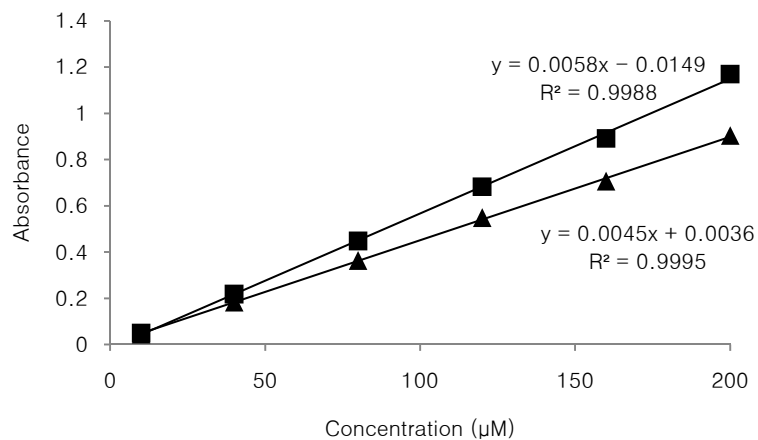
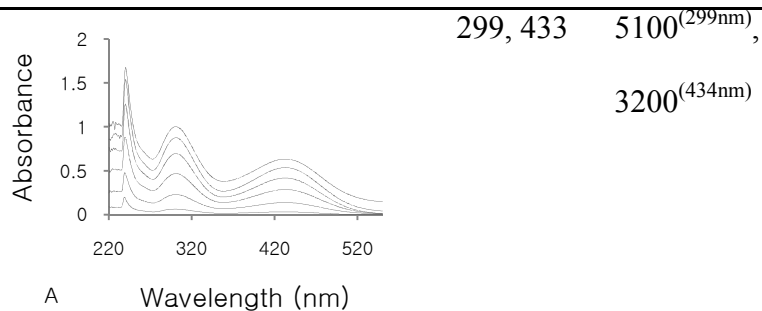
Nourescu et al. have reported that in ethanol-water at pH 3.5, 2-NE1 has an  $\lambda_{\text{max}}$  at 297 nm with a corresponding molar extinction coefficient ( $\epsilon$ ) of  $7940 \text{ M}^{-1} \text{ cm}^{-1}$ , and an  $\lambda_{\text{max}}$  at 425 nm with an  $\epsilon$  value of  $5337 \text{ M}^{-1} \text{ cm}^{-1}$  at pH 13 (Nourescu et al., 1998). 2-nitrophenol has an  $\epsilon$  of  $3470 \text{ M}^{-1} \text{ cm}^{-1}$  at pH 7.5 in phosphate buffer (Zeyer, 1986). Although spectral data for 2-NE1 at pH 3.5 and 13 have been reported before, we decided reexamine this and to also to determine the molar extinction coefficients of 2-NE1 at pH's more relevant to STS (pH 7-8). 2-NE1 and 2-NES were prepared by Christine Nicholas in the Taylor Group. The spectra data are summarized in Table 2.1. At pH 1.5 we noted an absorbance maximum at 300 nm. At pH's 7.5, 8.0 and 12.0 two maxima were found at about 300 and 430 nm. The extinction coefficient at pH 7.5 and pH 8.0, pH's at which STS is commonly assayed, at about 430 nm was  $3200 \text{ M}^{-1} \text{ cm}^{-1}$  while at 299 nm it was  $7100 \text{ (pH 7.5)}$  and  $5200 \text{ M}^{-1} \text{ cm}^{-1}$  (pH 8.0). 2-NES exhibits an absorbance maximum at 281 nm with an extinction coefficient of  $4200 \text{ M}^{-1} \text{ cm}^{-1}$ , absorbs relatively strongly at 299 nm and does not absorb at 430 nm (Table 2). So we decided to examine 2-NES as a substrate for STS at pH 8.0 monitoring the increase in absorbance at 433 nm even though the extinction coefficient of 2-NE1 at this wavelength was only  $3200 \text{ cm}^{-1}$ . If we use  $50 \mu\text{M}$  2-NES in the STS assay at pH 8.0 and if only 10% of the substrate were hydrolyzed we would only expect an OD change of 0.0235 when monitoring its production at 433 nm. This is not a very large OD

change. Indeed, when we incubated 9 nM STS with 50  $\mu$ M 2-NES, we could not detect the production of 2-NE1 at 433 nm in buffer containing 10% ethanol, 0.01% Triton X-100 and 0.1 M Tris-HCl at pH 8.0 in a 10 mm cuvette. Hence, we expect that amount of 2-NE1 produced by STS may be too small to be reliably detected or 2-NES is not a substrate for STS.

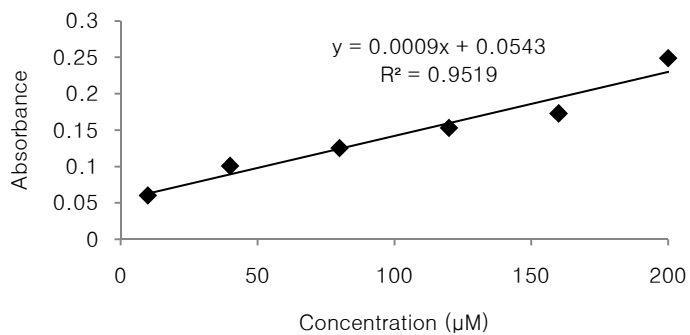
**Table 2.1.** Spectra of 2-NE1 at various pH. Concentrations of 2-NE1 beginning at the bottom curve are 10, 40, 80, 120, 160, and 200  $\mu$ M respectively for all pH except 7.5. At pH 7.5, concentrations of 2-NE1 beginning at the bottom curve are 4, 8, 12, 16, and 20  $\mu$ M.

pH	Spectra	$\lambda_{\text{maxima}}$ (nm)	Molar Extinction Coefficient ( $\epsilon$ ) ( $\text{M}^{-1} \text{cm}^{-1}$ )
1.5		300	900
12		299, 434	5800 <sup>(299nm)</sup> , 4500 <sup>(434nm)</sup>
7.5		299, 431	7100 <sup>(299nm)</sup> , 3200 <sup>(431nm)</sup>

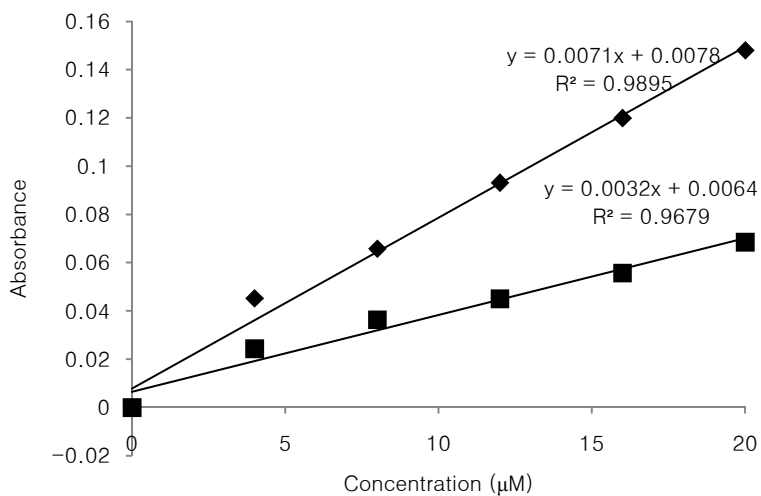
8.0



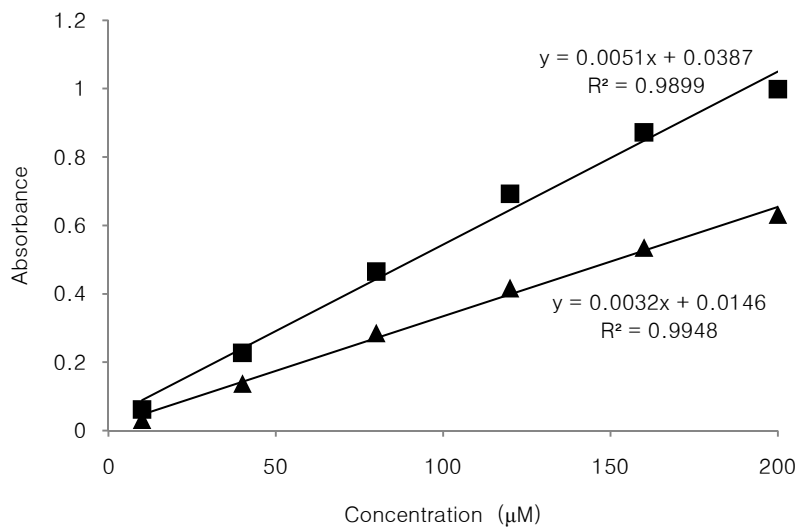
**Figure 2.5.** Replots of 2-NE1 spectra at pH 12 at wavelength 299nm (■) and 434 nm (▲)



**Figure 2.6.** Replots of 2-NE1 spectra at pH 1.5 at wavelength 300 nm (◆)



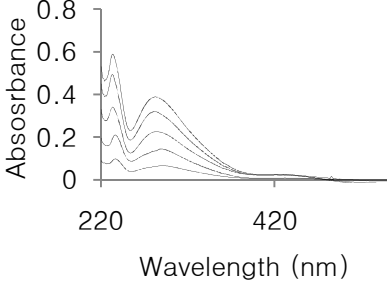
**Figure 2.7.** Replots of 2-NE1 spectra at pH 7.5 at wavelength 299 nm ( $\blacklozenge$ ) and 431 nm ( $\blacksquare$ )



**Figure 2.8.** Replots of 2-NE1 spectra at pH 8.0 at wavelength 299 nm ( $\blacksquare$ ) and 433 nm ( $\blacktriangle$ )



**Table 2.2** Spectra of 2-NES at pH 8. Concentrations of 2-NES beginning at the bottom curve are 20, 40, 60, 80, and 100 $\mu$ M.

pH	Spectra	$\lambda_{\text{maxima}}$ (nm)	Molar Extinction Coefficient ( $\epsilon$ ) $\text{M}^{-1}$ $\text{cm}^{-1}$
8.0		281	4200

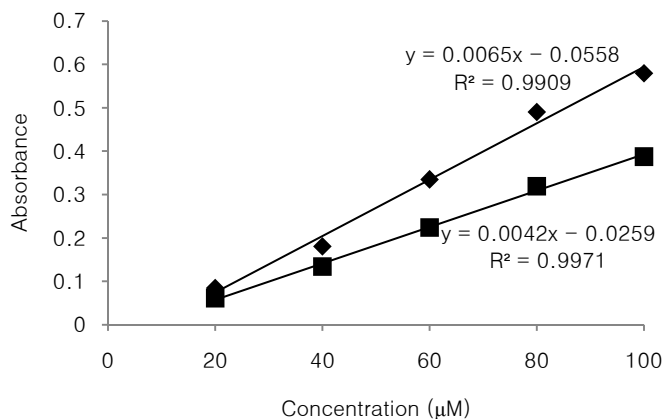


**Figure 2.9.** Replots of 2-NES spectra at pH 8.0 at wavelength 232 nm (◆) and 281 nm (■)

To determine if 2-NES is a substrate for STS we incubated 50  $\mu$ M 2-NES with 9 nM STS in buffer containing 10% ethanol, 0.01% Triton X-100 and 0.1 M Tris-HCl at pH 8.0 and looked for the production of 2-NE at 281 and 299 nm using HPLC. After 25 minutes all of the 2NES is completely converted to 2-NE (**Figures 2.10 and 2.11**), suggesting that 2-NES is indeed a substrate for STS. So it appears that although 2-NES is indeed a substrate for STS, the resulting

product, 2-NE1 is not a strong enough chromophore to allow 2-NES to be used as a chromogenic substrate for STS.

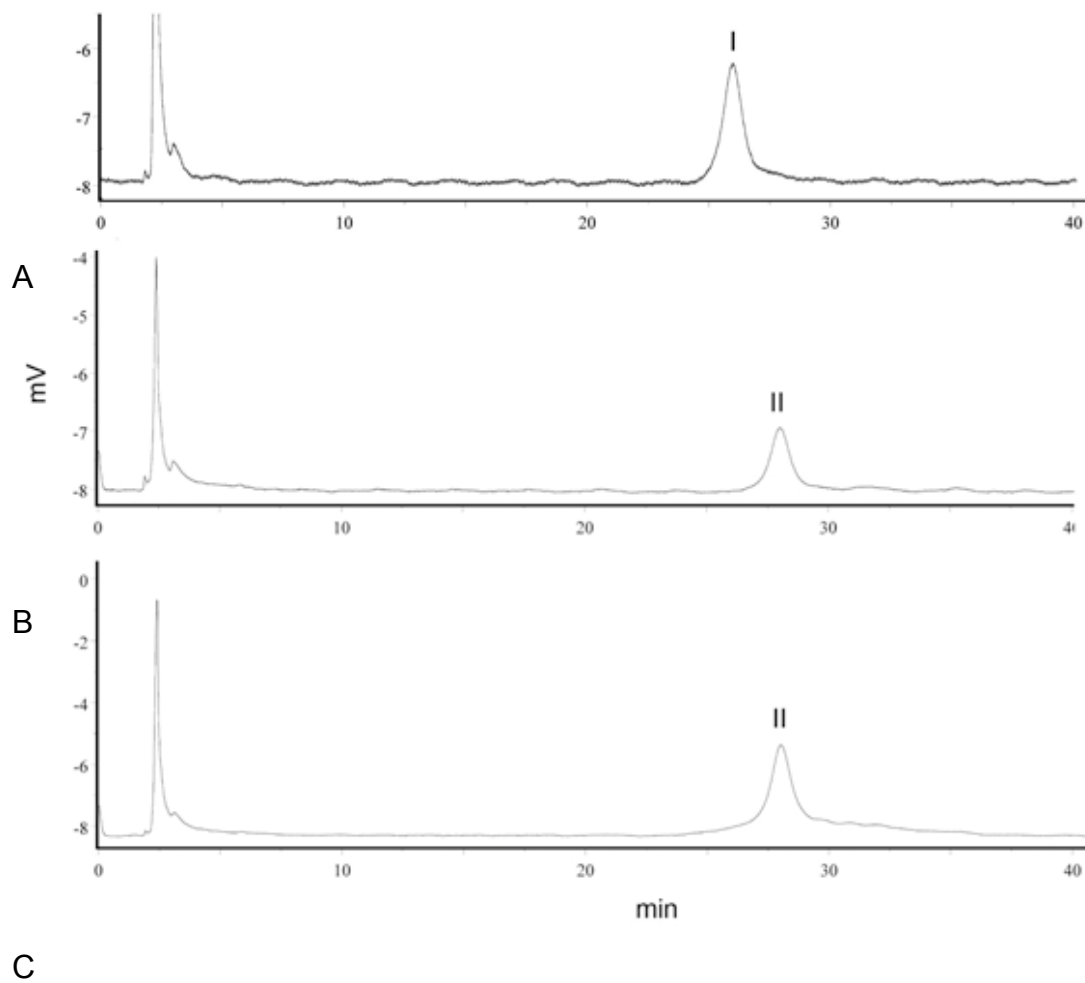


**Figure 2.10.** HPLC chromatograms for **A)** 2-NES; **B)** 2-NE1 and, **C)** a solution containing 9 nM STS, 50  $\mu$ M 2-NES after 25 min. A solutions were prepared in buffer containing 0.1 M Tris-HCl, 0.01 % Triton X-100, 10% ethanol at pH 8.0. The detector was set to 281 nm.

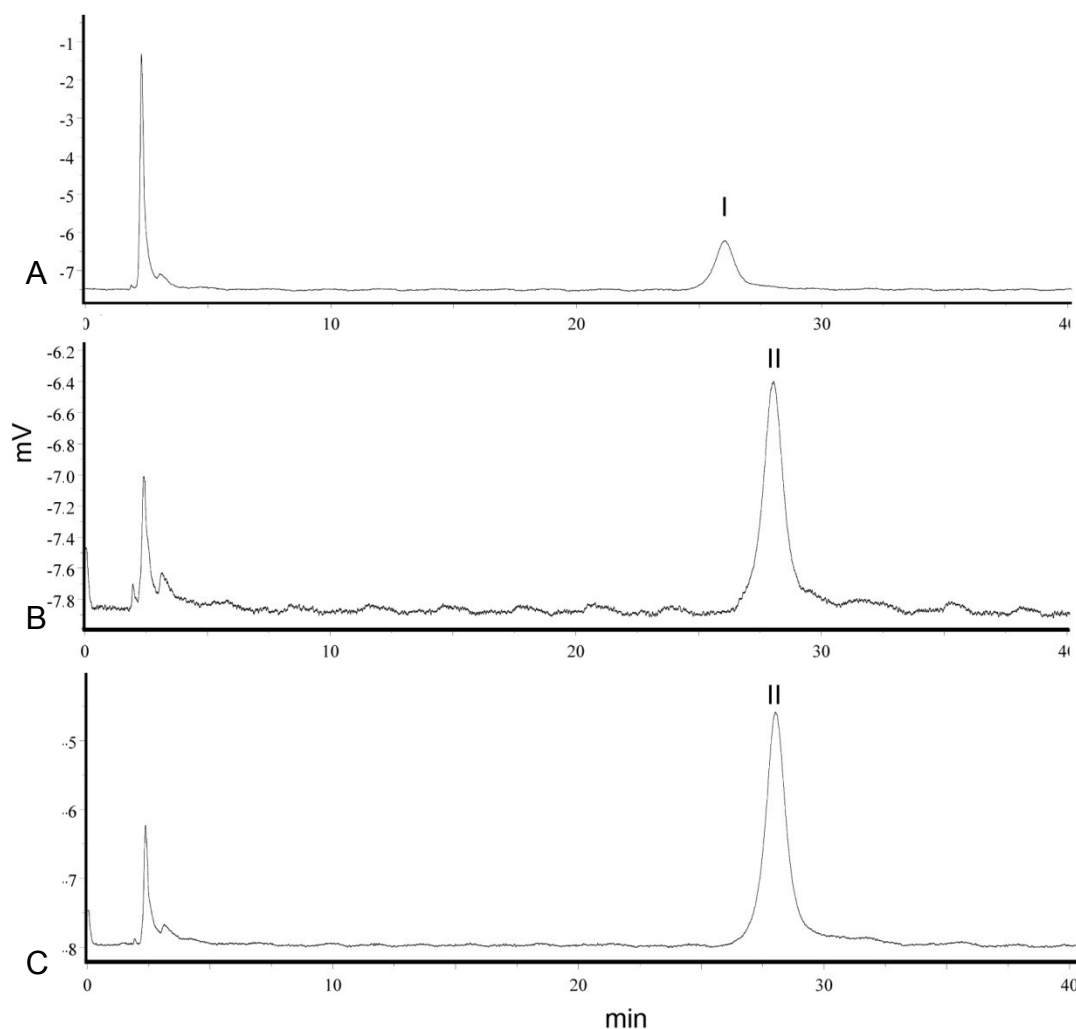


**Figure 2.11.** HPLC chromatograms for **A)** 2-NES; **B)** 2-NE1 and, **C)** a solution containing 9 nM STS, 50  $\mu$ M 2-NES in buffer containing 0.1 M Tris-HCl, 0.01 % Triton X-100, 10% ethanol at pH 8.0 after 25 minutes. The detector was set to 299 nm.

### 2.3 Conclusion and Future Work

The purification of STS is an important first step for accurate kinetic analysis of STS activity. In the Taylor lab, we have developed a reliable method for the purification of STS which yields the enzyme in very high purity. While 2-NES is a substrate for STS, 2-NE is not a sensitive enough chromophore to be used for the continuous assaying of STS. It looks like future studies on substrate inhibition in STS will have to be done using radiolabeled substrates.

## **2.4 Experimental**

### **2.4.1 Materials**

The biochemical reagents and buffers were purchased from Sigma-Aldrich (St. Louis, Missouri). Fresh human placenta was provided by Credit Valley Hospital (Mississauga, Ontario). The placenta is transported on dry ice and stored at -80°C for no longer than two days before its purification. DEAE cellulose was purchased from Whatman (Maidstone, England). The STS immunoaffinity column was prepared by Vanessa Ahmed, a graduate student in the Taylor group, by coupling an anti-STS monoclonal antibody, obtained as a gift from Novartis (Austria), to cyanogen bromide-activated Sepharose 4B obtained from Pharmacia at a density of 10mg/ml resin. The procedure for purification of STS by immunoaffinity chromatography was provided by Dr. Andreas Billich at Novartis (Austria). The DC Protein Assay kit was purchased from BioRad Laboratories (Richmond, California). Gel staining was achieved by PageBlue™ Protein staining solution from Fermentas Life Science (Vilnius, Lithuania). STS activity was determined, using the 4-MUS assay described above, on a SpectraMax Gemini XS plate reader from Molecular Devices (Sunnyvale, California) and analyzed with SOFTMAX Pro Version 3.1.1 and Microsoft Excel 2007. UV Spectra were obtained using an Agilent 8453 Spectrophotometer (Santa Clara, California) in a 10 mm quartz cuvette from Hellma (Germany).

### **2.4.2 STS purification**

The homogenization and centrifugation of human placenta were done according to procedures developed by Hernandez-Guzman and coworkers (Hernandez-Guzman et al., 2003). After removal of the membrane and umbilical cord, the full-term human placenta was cut into small pieces. 200 g of the chopped up placenta was homogenized using a Brinkman polytron in 50mM Tris-HCl pH 7.5, 0.25 sucrose, 1 g protease inhibitor cocktail (Sigma-Aldrich). The

resulting homogenate, approximately 400 mL, was centrifuged at 20 000g for 30 min at 4°C. The supernatant was discarded, and the pellet resuspended in the same buffer, and subjected to another centrifugation at 20,000 g for 30 min at 4°C. The supernatant was discarded again, and the pellet resuspended in 300 mL of extraction buffer consisting of 20 mM Tris-HCl, pH 7.4, 0.3 % Triton X-100. This sample is allowed to equilibrate for two hours before being subjected to ultracentrifugation at 100,000 g for 70 min at 4°C. The time the supernatant was collected, and the pellet was resuspended in 200 mL of the extraction buffer and subjected to another ultracentrifugation. The resulting supernatant was pooled with the previously collected supernatant, and the pellets were discarded. This microsomal sample, approximately 400 mL, was dialyzed into buffer containing 20 mM Tris-HCl, pH 7.4, 0.1% Triton X-100 (3 x 4 L) over 24 hours. The dialysate was loaded onto a DEAE column (radius = 2.5 cm, height = 16.5 cm), washed with 1500 mL of buffer containing 20 mM Tris-HCl, pH 7.4, 0.1% Triton X-100, and eluted off with a salt gradient reaching 1 M of NaCl in buffer 20 mM Tris-HCl, pH 7.4, 0.1% Triton X-100 over 1000 mL. Pooled fractions containing STS (250 mL) were dialyzed into 20 mM Hepes buffer pH 7.4 1% Triton X-100 (3 x 2 L) over 24 hours. This material was applied to an anti-STS immunoaffinity column (2.5 mL) that had been pre-equilibrated with 25 mL of the Hepes dialysis buffer. The column was washed with 40 mL of the same buffer, and STS fractions are eluted off with 40 mL of 50 mM citric acid, 140 mM NaCl, 0.1% Triton X-100. The fractions are pooled and dialyzed into storage buffer containing 20 mM Tris-HCl, pH 7.4, 0.1% Triton X-100 (3 x 4 L) over 24 hours and flash frozen with liquid nitrogen and stored at -80°C. \

### **2.4.3 STS activity in Purification**

STS activity in the fractions obtained at the various stages of the purification procedure was determined as follows. 20  $\mu\text{L}$  sample was added into the wells of a 96-well black microtiter plate containing 180  $\mu\text{L}$  of 222  $\mu\text{M}$  4-MUS in 0.1 M Tris-HCl, pH 7.0 such that the final concentration of STS was 10 fold diluted in buffer containing 200  $\mu\text{M}$  4-MUS 0.1 M Tris-HCl, pH 7.0 0.01% Triton X-100. The production of fluorescent 4-MU was monitored for 5 minutes ( $\lambda_{\text{ext}} = 360\text{nm}$ ,  $\lambda_{\text{em}} = 460 \text{ nm}$ ) using a SpectraMax Gemini XS plate reader. The enzyme activity was reported as relative fluorescent units per second (RFUs/second).

### **2.4.4 Protein determination**

The protein concentration was determined according to DC Biorad Laboratories (Richmond, CA) protein concentration determination kit instructions using bovine serum albumin (BSA) as a standard. This colorimetric assay is for the determination of protein concentration following solubilization with a detergent such as Triton X-100. The assay is based on the reaction of protein with an alkaline copper tartrate solution and Folin reagent (Bradford, 1976).

### **2.4.5 Spectral data**

2 mM solutions of 2-NE1 and 2-NES were prepared in ethanol. These solutions were diluted in buffer containing 0.11 M Tris-HCl, 0.011% Triton X-100 that was pH'd to the desired value (1.5, 7.5, 8.0 and 12). Serial dilutions of these two stock solutions in the same buffer at the appropriate pH were performed to obtain the solutions that were used for spectral determinations. 1 mL of these solutions was added to a 10 mm Helma cuvette and the spectra obtained using an Agilent 8453 spectrophotometer. Solutions containing 0.1 M Tris-HCl, 10% ethanol, 0.01% Triton X-100 were used as blanks. The extinction coefficients were determined by taking the

slopes of plots of OD versus concentration and fitting the data using linear regression analysis with Excel 2007.

#### **2.4.6 HPLC studies**

A solution of 9 nM STS and 50  $\mu$ M 2-NES in buffer containing 0.1 M Tris-HCl, 0.01 % Triton X-100, 10% ethanol, pH 8.0 was prepared and left standing at room temperature for 25 min. A 20  $\mu$ L aliquot was withdrawn and injected on to a Phenomex Jupiter analytical reversed-phase C-18 column (Torrance, CA, USA) attached to a Waters 600 HPLC system (Milford, MA, USA). The Waters 2487 dual wavelength detector was set to 299 nm and 281 nm. The compounds were eluted using 52% acetonitrile/48% water containing 0.1% trifluoroacetic acid. The retention times of 2-NES and 2-NE1 were determined by injecting 20  $\mu$ L samples of 50  $\mu$ M solutions of 2-NES and 2-NE1 in the same buffer in the absence of STS.

## Chapter 3 – 4-Substituted Estrogens as Reversible and Irreversible Inhibitors of STS

### 3.1 Introduction

In Chapter 1 we mentioned that 4-formyl estrone (**1.29**, **Figure 3.1**) was an irreversible inhibitor of STS (Ahmed et al., 2009). Kitz-Wilson analysis yielded a  $K_I$  of 1.5  $\mu\text{M}$  and a  $k_{\text{inact}}$  of 0.13  $\text{min}^{-1}$  ( $k_{\text{inact}}/K_I = 1 \times 10^5 \text{ M}^{-1} \text{ min}^{-1}$ ). With just 5  $\mu\text{M}$  of 4-FE1, STS is almost completely inactivated within 60 minutes. Only 2 % of STS activity could be recovered after extensive dialysis. We proposed that the compound forms a Schiff base with active site amine-bearing residues though this has yet to be proven. What was also interesting was that 2-formyl estrone (2-FE1, **3.1**) and estra-1,3,5(10)-triene-17-one-3-carbaldehyde (**3.2**) did not exhibit any inhibition at concentrations up to 10  $\mu\text{M}$  indicating that the inhibition is specific for the formyl group at the 4-position.

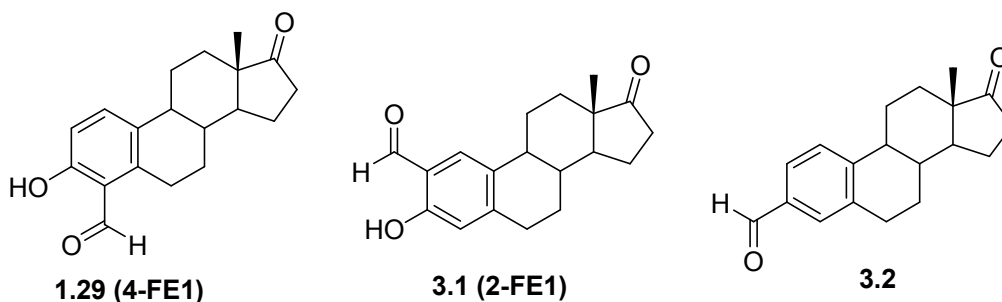


**Figure 3.1.** Structures of 4- (**1.29**) and 2-formyl estrone (**3.1**) and estra-1,3,5(10)-triene-17-one-3-carbaldehyde (**3.2**).

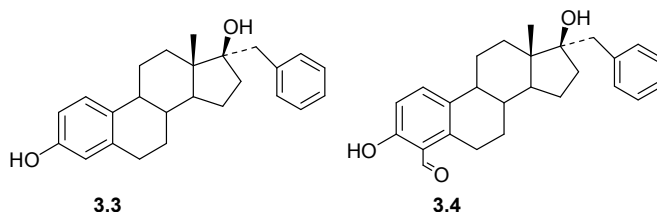
There have been almost no reports in the literature of STS inhibitors, reversible or irreversible, bearing substituents at the 4-position of E1 or E2. The objective of the work described in this chapter is to examine estrogen derivatives bearing functional groups at the 4-position as inhibitors of STS.



## 3.2 Results and Discussion

### 3.2.1 Inhibition of STS with 17- $\alpha$ -benzyl-4-formyl estradiol

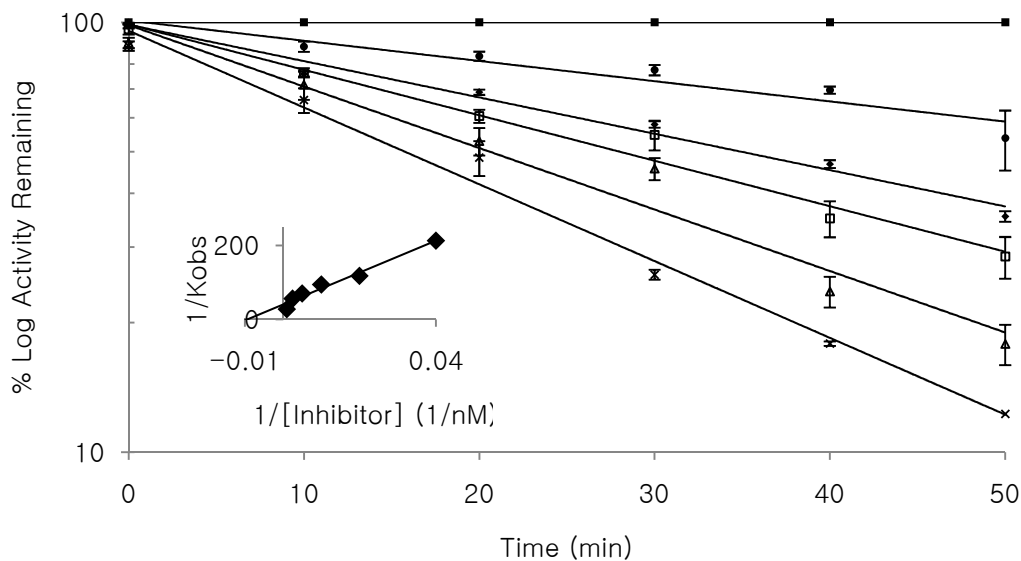
We wished to determine if we could improve upon the potency of 4-FE1 by modifying the steroid skeleton. As mentioned in Chapter 1, Poirier and coworkers have reported that estradiol modified at the 17-position with hydrophobic phenyl, benzyl or alkyl groups yields compounds that are highly potent reversible inhibitors of STS (see Table 1.2). (Poirier et al. 1998, Ciobanu and Poirier, 2006). One example of such an inhibitor is compound **3.3** which has an IC<sub>50</sub> value of 299 nM with purified STS (Ahmed et al., 2006) (**Figure 3.2**). Based on Poirier's work on 17-modified estradiol derivatives we decided to determine if the potency of 4-FE1 could be improved by modifying 4-FE1 at the 17-position. Towards this end, compound **3.4** (prepared by Byoungmoo Kim in the Taylor group) was examined as an inhibitor of STS.



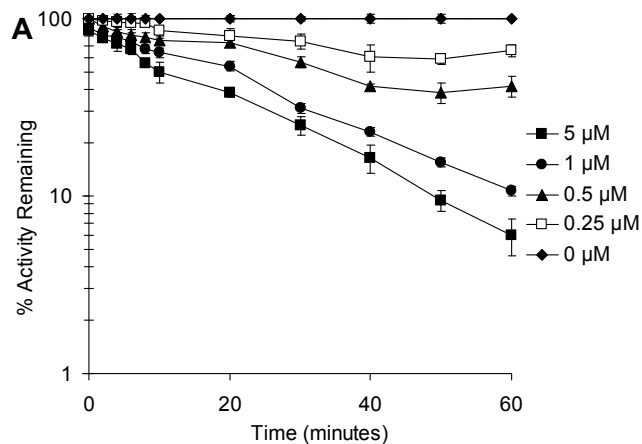
**Figure 3.2.** Structures of compounds **3.3-3.4**.

Incubation of STS with **3.4** resulted in time- and concentration-dependent inhibition as illustrated in **Figure 3.3**. From the Kitz-Wilson plot (inset, **Figure 3.3**) a  $K_i$  of 107 nM and  $k_{\text{inact}}$  of 0.025 min<sup>-1</sup> were obtained indicating that this compound is considerably more potent than 4-FE1 in terms of its affinity for STS but its rate of inactivation is less than that of 4-FE1. However,  $k_{\text{inact}}/K_i$  for **3.4** is  $2.3 \times 10^5 \text{ M}^{-1} \text{ min}^{-1}$  which is superior to 4-FE1. There are several other differences between compound **3.4** and 4-FE1. When STS is incubated with low concentrations ( $< 1 \mu\text{M}$ ) of 4-FE1 the inactivation plateaus after about 40 minutes while at higher concentrations ( $\geq 1 \mu\text{M}$ ) pseudo-first order behaviour was observed throughout (**Figure**

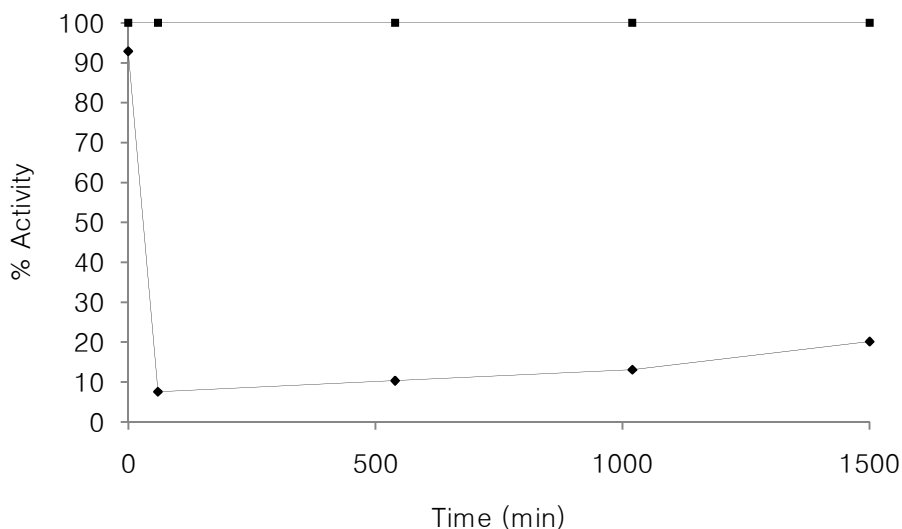
**3.4**). This behaviour may be due to multiple labelling events that are both productive and unproductive towards inactivation. This behaviour was not seen with **3.4** as more or less pseudo-first order behaviour was exhibited at all of the concentrations examined (**Figure 3.3**). Also, after inactivation of STS with compound **3.4**, about 14% of the activity was recovered after extensively dialyzing for 24 h (**Figure 3.5**). This is in contrast to 4-FE1 where almost no activity could be recovered after inactivation. Consequently, it is possible that these two inhibitors are targeting different residues.



**Figure 3.3.** Time- and concentration-dependent inhibition of STS with compound **3.4**. Reactions were conducted in 0.1 M Tris-HCl 5 % DMSO 0.01 % Triton X-100 at pH 7.0 using 310 nM STS. STS activity was determined by adding 4-MUS to the reaction mixture such that the final concentration of 4-MUS was 4 mM and then the production of 4-MU followed using fluorimetry. [**3.4**] =  $\square$  0,  $\bullet$  25,  $\blacklozenge$  50,  $\square$  100,  $\triangle$  200,  $\times$  400 nM.



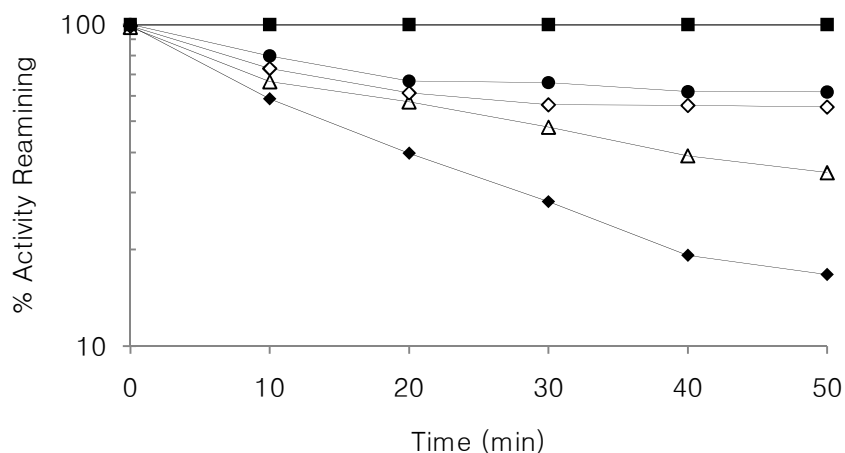
**Figure 3.4.** Time- and concentration-dependent inhibition of STS with **4-FE1** (Ahmed et al., 2009).



**Figure 3.5.** Dialysis experiment with  $1\ \mu\text{M}$  **3.4** incubated with  $277\ \text{nM}$  STS in buffer containing  $0.1\ \text{M}$  Tris-HCl,  $5\%$  DMSO,  $0.1\%$  Triton X-100 pH  $7.0$  in a  $200\ \mu\text{L}$  volume. Samples are diluted  $50$ -fold into a solution of the same buffer containing  $4\ \text{mM}$  4-MUS at  $0$ ,  $60$ ,  $540$ ,  $1200$ , and  $1500$  min. The sample is dialyzed into a  $1\ \text{L}$  buffer containing  $0.1\%$  Triton X-100  $0.1\ \text{M}$  Tris-HCl pH  $7.0$  every  $8\ \text{h}$  over a  $24\ \text{h}$  period beginning at time  $60$  min.

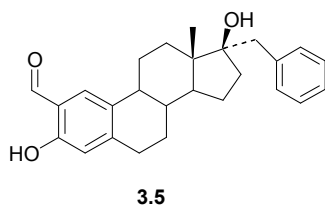
To determine whether compound **3.4** was labeling residues in the active site, a protection experiment was carried out with STS incubated with  $2.5$ ,  $5$ , and  $25\ \mu\text{M}$  of EP in  $0.1\ \text{M}$  Tris-HCl  $5\%$  DMSO pH  $7.0$ . The presence of EP, a competitive inhibitor of STS, protected the enzyme from inactivation by compound **3.4**. This protective effect increases with increasing

concentration of EP, suggesting that **3.4** must inactivate STS by reacting with an active site residue.

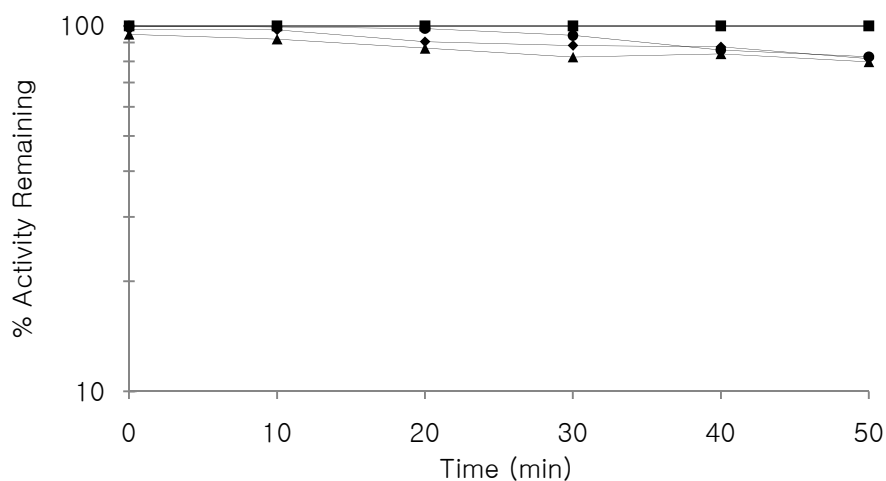


**Figure 3.6.** Time- and concentration-dependent inhibition of STS with 500 nM **3.4** in the presence varying amounts of EP at 0 (◆), 2.5 (△), 5 (◇), 25 (●) μM. A control was conducted in the absence of **3.4** and EP (■). Reactions were conducted in 0.1 M Tris-HCl, 5% DMSO 0.1 % Triton X-100 at pH 7.0 using 310 nM STS. STS activity was determined by adding 4-MUS to the reaction mixture such that the final concentration of 4-MUS was 4 mM and then the production of 4-MU followed using fluorimetry.

To determine if the inhibition was specific for the 4-position we examined compound **3.5** (Figure 3.6, prepared by Byoungmoo Kim in the Taylor group) for STS inhibition. This compound exhibited very little time- and concentration-dependent inhibition even at 10 μM (Figure 3.7). The  $IC_{50}$  for this compound was not determined due to solubility issues greater than 10 μM.



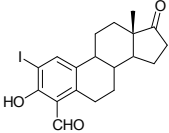
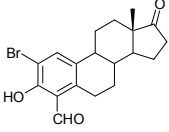
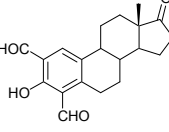
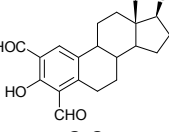
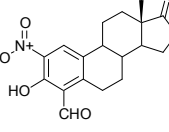
**Figure 3.7.** Structure of compound **3.5**.



**Figure 3.8.** Determination of time and concentration dependent inhibition of STS with compound **3.5**. Reactions were conducted as described in **Figure 3.3**. [inhibitor]=0.1(●), 1.0 (◆), 10  $\mu$ M (▲), control (■).

We also examined several other 4-formyl estrogen derivatives for STS inhibition that had previously been prepared by Yong Liu in the Taylor group. These 4-FE1 derivatives contained substituents at the 2-position and include the dialdehydes **3.8** and **3.9**. They were initially screened for time and concentration-dependent inhibition at 50  $\mu$ M. Surprisingly, none of these compounds exhibited time and concentration-dependent inhibition. The  $IC_{50}$ 's were determined for compounds **3.7-3.9** (compounds **3.6** and **3.10** were poorly soluble in the assay buffer at concentrations greater than 50  $\mu$ M) and found to be much greater than the  $K_i$  of 4-FE1 and compound **3.4**. Although this study is somewhat limited in scope, it suggests that substituents at the 2-position of 4-formyl estrogen derivatives have a detrimental effect on the binding of the inhibitor and the ability of the 2-formyl group to interact with a residue that results in time- and concentration dependent inhibition.

**Table 3.1.** Inhibition of STS with 2-substituted 4-FE1 Derivatives

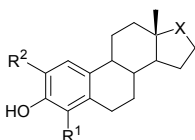
Compound	IC <sub>50</sub> (μM)
 3.6	ND
 3.7	145 ± 11
 3.8	224 ± 7
 3.9	157 ± 9
 3.10	ND

### 3.2.2 Reversible Inhibition of STS with 4-substituted estrogen derivatives

In addition to 4-formyl substituted estrogens, we also examined other 4-substituted estrogen derivatives as STS inhibitors which had been prepared in the Taylor group by Yong Liu. These compounds and the results consisting of their percent inhibition (at 50 μM) and/or their IC<sub>50</sub>'s are shown in **Table 3.2**. We reasoned that if a residue was forming a Schiff base with the aldehyde group of 4-FE1 then it might form a salt bridge with a carboxyl group at the 4-position and a potent reversible inhibitor might result. However, 4-carboxy estrone (**3.11**), was a very poor inhibitor. The 4-hydroxymethyl, 4-aminomethyl and 4-amino derivatives (**3.12-3.14**) were also poor inhibitors as was the 4-vinyl derivative (**3.15**). However, when we substituted the

4-position with a non-ionizable electron withdrawing group (compounds **3.16-3.20**) the potency of these compounds increased considerably especially for the E1 derivatives. The 4-NO<sub>2</sub> E1 derivative (**3.19**) exhibited the lowest IC<sub>50</sub> (2.4 μM) from amongst this group of compounds. 4-NO<sub>2</sub>-E2 (**3.20**) exhibited a similar IC<sub>50</sub>. The 2-nitro (**3.21**), 2,4-dinitro (**3.22**) and the 4-nitro-2-bromo derivatives (**3.23**) were all less potent than **3.19**. The 2,4-dibromo derivative **3.24** was a surprisingly good inhibitor and almost as good as compound **3.19**.

**Table 3.2.** Inhibition of STS with 4-substituted estrogen derivatives.



compound	R <sup>1</sup>	R <sup>2</sup>	X	% inhibition at 50 μM	IC <sub>50</sub> (μM)
E1	H	H	C=O	ND	51 ± 8
E2	H	H	CHOH	ND	11 ± 1
<b>3.11</b>	CO <sub>2</sub> H	H	C=O	35	286 ± 13
<b>3.12</b>	CH <sub>2</sub> OH	H	C=O	46	ND
<b>3.13</b>	CH <sub>2</sub> NH <sub>2</sub>	H	CHOH	4	ND
<b>3.14</b>	NH <sub>2</sub>	H	CHOH	43	ND
<b>3.15</b>	CH=CH <sub>2</sub>	H	C=O	45	ND
<b>3.16</b>	Br	H	C=O	84	4.8 ± 0.4
<b>3.17</b>	F	H	C=O	84	3.3 ± 0.2
<b>3.18</b>	CN	H	C=O	71	6.7 ± 0.3
<b>3.19</b>	NO <sub>2</sub>	H	C=O	98	2.4 ± 0.1
<b>3.20</b>	NO <sub>2</sub>	H	CHOH	ND	2.8 ± 0.2
<b>3.21</b>	H	NO <sub>2</sub>	C=O	ND	17 ± 1
<b>3.22</b>	NO <sub>2</sub>	NO <sub>2</sub>	C=O	ND	26 ± 1
<b>3.23</b>	NO <sub>2</sub>	Br	C=O	ND	9.5 ± 0.9
<b>3.24</b>	Br	Br	C=O	85	3.0 ± 0.1

Studying the mode of reversible inhibition can help reveal secondary binding sites which may elicit inhibitory effects. Here we briefly describe the modes of inhibition related to our project objectives. The first is competitive inhibition, in which the inhibitor binds directly to the active site. As such, competitive inhibitors have the effect of diminishing the initial velocity of the catalytic reaction, and consequently increasing  $K_m$  in the presence of the inhibitor. The same  $V_{max}$  however can still be achieved in the presence of excess substrates. Non-competitive inhibitors have identical affinity to the free enzyme and the enzyme-substrate complex, and bind at a secondary site. For this reason, they inhibit the enzyme by alternative mechanisms, and cannot be displaced by high substrate concentrations. Non-competitive inhibitors consequently reduce the overall  $V_{max}$  but  $K_m$  remains unchanged. In addition to these two types of inhibitors are mixed inhibitors, which can bind to both the active site and the secondary binding site (Copeland, 1996).

One way to study the modes of inhibition is by analyzing data using a Lineweaver-Burk Plot. While there are other graphical determination methods available, the Lineweaver Burk Plot, or double-reciprocal plot of the Michaelis-Menten equation, is one of the commonly used transformations to analyze modes of inhibition. In this plot, the y-axis represents  $1/\text{velocity}$  and the x-axis corresponds to the  $1/[\text{substrate}]$ . The y-intercept of these lines corresponds to the observed  $1/V_{max}$  and the x-intercept corresponds to  $-1/K_m$ . Typically, several experiments are conducted with various concentrations of substrate in the presence of different concentrations of inhibitors. The results are usually several lines which intersect at a particular point which reflect a particular inhibitor type. Depending on the mode of inhibition, the observed  $V_{max}$  and  $K_m$  are replotted accordingly on a Dixon Plot to obtain a  $K_i$  value for the inhibitor (Copeland, 1996).



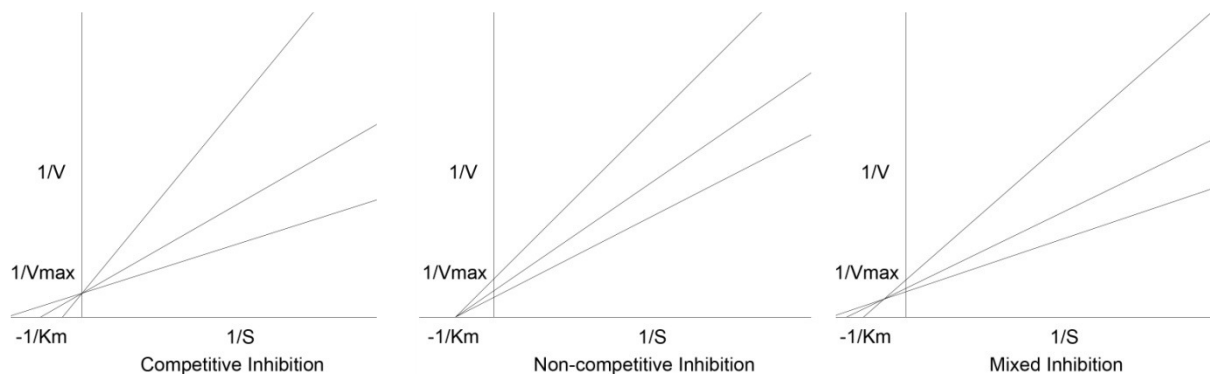


**Figure 3.9.** Lineweaver-Burk plot for competitive (A), non-competitive (B), and mixed inhibition (C) (Adapted from Copeland, 1996)

We investigated the mode of inhibition for compounds **3.19** (4-NO<sub>2</sub>E1), **3.16** (4-BrE1), and **3.20** (4-NO<sub>2</sub>E2) which were among the most potent ones listed in **Table 3.2**. All three compounds showed almost exclusively non-competitive inhibition (**Figures 3.9-3.11**). Replots of these graph to the corresponding Dixon-plot yielded non-competitive  $K_i$  for these compounds, and is displayed in **Table 3.3**. So it appears that these compounds inhibit STS by binding at a secondary site and inhibit via a different mechanism than regular competitive inhibitors. This is strong evidence suggesting the presence of a secondary binding site available to analogues of estrone, and estradiol, and potentially ES and EP.

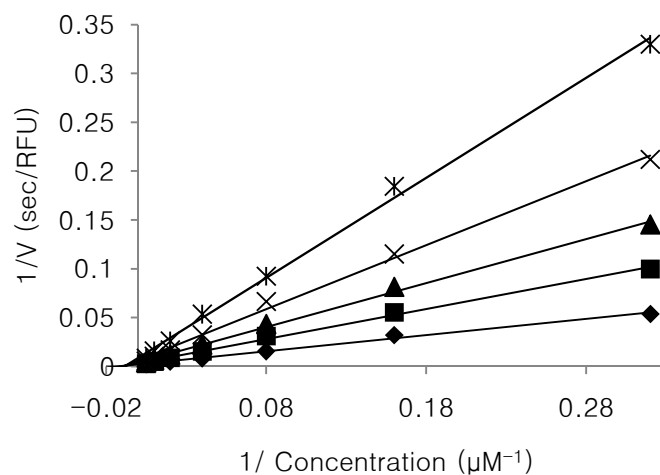


**Figure 3.10.** Lineweaver-Burk plot for **3.19**  $\blacklozenge$  0  $\mu\text{M}$   $\blacksquare$  0.5  $\mu\text{M}$   $\blacktriangle$  1  $\mu\text{M}$   $\times$  2  $\mu\text{M}$   $*$  4  $\mu\text{M}$

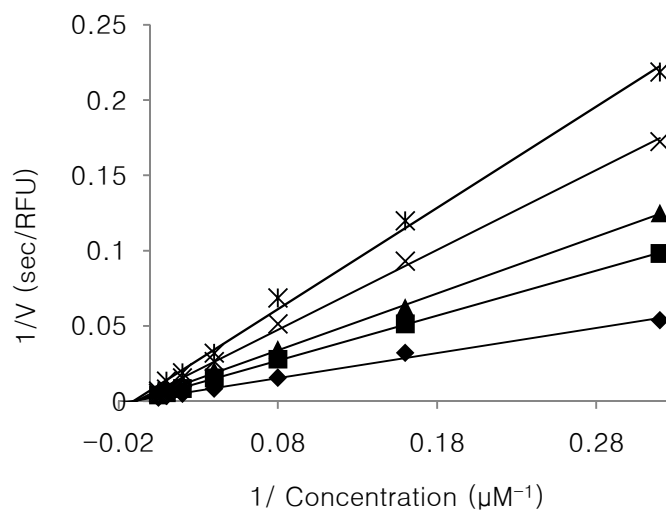


**Figure 3.11.** Lineweaver-Burk plot for **3.20**  $\blacklozenge$  0  $\mu\text{M}$   $\blacksquare$  0.5  $\mu\text{M}$   $\blacktriangle$  1  $\mu\text{M}$   $\times$  2  $\mu\text{M}$   $*$  4  $\mu\text{M}$

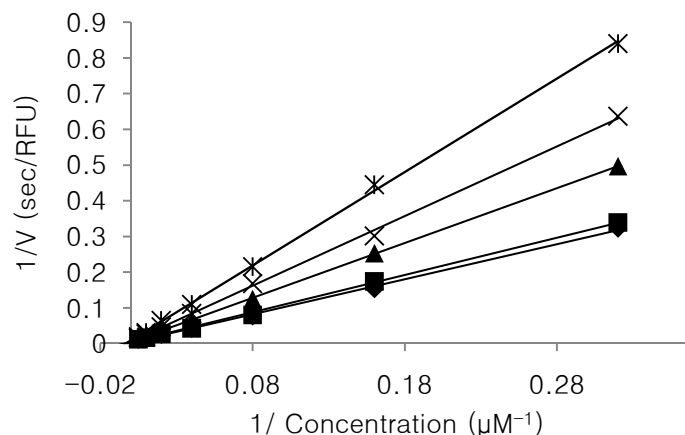


**Figure 3.12.** Lineweaver-Burk plot for **3.16** ◆ 0μM ■ 0.6125 μM ▲ 1.25 μM × 2.5 μM \* 5 μM

**Table 3.3.**  $K_i$ 's for compounds **3.19**, **3.20** and **3.24**

Compound	$K_i$ (μM)
<b>3.19</b>	1.4
<b>3.20</b>	1.8
<b>3.16</b>	2.5

If the above compounds are binding at a secondary site then the question remains as to where this second site is. The detergent  $\beta$ -*n*-octyl-D-glucopyranoside (**BOG**, **3.25**, **Figure 3.12**) is present during the crystallization of STS to help solubilize the enzyme (Hernandez-Guzman et al., 2001). It co-crystallizes with STS. It crystallizes in the tunnel formed by two transmembrane  $\alpha$ -helices, and on a secondary site on the surface of the enzyme (**Figure 3.13**). The hydrophobic chain of **BOG** inserts itself in the hydrophobic tunnel towards the active site, suggesting a possible orientation for the substrate as it enters the active site or the product as it exits STS. In vitro, the substrate may have access to this secondary binding site, which may be inhibitory, and result in the observed substrate inhibition at high concentration of substrate. It is also possible that inhibitors such as **3.19** also bind at this site.

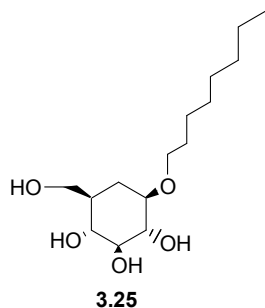


**Figure 3.13.** Structure of BOG

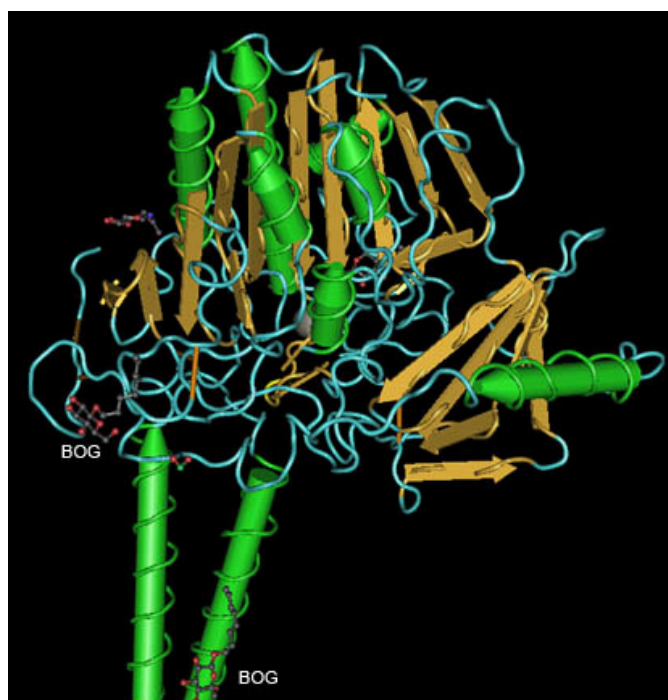


**Figure 3.14.** Crystal structure of STS showing the location of bound BOG (Hernandez-Guzman et al., 2003).

### 3.3 Conclusion and Future Work

We have shown that the inhibition of STS with 4-formyl estrogen derivatives can be enhanced, in terms of binding affinity, by introducing a hydrophobic benzyl group at the 17-position of 4-FE1. As with 4-FE1, the inhibition is still concentration and time-dependent. Future studies with these compounds will include determining if 4-FE1 and **3.4** are inhibiting STS by forming a Schiff base with a lysine or arginine residue. These studies will involve

subjecting the inactivated enzyme to a reducing agent such as NaCNBH<sub>3</sub> to reduce the imine (if formed) to a stable amine, followed by deglycosylation of the enzyme, enzymatic digestion and MS analysis of the resulting fragments.

Preliminary studies suggest that introducing substituents at the 2-position of 4-formyl estrogen derivatives results in loss of concentration and time-dependent inhibition and a considerable decrease in inhibitor affinity. Studies with estrogen derivatives substituted at the 4-position with groups other than a formyl revealed that a good reversible inhibitor can be obtained simply by introducing an electron withdrawing group at this position (such as 4-nitroestrone). However, these types of inhibitors are non-competitive inhibitors suggesting an alternative steroid binding site. These compounds will be used as lead compounds for the design of future inhibitors for STS. Preparing estrogens bearing substituents at both the 17- and 4-positions could lead to highly potent inhibitors.

### **3.4 Experimental**

#### **3.4.1 Materials**

Materials were the same as described in section 2.4.1 chapter 2.

#### **3.4.2 IC<sub>50</sub> determinations**

20 µL of the inhibitor solutions of various concentrations of inhibitor in (1:1) DMSO/0.1 M Tris-HCl pH 7.0 were added to the wells of a 96-well microtiter plate containing 160 µL of a 2 mM 4-MUS solution in 0.1 M Tris-HCl, pH 7.0. The reaction is initiated by the addition of 20 µL of 80 nM STS in 20 mM Tris-HCl, pH 7.4, 0.1% Triton X-100 into to the well, yielding a final concentration of 8 nM STS, 200 µM 4-MUS in 0.1M Tris-HCl, pH 7.0, 0.01% Triton X-100, and 5% DMSO. STS activity was measured by monitoring the production of 4-MU by fluorescence for 10 minutes as described in section 2.4.3 in chapter 2. The activity of

STS in the presence of inhibitor was compared to the activity of STS in the absence of inhibitor, and a percent activity was calculated. This percent activity was plotted on a semi log graph against the log concentration of the inhibitor, and fitted in Grafit from Erithacus Software (Surrey, U.K.) using the equation:  $V_i = V_o/[1+([I]/IC_{50})^s] + B$  where  $V_i$  = initial rate of reaction at inhibitor concentration  $[I]$ ;  $V_o$  = velocity in the absence of inhibitor;  $B$  = background activity;  $s$  = slope factor. All reactions were performed in triplicate.

### **3.4.3 $K_i$ determination**

Various solutions of inhibitors **3.19**, **3.20**, and **3.24** were prepared in DMSO/0.1M Tris-HCl pH 7.0 (1:1). 20  $\mu$ L of these solutions were added to the wells of a black 96-well microtiter containing 160  $\mu$ L of varying concentrations of 4-MUS ranging from 0-222.2  $\mu$ M. The reaction is initiated by the addition of 20  $\mu$ L of 80 nM STS in buffer containing 20 mM Tris-HCl 0.1% Triton X-100 pH 7.0. STS activity was monitored as described previously. A positive control was done in a similar manner, with the exception of adding STS and replacing the volume with 20  $\mu$ L of 20mM Tris-HCl, 0.1% Triton X-100, pH 7.0. The initial rates of the reaction obtained as relative fluorescent units over time (RFU/sec) for each 4-MUS concentration are plotted as a Lineweaver-Burk graph using Excel 2007. The slopes and intercepts of the Lineweaver-Burk plots are replotted based on the equations for mixed or competitive inhibition to obtain the desired  $K_i$  values. All reactions were performed in triplicate.

### **3.4.4 Determination of time and concentration dependent inhibition of STS with 3.4.**

Stock solutions of compound **3.4** were prepared in DMSO/0.1M Tris-HCl pH 7.0 (1:1). 20  $\mu$ L of these samples were added to an Eppendorf tube containing 160  $\mu$ L of 0.1M Tris-HCl pH 7.0 and 20  $\mu$ L of 3.1  $\mu$ M STS in 20 mM Tris-HCl, 0.1% Triton X-100 pH 7.4. 4  $\mu$ L aliquots were withdrawn every 10 minutes and added to a well containing 196  $\mu$ L of 4 mM 4-MUS in 0.1

M Tris-HCl pH 7.0. This was repeated in triplicate. STS activity was determined as described above. A similar procedure was carried out for a control which contained 20  $\mu\text{L}$  of DMSO/0.1 M Tris-HCl pH 7.0 (1:1) in place of the inhibitor solutions. The production of 4-MU was followed as described above. The percent activity remaining as a function of time was plotted as a semilog graph. The slopes of these plots, which represent the pseudo-first order rate constants ( $k_{\text{obs}}$ ), were used to generate a Kitz-Wilson double reciprocal plot. A linear regression model was used to calculate the inhibition constant,  $K_I$  (-1/x-intercept) and  $k_{\text{inact}}$  (1/y-intercept).

### **3.4.5 Time and concentration-dependent inhibition of STS in the presence of estrone phosphate (EP) (protection experiments)**

Protection experiments with EP were carried out in the same procedures as above for time and concentration-dependent inhibition of compounds **3.4**, with the exception of varying concentration of EP (2.5, 5, and 25 $\mu\text{M}$ ). The concentration of **3.4** was 500 nM.

### **3.4.6 Dialysis Experiment**

A 200  $\mu\text{L}$  solution containing 1  $\mu\text{M}$  of **3.4** and 277 nM STS in 0.1M Tris-HCl, 5% DMSO, 0.1 % Triton X-100, pH 7.0 was incubated for 60 minutes at room temperature. 4  $\mu\text{L}$  aliquots were withdrawn at  $t = 0$  and  $t = 60$  min and added to the wells of a 96-well microtiter plate containing 196  $\mu\text{L}$  of 4 mM 4-MUS. STS activity is monitored as described previously. This was performed in triplicate. The remaining 176  $\mu\text{L}$  was transferred to a dialysis bag and dialyzed against 1 L buffer containing 0.1 M Tris-HCl pH 7.0, 0.1% Triton X-100. 4  $\mu\text{L}$  aliquots were withdrawn at 540, 1020, and 1500 min and STS activity was determined as described above. After withdrawing aliquots at 540 and 1020 minutes the dialysis buffer was changed. A control was performed in an identical manner except no inhibitor was present.

## Chapter 4 – Photoaffinity Labeling to Reveal Mode of Substrate and Product Transport in STS

### 4.1 Introduction

#### 4.1.1 Photoaffinity labeling

In Chapter 1 we mentioned that it is not yet known how STS substrates enter the active site (see section 1.2.3). The substrate could enter via a tunnel between the two antiparallel hydrophobic  $\alpha$ -helices. Alternatively, the tunnel could also serve as an exit for the product. An alternative mode of entry to the active site is for the substrate to enter from the lumen side via three flexible loops surrounding the active site. In order for this to occur, the sulfated substrate must first be transported through the ERit membrane via a specific transporter into the lumen of the ERit. One technique that may allow us to learn more about substrate entry and product release in STS is photoaffinity labeling.

Photoaffinity labeling (PAL) is a labeling procedure which can be used to gain insight on ligand-protein interaction, such as drug-protein or substrate-protein interactions, otherwise not possible with regular protein identification and characterization techniques. In brief, PAL involves a ligand containing a photosensitive group which is able to form a non-covalent interaction with its receptor. As such, majority of photoaffinity labels are derivatives of natural substrates. When activated by UV irradiation, the ligand breaks down to form a reactive intermediate which reacts to form a covalent bond with residues near the binding site. The covalently linked ligand-receptor complex formed by PAL allows for vigorous downstream applications such SDS-PAGE, protein digests, HPLC, and mass spectrometry (Robinette et al., 2006) (**Figure 4.1**). These techniques, in particular mass spectrometry, when combined with PAL can reveal secondary binding sites and mode of substrate-protein interactions. Amongst



other cross linking methods, PAL remains attractive due to its formation of highly reactive intermediates, capable of virtually reacting with any residues in proximity (Robinette et al., 2006). In addition, PAL has been successful in the past to label various binding sites on proteins, including the estrogen receptor (Payne et al., 1980).

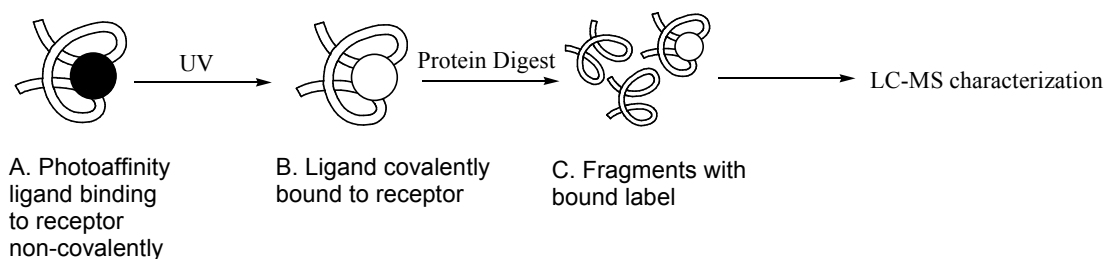
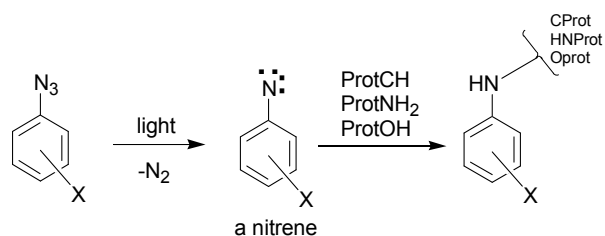


**Figure 4.1.** The photolabelled ligand is covalently linked by UV irradiation to the binding site on the enzyme. The digestion of the labeled protein followed by MS allows for the identification of the labeled amino acids (Robinette et al., 2006)

#### 4.1.2 Photoaffinity Probes

The choice of a photoaffinity probe depends on the compatibility with the ligand and receptor in question. Ideally, the photo label should have a lifespan under UV irradiation that is short enough so the covalent linkage can occur before the dissociation of the ligand-protein complex, but also long enough so that sufficiently covalent bonding is able to occur. In addition, it should be able to attack C-H and X-H bonds at wavelengths that do not cause extensive photolytic damage to the protein. The three main types of photoactivating groups commonly used in PAL are the benzophenone groups, diazirines, and azido. Photolysis of these groups generally produces highly reactive carbenes and nitrenes. A general reaction scheme for an azido group is shown in **scheme 4.1**. These intermediates are highly reactive electrophiles capable of reacting with double bonds and heteroatoms with lone pairs such as nitrogen, oxygen, and sulfur. However, their star role in PAL is due to their ability to attack inert aliphatic C-H

bonds, allowing them to react with almost all functional groups found in proteins (Robinette et al., 2006).



**Scheme 4.1.** General mechanism for photoaffinity labeling of proteins with aryl azides

The objective of the work described in this chapter is to evaluate compounds **4.1-4.5** (**Figure 4.2**) as photoaffinity labels of STS. Should any of these compounds prove to be photoaffinity labels of STS then, by identifying which residues are being modified by these labels, we will be able to learn more about substrate entry and product release in STS.

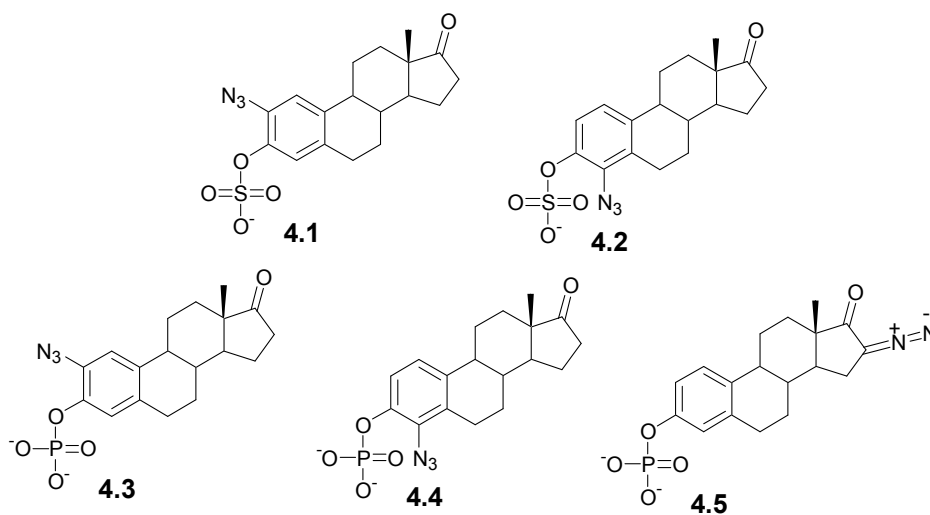


**Figure 4.2.** Proposed PAL's for STS.

## 4.2 Results and Discussion

### 4.2.1 Studies with compounds 4.1 and 4.2

We initially focused our attention on phenyl azides **4.1** and **4.2** which were synthesized by Christine Nicolas in the Taylor group. We initially chose these compounds since it is known that phenylazides can be photolyzed under mild conditions (wavelengths between 300-350 nm are often employed [Payne et al., 1980]). However, we did not know what affect irradiating STS at wavelengths between 300-350 nm would have on its activity. To determine this a solution of STS in 0.1M Tris-HCl, 0.01% Triton X-100, 5% DMSO, pH 7.0 was irradiated at room lighting (control), 300 nm and 350 nm over 25 minutes (**Figure 4.3**) using a Rayonet Photochemical Reactor (Southern New England Ultraviolet). At 300 nm irradiation, almost 45% of enzyme activity is lost over 25 minutes which is considerable. The loss of activity at 350 nm was about 15%, which is reasonably acceptable and thus selected as the irradiation wavelength for the PAL experiments.

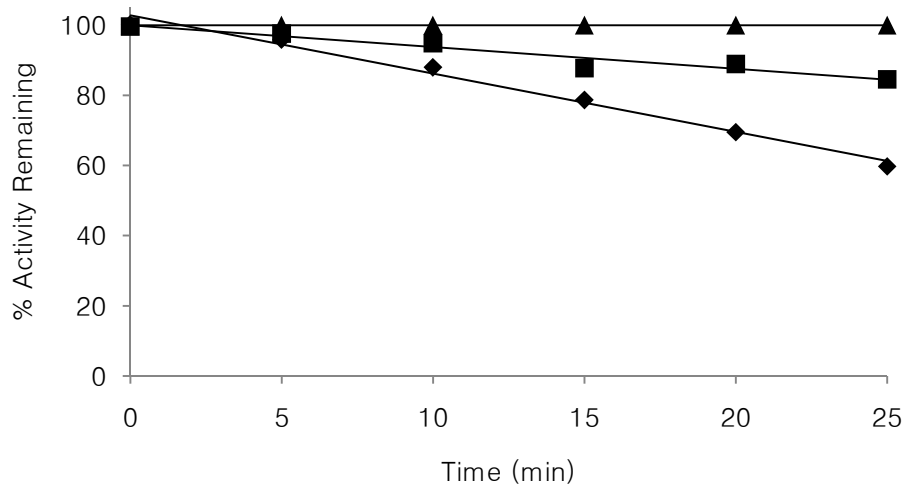


**Figure 4.3.** Effect of irradiation at 300 or 350 nm on the activity of STS. 300 nm (◆) 350 nm (■) and no irradiation (▲)

The next step was to determine if **4.1** and **4.2** breakdown within a reasonable amount of time (30 min) upon irradiation at 350 nm. Thus, estrone sulfate (ES), **4.1** and **4.2** were irradiated at 350 nm and their absorbance spectrum was obtained every 5 minutes over a 20 minute period (**Figure 4.4-4.6**). **4.1** and **4.2** exhibit absorbance maxima at around 250-260 nm (**Figures 4.4 and 4.5**). Although neither of these compounds absorb at 350 nm there was a significant change in their absorbance spectrum upon irradiation at 350 nm over the 20 minute time period suggesting that breakdown of the azide was occurring. The spectrum of ES did not change upon irradiation at 350 nm (**Figure 4.5**).

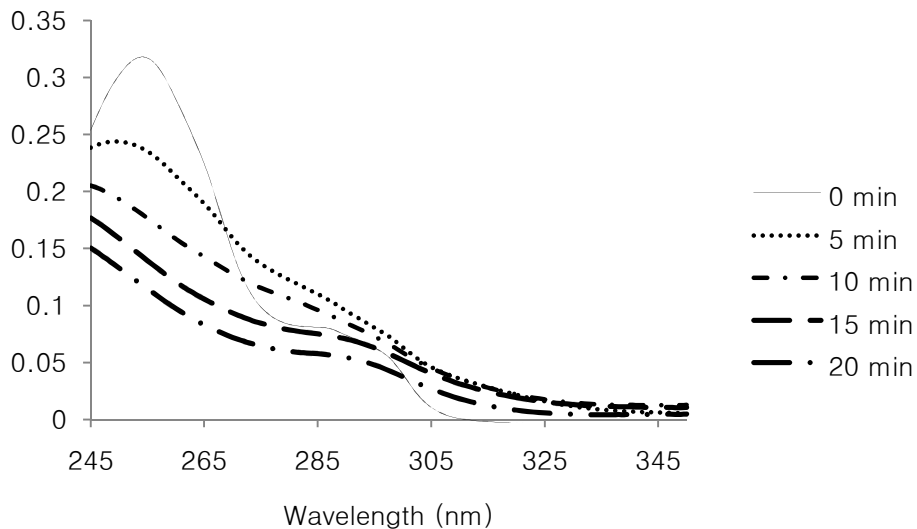


**Figure 4.4.** Absorbance spectra of a 30  $\mu$ M solution of **4.1** in 0.1M Tris-HCl, 0.01% Triton X-100, 5% DMSO, pH 7.0 at 350 nm for 0, 5, 10, 15, 20 and 25 min.

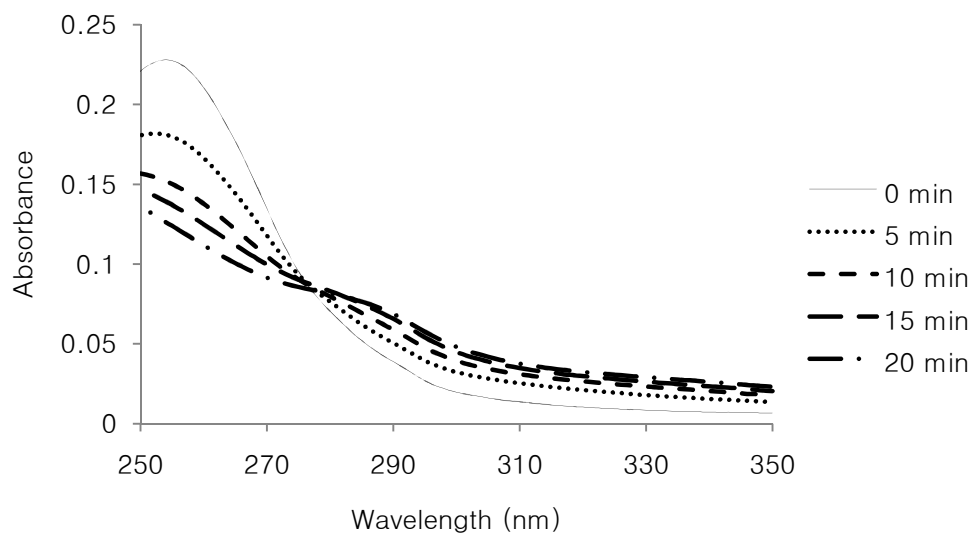


**Figure 4.5.** Absorbance spectra of a 30  $\mu$ M solution of **4.2** in 0.1M Tris-HCl, 0.01% Triton X-100, 5% DMSO, pH 7.0 at 350 nm for 0, 5, 10, 15, 20 and 25 min.

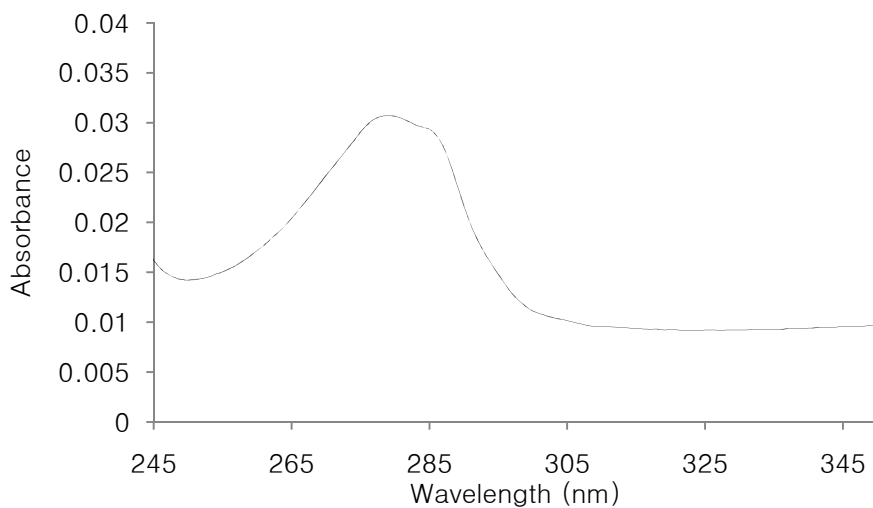


**Figure 4.6.** Absorbance spectra of 50 $\mu$ M ES in 0.1 M Tris-HCl, 0.01% Triton X-100, 5% DMSO, pH 7.0

One potential complication of using **4.1** and **4.2** as PAL's for STS is that they are potential STS substrates. Upon treatment with STS **4.1** and **4.2** could produce 2- (**4.6**) and 4-

azidoestrone (**4.7**) which could also act as photolabels of STS (**Figure 4.7**). Indeed, compound **4.7** has been used by Payne et al as a PAL for the estrogen receptor (Payne et al., 1980).

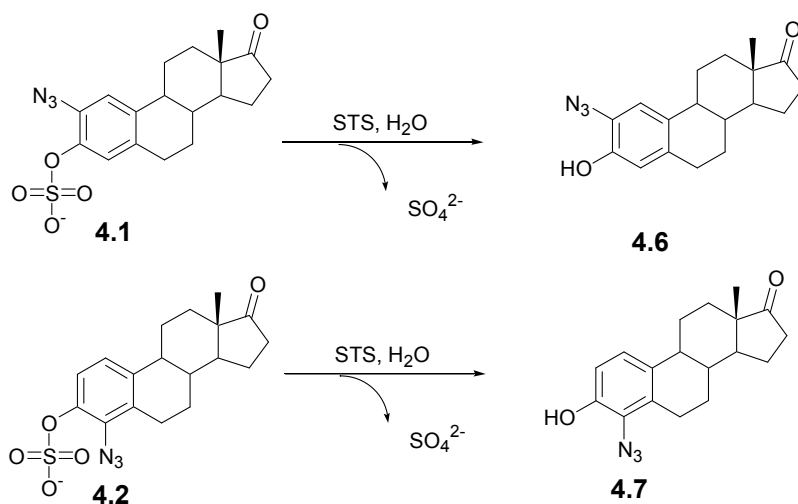


**Figure 4.7.** Products (**4.6** and **4.7**) resulting from the STS-catalyzed hydrolysis of **4.1**, and **4.2**.

Compounds **4.6** and **4.7** were prepared in the Taylor lab by Christine Nicolas. Compound **4.6** was readily soluble in our assay buffer. Its absorbance spectrum was obtained and one of its absorption maxima is at 299 nm (**Figure 4.8**). We also found that its spectrum undergoes considerable changes upon irradiation at 350 nm (**Figure 4.8**). Compound **4.7** did not dissolve at all in our assay buffer and we had to obtain its spectrum in pure ethanol. Nevertheless, **4.7** appears to also absorb strongly at around 295 nm and there was an observable change in the spectrum upon irradiation at 350 nm (**Figure 4.9**).

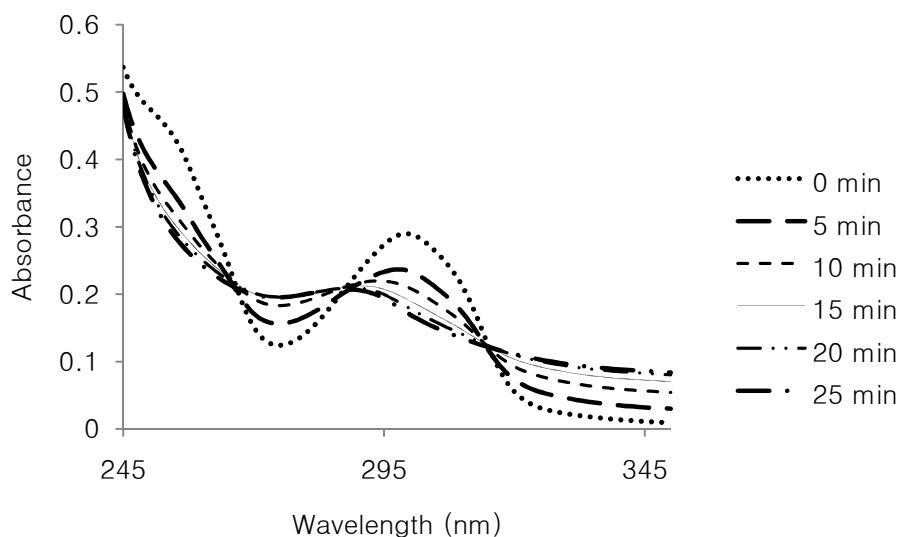


**Figure 4.8.** Absorbance spectra of a 50  $\mu$ M solution of **4.6** in 0.1M Tris-HCl, 0.01% Triton X-100, 5% DMSO, pH 7.0 after irradiation at 350 nm for 0, 5, 10, 15, 20 and 25 min.

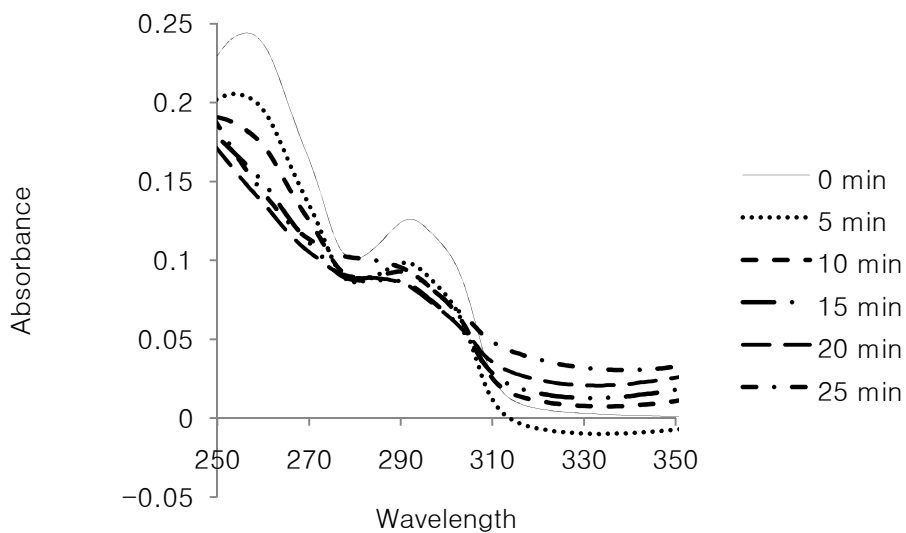


**Figure 4.9.** Absorbance spectra of a 50  $\mu$ M solution of **4.7** in ethanol after irradiation at 350 nm for 0, 5, 10, 15, 20 and 25 min

To find out if **4.1** and **4.2** were substrates for STS, we incubated 50  $\mu$ M **4.1** and **4.2** with 55 nM of STS in buffer containing 0.1 M Tris-HCl, 0.01 % Triton X-100, 5% DMSO at pH 7.0. Controls were also carried out for **4.1**, **4.2**, **4.3**, and **4.4** in the absence of STS in the same buffer.

After 25 minutes, 20  $\mu\text{L}$  of each sample were injected into HPLC and their HPLC chromatograms obtained (**Figures 4.10** and **4.11**). The samples were monitored at 255 nm, corresponding to the  $\lambda_{\text{max}}$  of **4.1** and **4.2**, (**Figure 4.10**) and 299 nm corresponding to the  $\lambda_{\text{max}}$  of **4.6** and one of the peaks of **4.7** (**Figure 4.11**). After 25 minutes, almost all of **4.1** was consumed. In contrast, almost none of **4.2** was consumed. So it appears that **4.1** is a substrate for STS while **4.2** is not.

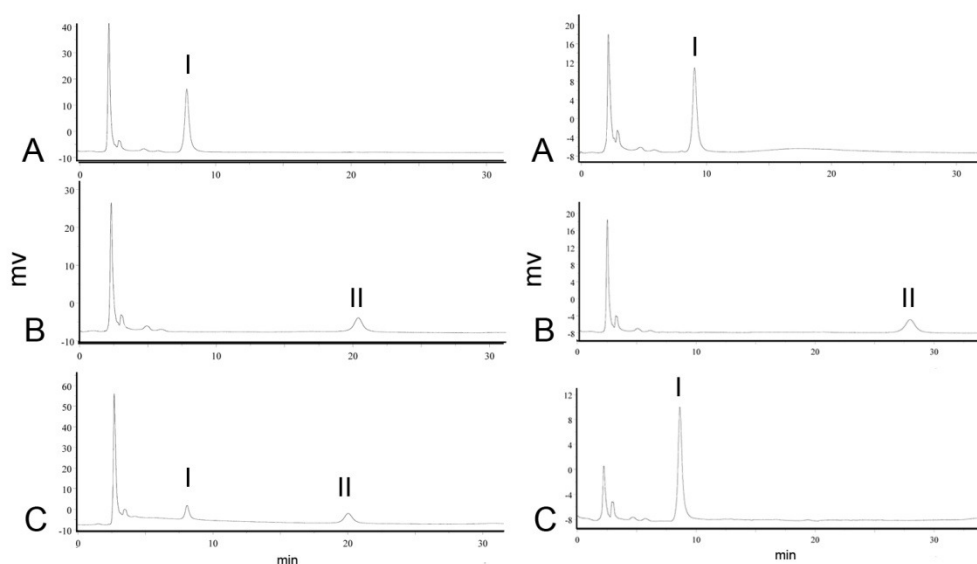


**Figure 4.10.** HPLC chromatograms for **A**) 50  $\mu\text{M}$  **4.1** (left) or **4.2** (right) **B**) 50  $\mu\text{M}$  **4.6** (left) or **4.7** (right) **C**) 55 nM STS with 50  $\mu\text{M}$  **4.1** (left) or **4.2** (right) after 25 minutes. All solutions consisted of compound in 0.1 M Tris-HCl, 0.01 % Triton X-100, 5% DMSO, pH 7.0 prior to injection into the HPLC. Chromatograms were recorded at 255 nm.



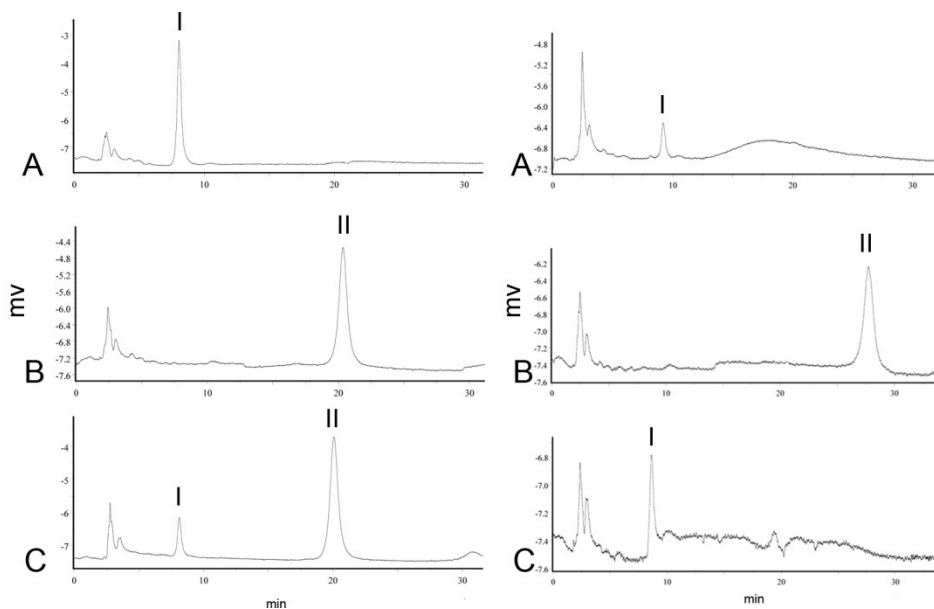


**Figure 4.11.** HPLC chromatograms for **A**) 50  $\mu\text{M}$  **4.1** (left) or **4.2** (right) **B**) 50  $\mu\text{M}$  **4.6** (left) or **4.7** (right) **C**) 55 nM STS with 50  $\mu\text{M}$  **4.1** (left) or **4.2** (right) after 25 minutes. All solutions consisted of compound in 0.1 M Tris-HCl, 0.01 % Triton X-100, 5% DMSO, pH 7.0 prior to injection into the HPLC. Chromatograms were recorded at 299 nm.

Although compound **4.2** is not an STS substrate, we did find that it is a good STS inhibitor exhibiting an  $\text{IC}_{50}$  of  $7.4 \pm 0.4 \mu\text{M}$ . A more detailed analysis revealed that this compound exhibits mixed non-competitive inhibition (**Figure 4.12**) with a  $K_i$  of  $8.3 \mu\text{M}$  and  $\alpha K_i$  of  $19.5 \mu\text{M}$ . So this compound binds to STS but is not a substrate. It is not surprising that this compound exhibits mixed non-competitive inhibition since we demonstrated in Chapter 3 that estrogen derivatives bearing substituents at the 4-position were noncompetitive STS inhibitors. We also found that the  $\text{IC}_{50}$  for compound **4.1** ( $\text{IC}_{50} = 8.3 \pm 0.2 \mu\text{M}$ ) is very similar to that of compound **4.2**. Compound **4.1** exhibits mainly competitive inhibition with a  $K_i$  of approximately  $5.5 \mu\text{M}$  (**Figure 4.13**) which is consistent with it being a good STS substrate. However, the fact that it is a substrate for STS means that the  $\text{IC}_{50}$  and  $K_i$  values that we have reported for **4.1** must

be regarded with caution since its concentration would be changing (due to STS-catalyzed hydrolysis) during the course of the inhibition experiments.

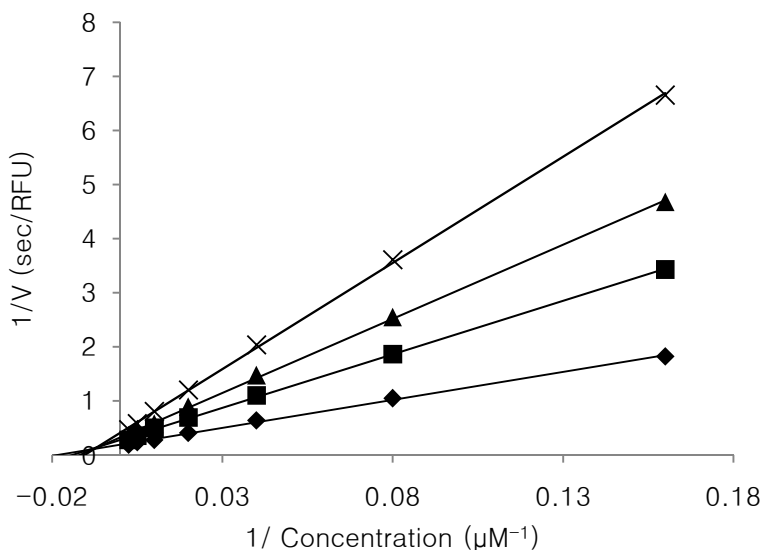


**Figure 4.12.** Lineweaver-Burk plot for **4.2** ◆ 0 $\mu\text{M}$  ■ 5  $\mu\text{M}$  ▲ 10  $\mu\text{M}$  × 20  $\mu\text{M}$

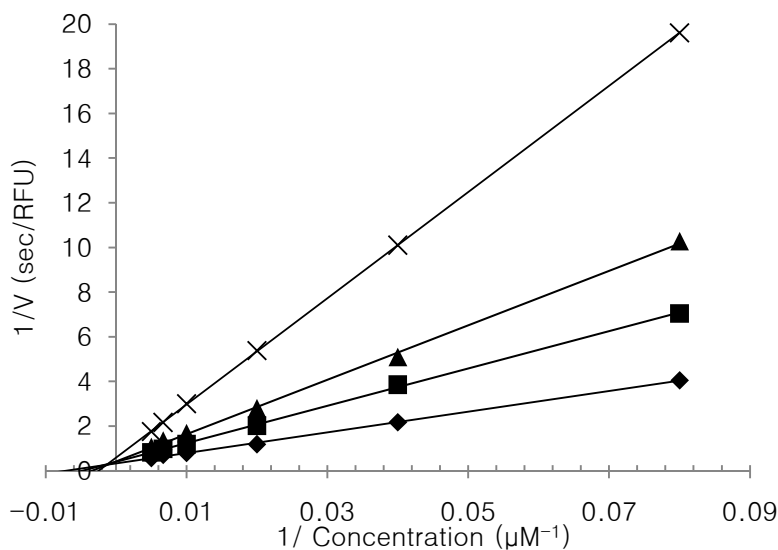


**Figure 4.13.** Lineweaver-Burk plot for **4.1**. 0 $\mu\text{M}$  (◆), 2.5  $\mu\text{M}$  (■), ▲ 5  $\mu\text{M}$  × 10  $\mu\text{M}$

Before examining **4.1** and **4.2**, as well as **4.6** and **4.7** as PAL's, we determined whether these compounds would exhibit time-dependent inhibition of STS in the absence of irradiation at

350 nm. 10  $\mu$ M (compound **4.7**) or 50  $\mu$ M (compounds **4.1**, **4.2** and **4.6**) of these compounds was incubated with STS in buffer containing 0.1M Tris-HCl 5% DMSO pH 7.0, aliquots were removed at various time intervals and added to a 2mM solution of 4-MUS in the same buffer and the activity of the enzyme determined. We did not observe any time-dependent inhibition over 25 minutes as shown in **Figure 4.14**.

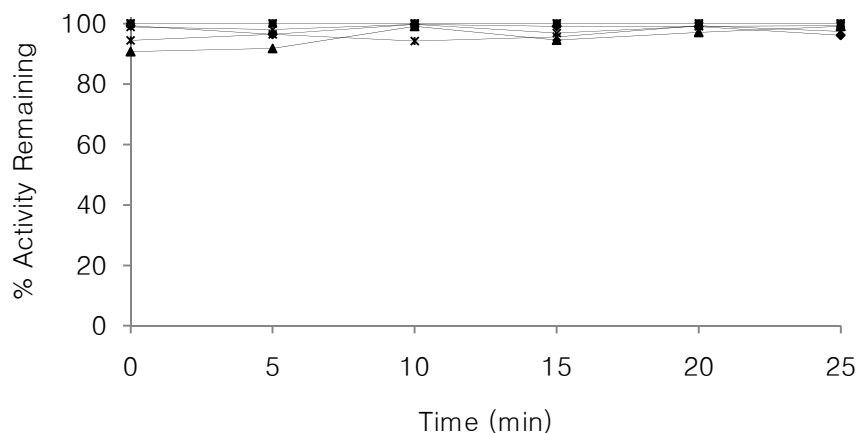


**Figure 4.14.** Percent STS activity recovered versus time upon a ten-fold dilution of a solution of STS containing no photoaffinity label (■), 50  $\mu$ M **4.1** (◆), 50  $\mu$ M **4.2** (▲), 50  $\mu$ M **4.6** (×) or 10  $\mu$ M **4.7** (\*) into a solution of 2 mM 4-MUS. All solutions contained 0.1 M Tris-HCl, 5% DMSO at pH 7.0.

Preliminary photoaffinity labeling experiments were carried out using varying concentrations of **4.1** and **4.2** ranging from 0-100  $\mu$ M over 20 minutes with 30 nm STS to determine an ideal concentration of photoaffinity label to use. The compounds were incubated with STS in buffer and the solution irradiated at 350 nm. An aliquot was withdrawn every 5 minutes and transferred to a solution containing 2 mM of 4-MUS and STS activity was determined in the usual manner. Both compounds exhibited time- and concentration-dependent inhibition when irradiated at 350nm (**Figure 4.15** and **4.16**). In both cases, we observe that 50  $\mu$ M of photoaffinity label is sufficient for our desired PAL experiments.

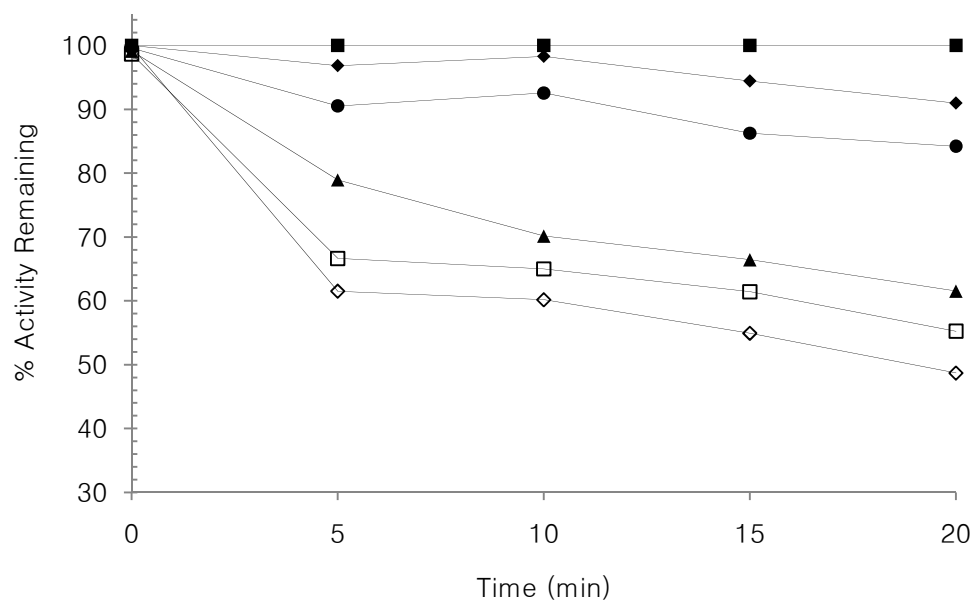


**Figure 4.15.** Percent STS activity remaining versus time in the absence of **4.1** with no irradiation (■) and upon irradiation at 350 nm in the presence of 5(◆), 10(●), 25 (▲), 50 (□) and 100 (◇) μM **4.1** in 0.1M Tris-HCl, 2% DMSO, pH 7.0. STS activity was determined by diluting the mixtures ten-fold into a solution containing 2 mM 4-MUS and following the production of MU as described in the experimental section. Activity loss due to the effect of 350 nM radiation on STS alone (see **Figure 4.3**) has been subtracted from the data.

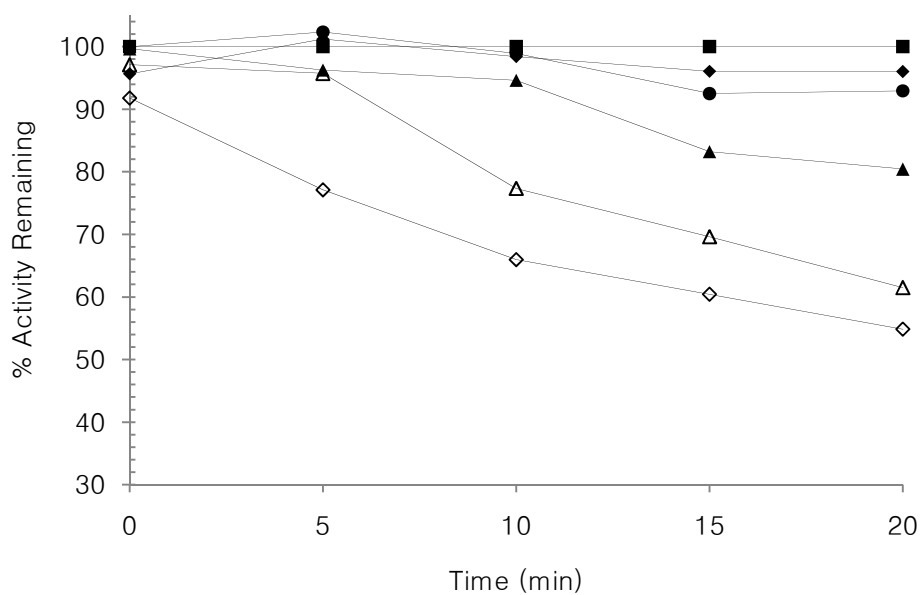


**Figure 4.16.** Percent STS activity remaining versus time in the absence of **4.2** with no irradiation (■) and upon irradiation at 350 nm in the presence of 5(◆), 10(●), 25 (▲), 50 (△) and 100 (◇)  $\mu\text{M}$  **4.2** in 0.1M Tris-HCl, 2% DMSO, pH 7.0. STS activity was determined by diluting the mixtures ten-fold into a solution containing 2 mM 4-MUS and following the production of MU as described in the experimental section. Activity loss due to the effect of 350 nM radiation on STS alone (see **Figure 4.3**) has been subtracted from the data.

Photoaffinity of **4.1** and **4.2** with the above procedures produced very desirable results.

We observe that for both compounds, the inhibition generally plateaus after 20 minutes. This is likely due to the complete breakdown of the photoaffinity label in solution. We also note that **4.1** exhibits a sharper decline in activity compared to that of **4.2**, which exhibits an initial lag phase. Overall, both **4.1** and **4.2** appear to be effective photoaffinity labels, with **4.1** only being slightly better. We also examined the effect of DMSO on their ability to label STS by repeating the above experiments using 5% instead of 2% DMSO. Increasing the DMSO from 2 to 5% had little or no effect on the ability of these compounds to label STS (**Figure 4.17**).

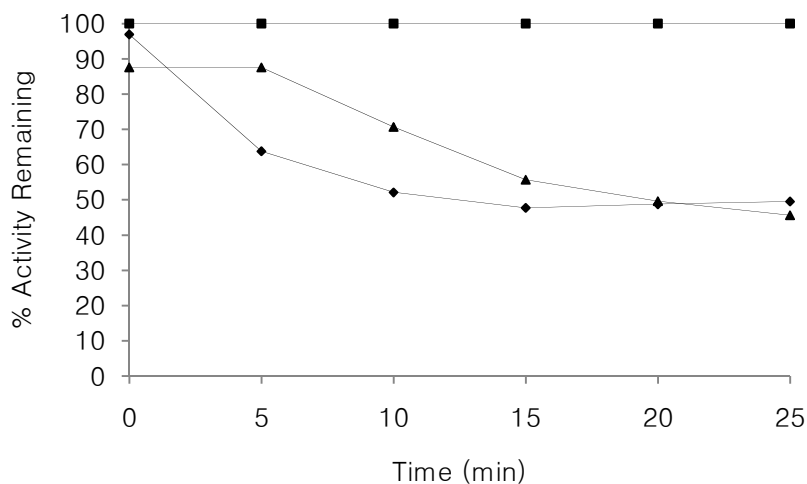


**Figure 4.17.** Percent STS activity remaining versus time in the absence of **4.1** and **4.2** with no irradiation (■), and in the presence of 50  $\mu\text{M}$  (◆) **4.1** or 50  $\mu\text{M}$  (▲) **4.2** in 0.1M Tris-HCl, 5% DMSO, pH 7.0. STS activity was determined by diluting the mixtures ten-fold into a solution containing 2 mM 4-MUS and following the production of MU as described in the experimental section. Activity loss due to the effect of 350 nM radiation on STS alone (see **Figure 4.3**) has been subtracted from the data.

One complicating issue when using **4.1** and **4.2** as photoaffinity labels is that the STS hydrolysis products **4.6** and **4.7** can also potentially act as photoaffinity labels. This is not a major problem with **4.2** since it does not appear to be a good substrate. However, **4.1** is a good substrate and is certainly being hydrolyzed under the conditions of the PAL experiment. Therefore we checked whether **4.6** and **4.7** could act as photoaffinity labels of STS. While we were able to solubilize **4.6** at 50  $\mu\text{M}$ , we were unable to do so for **4.7** at concentrations greater than 10  $\mu\text{M}$ . The data in **Figure 4.18** reveal that **4.6** is a good photoaffinity label for STS. Compound **4.7** also appears (**Figure 4.19**) to be capable of labeling STS though the loss of activity is very small but this could be due to the fact that we are using a much lower concentration of label compared to what was used for our studies with **4.1**, **4.2** and **4.6**. Thus using **4.1** as a photoaffinity label is not ideal since labeling by the desulfated product can also occur and it is very possible that the loss of activity we observe with **4.1** (**Figure 4.16**) may be completely due to labeling by **4.6**. However, since **4.3** labels STS fairly well and is not a good substrate it could be a promising photoaffinity label for STS. One drawback of **4.3** is that it begins to experience solubility problems above 50 $\mu\text{M}$ , and hence can only be used as photoaffinity labels below this concentration.

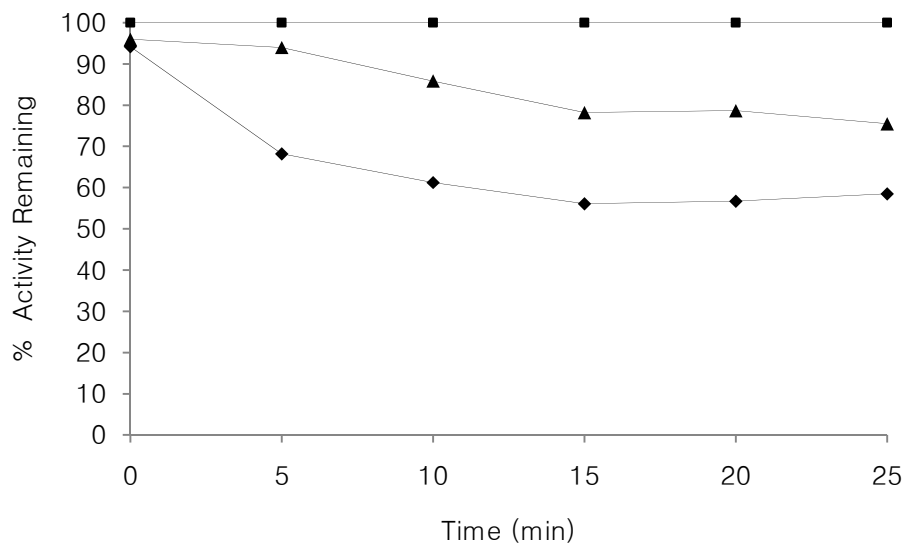


**Figure 4.18.** Percent STS activity remaining versus time in the absence of **4.6** and **4.7** with no irradiation (■) and upon irradiation at 350 nm and in the presence of 50 μM **4.6** (◆) or 10 μM **4.7** (▲) in 0.1M Tris-HCl, 5% DMSO, pH 7.0. STS activity was determined by diluting the mixtures ten-fold into a solution containing 2 mM 4-MUS and following the production of MU as described in the experimental section. Activity loss due to the effect of 350 nm radiation on STS alone (see **Figure 4.3**) has been subtracted from the data obtained from radiated solutions.

#### 4.2.2 Studies with compounds 4.3-4.5

One way to avoid the problem of the STS-catalyzed hydrolysis of the photoaffinity labels is to use photoaffinity labels that are based on an STS inhibitor instead of an STS substrate. Estrone-3-phosphate (EP, the phosphate analog of the natural STS substrate, ES) is a well-known inhibitor of STS with a  $K_i$  of 0.4 μM at pH 7.0 (Li et al., 1995).; Therefore we decided to examine compounds **4.3-4.5** as PAL's for STS (**Figure 4.2**). These compounds should bind (non-covalently) to STS at least as well as **4.1** and **4.2** and they should be more soluble in solution due to the phosphate group. Unlike compounds **4.1-4.4**, diazoketone **4.5** should inactivate STS by forming a reactive carbene (not a nitrene) upon irradiation. Carbenes are highly reactive compounds that can insert into C-H bonds. Compound **4.5** is very similar to compound **4.8** (**Figure 4.19**) which has been used for photoaffinity labeling of the estrogen

receptor (Payne et al., 1980). Compounds **4.3-4.5** and **4.8** were prepared by Professor Scott Taylor.

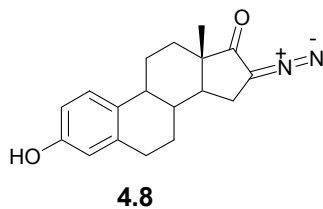


**Figure 4.19.** Structure of compound **4.8**.

As with the first generation of photoaffinity labels, we carried out experiments to check whether EP and **4.3-4.5** break down upon irradiation at 350 nm (Figures **4.20-4.23**). Compounds **4.3-4.5** exhibit significant changes in their absorbance spectra upon irradiation at 350 nm suggesting that structural changes are indeed occurring upon irradiation (Figures **4.20-4.22**). The spectrum of EP did not change upon irradiation at 350 nm (**Figure 4.23**).

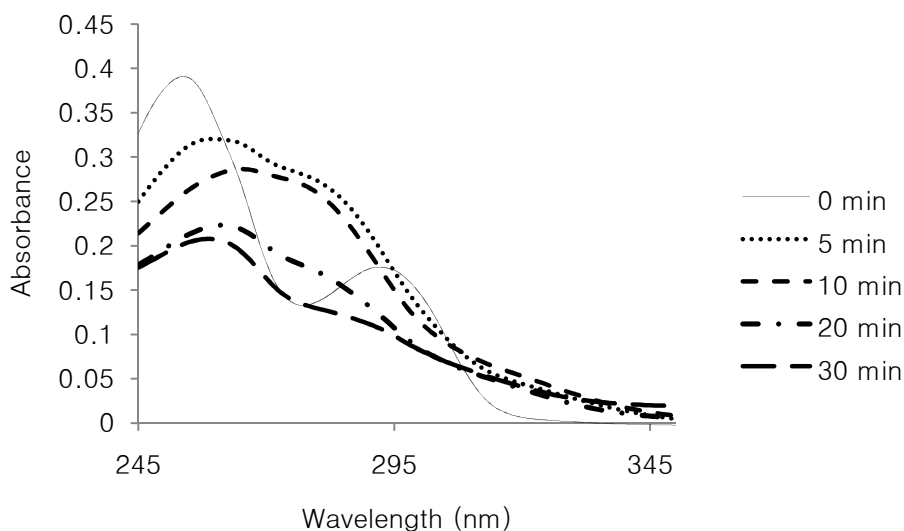


**Figure 4.20.** Absorbance spectra of a 50 μM solution of **4.3** in 0.1M Tris-HCl, 0.01% Triton X-100, 5% DMSO, pH 7.0 after irradiation at 350 nm for 0, 5, 10, 15, 20 and 30 min.



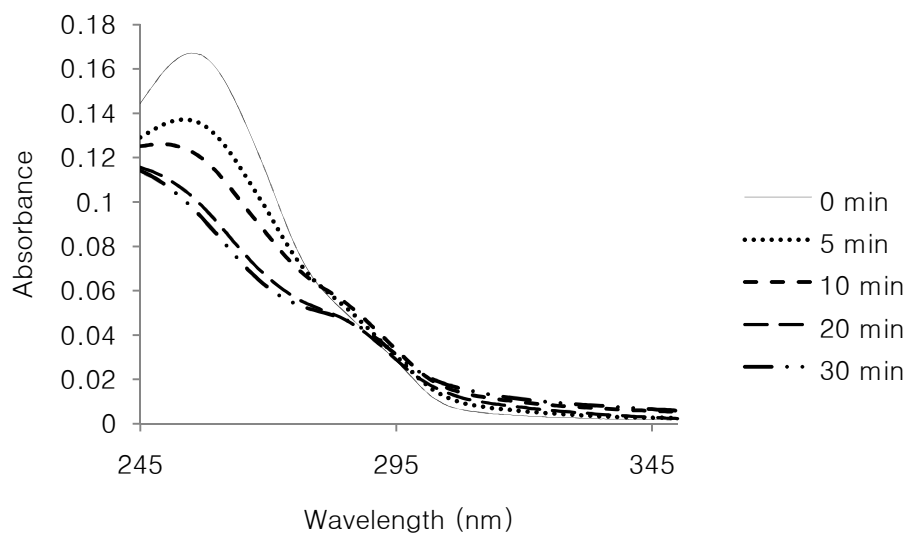


**Figure 4.21.** Absorbance spectra of a 50 μM solution of **4.4** in 0.1M Tris-HCl, 0.01% Triton X-100, 5% DMSO, pH 7.0 after irradiation at 350 nm for 0, 5, 10, 15, 20 and 30 min.

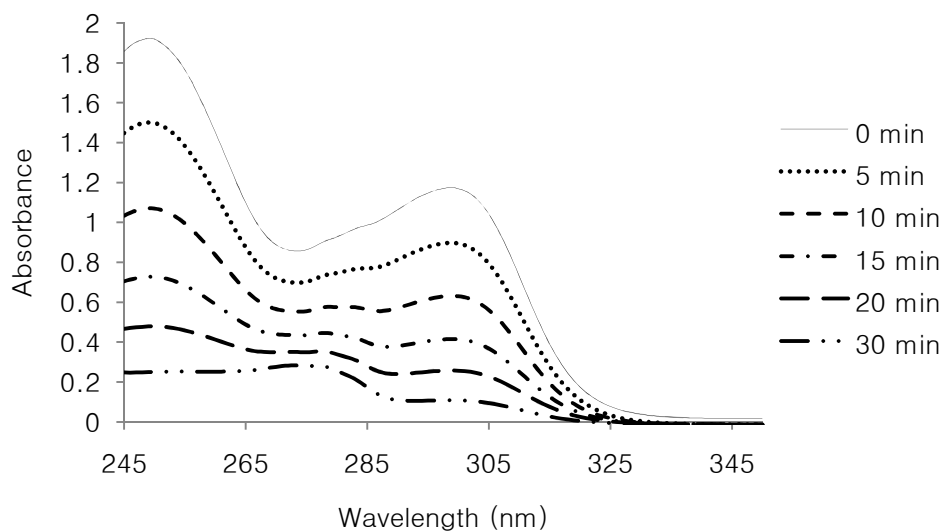


**Figure 4.22.** Absorbance spectra of a 200 μM solution of **4.5** in 0.1M Tris-HCl, 0.01% Triton X-100, 5% DMSO, pH 7.0 after irradiation at 350 nm for 0, 5, 10, 15, 20 and 30 min.

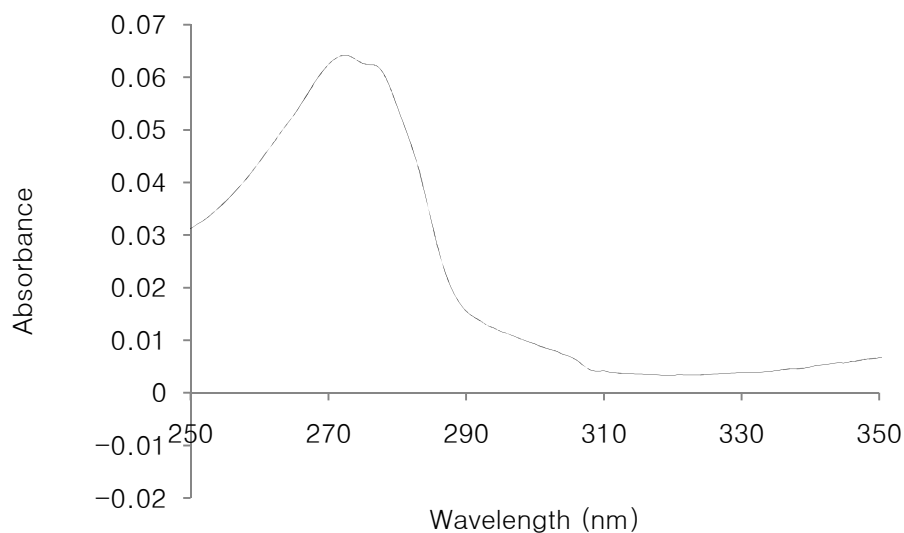


**Figure 4.23.** Absorbance spectra of 50  $\mu$ M EP in 0.1M Tris-HCl, 0.01% Triton X-100, 5% DMSO, pH 7.0.

The change in the absorbance spectrum of compound **4.8** upon irradiation at 350 nm was also examined. Surprisingly, the absorbance spectrum for compound **4.8** exhibited relatively minor changes upon irradiation at 350 nm (**Figure 4.24**). The  $\lambda_{\max}$  and  $\lambda_{\min}$  stayed more or less the same throughout the time course of the experiment while the absorbance intensity decreased, but not to a large extent, across the spectrum and with time. This is in contrast to its phosphate derivative **4.5** which absorbs much more strongly and exhibited significant changes.

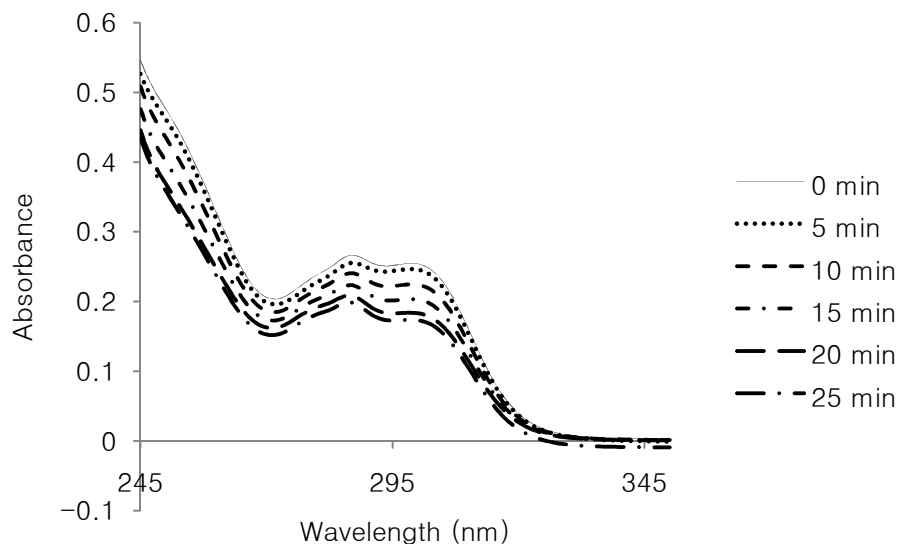


**Figure 4.24.** Absorbance spectra of a 50  $\mu\text{M}$  solution of **4.8** in 0.1M Tris-HCl, 0.01% Triton X-100, 5% DMSO, pH 7.0 after irradiation at 350 nm for 0, 5, 10, 15, 20 and 25 min.

To determine if compounds **4.3-4.5** and **4.8** exhibit time-dependent inhibition of STS in the absence of irradiation at 350 nm, 50  $\mu\text{M}$  of each of these compounds was incubated with STS, aliquots were removed at various time intervals and then diluted 10-fold into a solution of 4 mM 4-MUS for compounds **4.3** and **4.5**, and 2mM 4-MUS for compounds **4.4** and **4.8**, and the activity of the enzyme determined. Once again, we did not observe any time-dependent inhibition of STS in the absence of light (**Figure 4.25**). Only 40 % of the activity was recovered when STS was incubated with compounds both **4.3** and **4.5**. This suggested to us that these two compounds were perhaps very potent reversible inhibitors of STS and 4 mM 4-MUS was unable to completely displace these compounds from the active site after the initial solutions were diluted into the 4-MUS solution. We therefore determined the  $\text{IC}_{50}$ 's and/or  $\text{K}_i$ 's of these compounds.

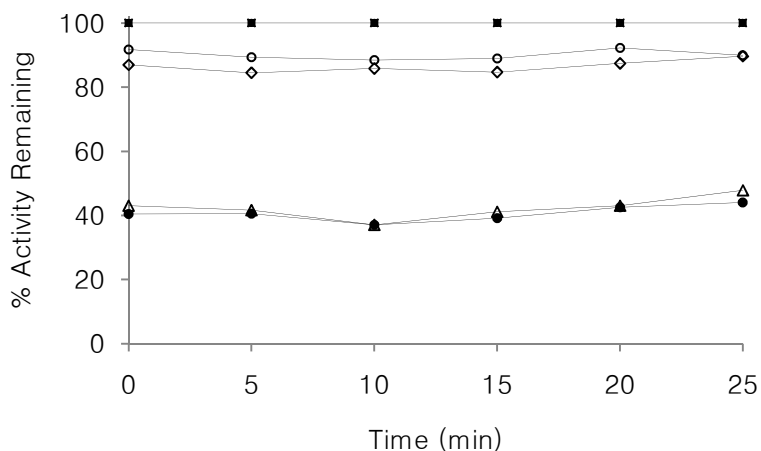


**Figure 4.25.** Percent STS activity recovered versus time upon a 1/10 dilution of a solution of STS containing no inhibitor (■), 50 μM 4.8 (◇), 50 μM 4.3 (△), 50 μM 4.5 (●), or 50 μM 4.4 (○) into a solution of 4 mM 4-MUS for compounds 4.3 and 4.5, and 2mM 4-MUS for compounds 4.4 and 4.8. All solutions contained 0.1 M Tris-HCl, 5% DMSO at pH 7.0.

Compound 4.5 exhibited competitive inhibition with a  $K_i$  of 1.4 μM, which is very similar to that of EP (Figure 4.26). Nonetheless, it was not a significantly better inhibitor than compounds 4.1 and 4.2 though these compounds exhibited, to varying extents, mixed inhibition. Compound 4.3 was also a competitive inhibitor with a  $K_i$  of 6.8 μM (Figure 4.27). Our ability to recover only 40 % of STS activity when incubating STS 4.3 and 4.5 does not seem to be related to the presence of the diazo or azido group in these compounds since we found that we were only able to partially recover STS activity when incubating STS with 10 μM EP which has a  $K_i$  very similar to that of compound 4.5 (Figure 4.28). An examination of the percent activity recovered versus 4-MUS concentration (Figure 4.28) after incubation of STS with just 10 μM EP or 4.5 revealed that the amount of activity recovered was dependent upon the concentration of 4-MUS. So it appears that even a high concentration of 4-MUS is unable to displace these inhibitors (after a 1/10 dilution into 4 mM 4-MUS). Compound 4.4 was a relatively poor inhibitor of STS exhibiting mixed inhibition (Figure 4.29) with an  $IC_{50}$  value of  $129 \pm 10$  μM, a

$K_i$  of  $64 \mu\text{M}$  and an  $\alpha K_i$  of  $127 \mu\text{M}$ . As shown in **Figure 4.24**, STS activity was readily recovered upon dilution of a solution of STS containing  $50 \mu\text{M}$  **4.4** into a solution of  $2 \text{ mM}$  4-MUS.

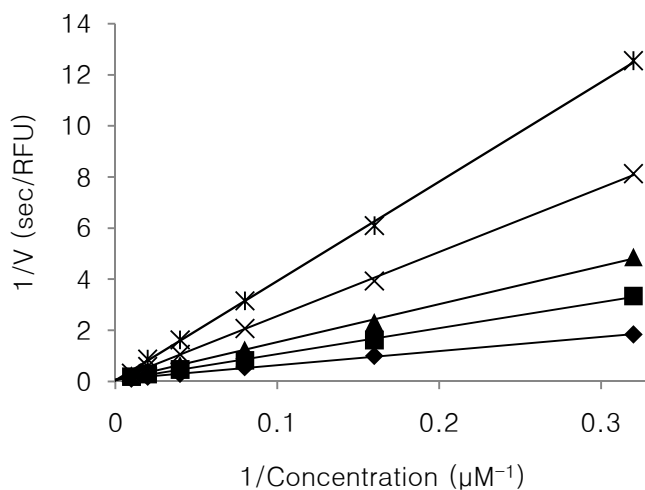


**Figure 4.26.** Lineweaver-Burk plot for **4.5**.  $0 \mu\text{M}$  ( $\blacklozenge$ ),  $3.13 \mu\text{M}$  ( $\blacksquare$ ),  $6.25 \mu\text{M}$  ( $\blacktriangle$ ),  $12.5 \mu\text{M}$  ( $\times$ ),  $25.0 \mu\text{M}$  ( $*$ ).

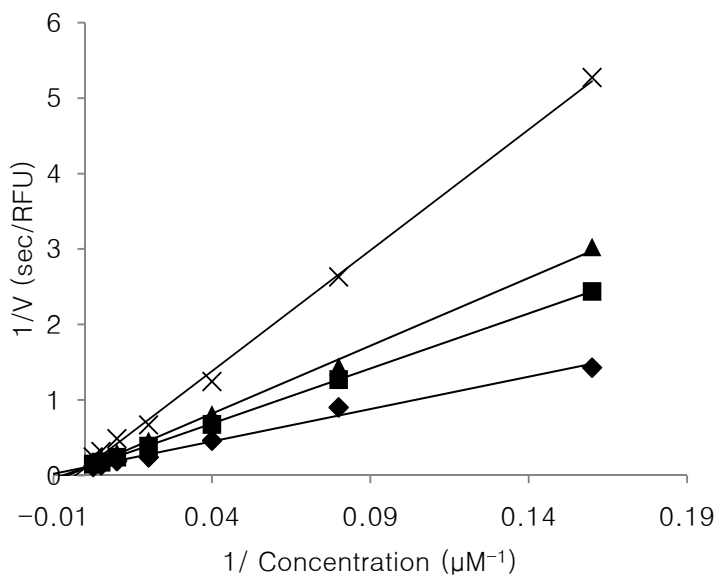


**Figure 4.27.** Lineweaver-Burk plot for **4.3**  $\blacklozenge$   $0 \mu\text{M}$   $\blacksquare$   $5.0 \mu\text{M}$   $\blacktriangle$   $10.0 \mu\text{M}$   $\times$   $20.0 \mu\text{M}$

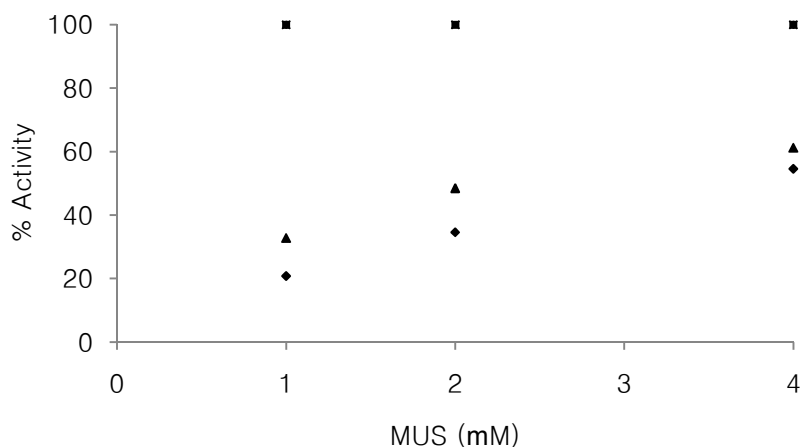


**Figure 4.28.** Effect of 4-MUS concentration on the recovery of STS activity after incubating STS with 10  $\mu\text{M}$  EP (◆) and 10  $\mu\text{M}$  4.5 (▲). STS activity was determined by diluting the mixtures of STS and EP or STS and 4.5 ten-fold into a solution containing various concentrations of 4-MUS and following the production of MU as described in the experimental section. Control without inhibitor (■).

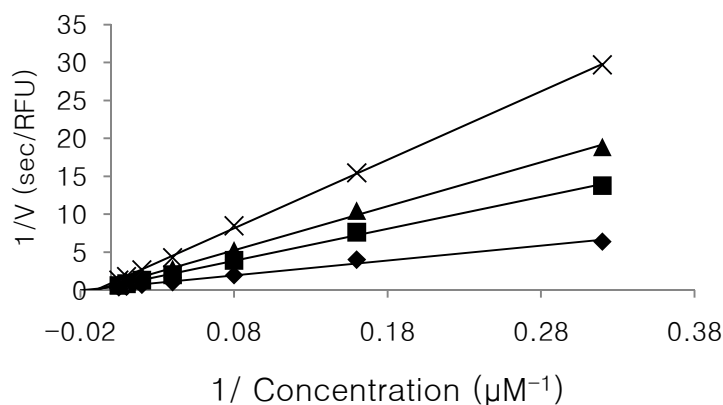


**Figure 4.29.** Lineweaver-Burk plot for compound 4.4. 0  $\mu\text{M}$  (◆), 50  $\mu\text{M}$  (■), 100  $\mu\text{M}$  (▲), 200  $\mu\text{M}$  (×).

To our surprise, we did not observe labeling occurring with 4.5 (Figure 4.30). One immediate assumption is that the diazo group in 4.5 is not breaking down when irradiated at 350 nm. However, the data presented in Figure 4.22 suggests that it is indeed breaking down under the irradiation conditions as a small amount of activity was recovered (~10%). It is possible that

the diazo group is indeed forming a carbene but the carbene is not reacting with a residue on the enzyme and the resulting product may still be a good inhibitor of STS since the phosphate group and much of the steroid skeleton should still be intact.

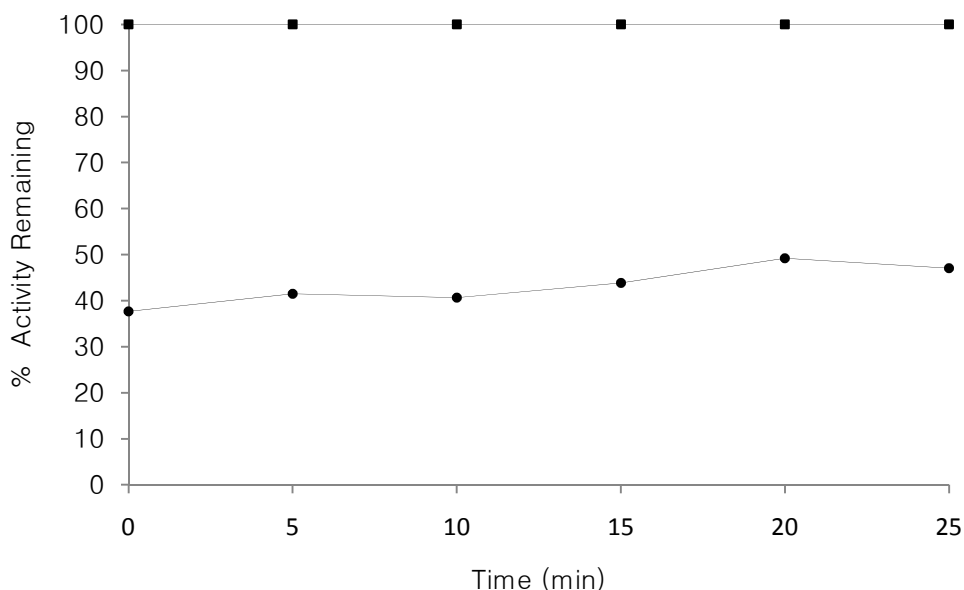


**Figure 4.30.** Percent STS activity remaining versus time in the absence of **4.5** with no irradiation (■) and upon irradiation at 350 nm and in the presence of 50 μM **4.5** (●) in 0.1M Tris-HCl, 5% DMSO, pH 7.0. STS activity was determined by diluting the mixture ten-fold into a solution containing 4 mM 4-MUS and following the production of MU as described in the experimental section. Activity loss due to the effect of 350 nm radiation on STS alone (see **Figure 4.3**) has been subtracted from the data obtained from radiated solution.

Surprisingly, photoaffinity labeling experiments with **4.8** reveal that it is able to label STS moderately as shown in **Figure 4.31**. This suggests that compounds **4.5** and **4.8** bind very differently to STS. The phosphate group may bind in a way that prevents the diazo group from reacting with the residues important in the transport or catalysis of STS. Compound **4.8** has an  $IC_{50}$  of 24 μM. We have not yet determined its mode of inhibition.

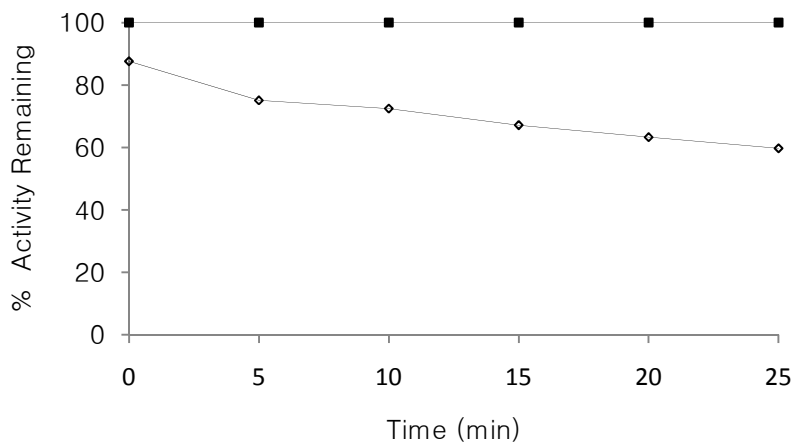


**Figure 4.31.** Percent STS activity remaining versus time in the absence of **4.8** with no irradiation (■) and upon irradiation at 350 nm and in the presence of 50  $\mu$ M **4.8** (●) in 0.1 M Tris-HCl, 5% DMSO, pH 7.0. STS activity was determined by diluting the mixture ten-fold into a solution containing 2 mM 4-MUS and following the production of MU as described in the experimental section. Activity loss due to the effect of 350 nm radiation on STS alone (see **Figure 4.3**) has been subtracted from the data obtained from radiated solution.

Photoaffinity labeling experiments with **4.3** yielded results that were similar to **4.5** (**Figure 4.31**). Since **4.6** is a good photoaffinity label for STS, it suggests that the phosphate group may indeed be the culprit preventing labeling from occurring. As shown earlier (**Figure 4.20**), **4.3** breaks down upon irradiation at 350 nm. The fact that activity is slowly being restored over time suggests that degradation of the label occurring. A reaction might be occurring between the photo-generated nitrene and the phosphate group which is in very close proximity. This results in destruction of the phosphate groups and loss of inhibitory activity. Compound **4.4** is a good photoaffinity label of STS (**Figure 4.32**) with only 35 % STS activity remaining after being irradiated in the presence of 50  $\mu$ M **4.4** for 25 minutes. This was surprising considering that this compound exhibited the poorest affinity for STS amongst all of the compounds studied. The fact that it exhibits mixed inhibition suggests that it is possible that the labeling might be



occurring at a secondary site (a site other than the active site) and this is somehow affecting enzymatic activity.

We conducted a protection experiment to determine if compound **4.4** is reacting with active site residues. The experiment was done similar to previous PAL experiments, with the addition of varying concentrations of estrone phosphate, a competitive inhibitor. Estrone phosphate protects STS from inactivation by **4.4** when irradiated at 350 nm (**Figure 4.34**) indicating that at least some labeling is occurring at the active site. A summary of our results with compounds **4.1-4.8** is given in Table 4.1.

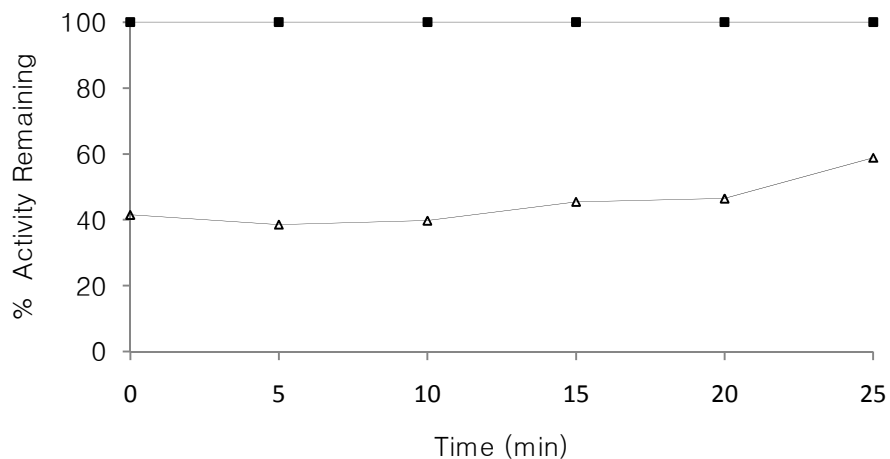


**Figure 4.32.** Percent STS activity remaining versus time in the absence of **4.3** with no irradiation (■) and upon irradiation at 350 nm and in the presence of 50  $\mu$ M **4.3** (●) in 0.1 M Tris-HCl, 5% DMSO, pH 7.0. STS activity was determined by diluting the mixture ten-fold into a solution containing 4 mM 4-MUS and following the production of MU as described in the experimental section. Activity loss due to the effect of 350 nm radiation on STS alone (see **Figure 4.3**) has been subtracted from the data obtained from radiated solution.

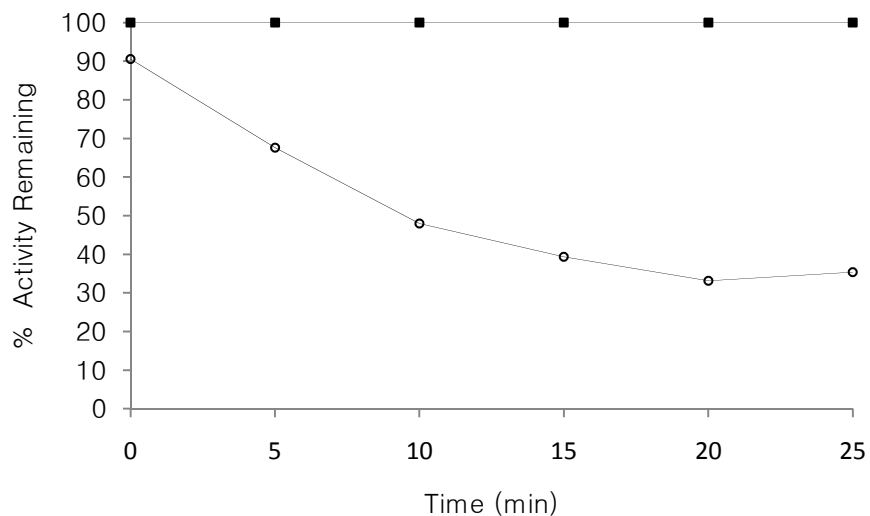


**Figure 4.33.** Percent STS activity remaining versus time in the absence of **4.4** with no irradiation (■) and upon irradiation at 350 nm and in the presence of 50  $\mu\text{M}$  **4.4** (●) in 0.1 M Tris-HCl, 5% DMSO, pH 7.0. STS activity was determined by diluting the mixture ten-fold into a solution containing 2 mM 4-MUS and following the production of MU as described in the experimental section. Activity loss due to the effect of 350 nm radiation on STS alone (see **Figure 4.3**) has been subtracted from the data obtained from radiated solution.

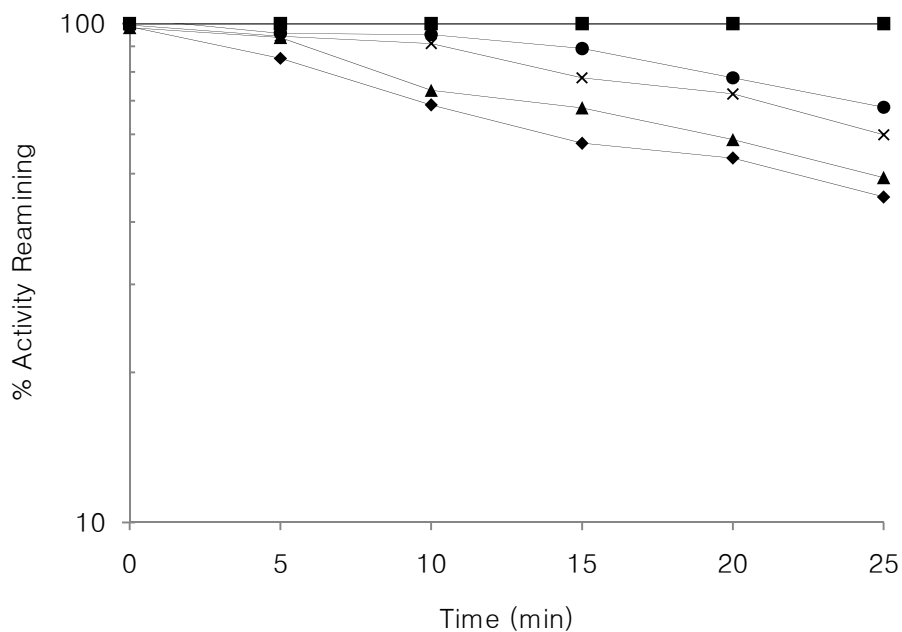


**Figure 4.34.** Percent STS activity remaining versus time in the absence of **4.4** with no irradiation (■) and upon irradiation at 350 nm and in the presence of 50  $\mu\text{M}$  **4.4** and 0  $\mu\text{M}$  EP (◆), 2.5  $\mu\text{M}$  EP (▲), 5  $\mu\text{M}$  EP (×), and 25  $\mu\text{M}$  EP (●) in 0.1 M Tris-HCl, 5% DMSO, pH 7.0. STS activity was determined by diluting the mixture ten-fold into a solution containing 4 mM 4-MUS and following the production of MU as described in the experimental section. Activity

loss due to the effect of 350 nm radiation on STS alone (see **Figure 4.2**) has been subtracted from the data obtained from radiated solution.

**Table 4.1.** Summary of results with compounds **4.1-4.8**

<b>Compound</b>	<b>IC<sub>50</sub> (μM)</b>	<b>K<sub>i</sub>(μM)</b>	<b>% activity remaining<sup>a</sup></b>	<b>Mode of inhibition</b>	<b>Substrate</b>
<b>4.1</b>	8.3 ± 0.2	5.5	55	Competitive	Yes
<b>4.2</b>	7.4 ± 0.4	8.3 (αK <sub>i</sub> = 20)	45	Mixed	No
<b>4.3</b>	8.3 ± 0.2	6.8	61 <sup>d</sup>	Competitive	No
<b>4.4</b>	129 ± 11	64 (αK <sub>i</sub> = 127)	35	Mixed	No
<b>4.5</b>	12.4 ± 0.4	1.4	47 <sup>d</sup>	Competitive	No
<b>4.6</b>	ND*	ND <sup>c</sup>	58	ND	No
<b>4.7</b>	ND*	ND <sup>c</sup>	87 <sup>b</sup>	ND	No
<b>4.8</b>	24 ± 3	ND	64	ND	No

<sup>a</sup>Percent activity remaining after irradiation of a solution of STS and 50 μM compound at 350 nm for 25 minutes followed by a 10-fold dilution into a 2 mM solution of 4-MUS for all compounds except **4.3** and **4.5** in which 4mM 4-MUS was used. <sup>b</sup>Only 10 μM of compound used due to limited solubility of the compound. <sup>c</sup>Not determined due to limited solubility. <sup>d</sup>Time-dependent inhibition was not observed upon irradiation.

Out of the five sulfated and phosphorylated compounds studied compounds **4.2** and **4.4** are most promising. While **4.1** appeared to photolabel STS it is very possible that this was due to labeling by its hydrolysis product **4.6**. Compounds **4.3** and **4.5** did not exhibit time-dependent inhibition upon irradiation. Compounds **4.6** and **4.7** also act as photolabels of STS and might be useful for examining product release pathways in STS.

### 4.2.3 Deglycosylation of STS

We would like to use mass spectrometry to determine which residues in STS are being modified by our photoaffinity labels. This will require that the modified STS be deglycosylated before MS analysis. STS is glycosylated at four Asn residues. Mortaud et al. report deglycosylation of STS by a N-glycosidase F (PNGase F) (Mortaud et al., 1995). PNGase is an endoglycosidase that catalyzes the release of N-linked oligosaccharides from proteins (Tarentino et al., 1985). We purchased PNGase F from New England Biolabs, and followed the procedure provided with the kit. Mortaud et al. have shown that deglycosylated STS exhibits enhanced mobility on SDS PAGE compared to native STS and our results (**Figure 4.35**) are consistent with this observation. PNGase usually appears on an SDS gel as 35.5 kDa (Tarentino et al., 1985), but we did not observe any band in this region due to a low concentration of PNGase F used.

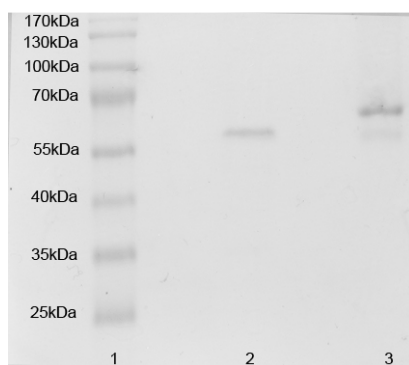


**Figure 4.35.** SDS PAGE of purified STS. The gel was stained in Fermentas PageBlue Protein staining solution. Lane 1 contains Fermentas PageRuler™ Prestained Protein Ladder. Lane 2 contains deglycosylated STS. Lane 3 contains purified STS.

### 4.3 Conclusion and Future Work

A series of estrone derivatives were examined as photoaffinity labels of STS. Of the sulfated and phosphorylated compounds examined, two of these compounds, **4.2** and **4.4** exhibit properties that are suitable for PAL studies with STS. These labels may be useful for

ascertaining pathways of substrate entry into the STS active site. All of the non-sulfated or non-phosphorylated compounds **4.6-4.8**, acted as photoaffinity labels to varying degrees. These labels may be useful for ascertaining pathways of product release into the STS active site. Our future studies will involve identifying which residues are being modified using mass spectrometry. We have shown, by SDS PAGE, that we can deglycosylate STS. The band corresponding to the deglycosylated enzyme has been excised from the gel (**Figure 4.35**) and sent to The University of Guelph mass spectrometry facility where an in-gel tryptic digest has been performed and the resulting fragments sequenced by LC-MSMS. The next step is to perform this type of analysis on the modified enzyme.

## **4.4 Experimental**

### **4.4.1 Materials**

Most materials were the same as described in section **2.4.1** chapter 2. Photoaffinity labeling of STS is carried out in quartz test tubes using a Rayonet Photochemical Reactor from Southern New England Ultraviolet (Branford, Connecticut). PNGase F deglycosylation kit (glycerol free) was purchased from New England Biolabs (Ipswich, MA).

### **4.4.2 Effect of 350 nm light on STS activity**

30 nM of STS in buffer containing 0.1% Triton X-100, 0.1M Tris-HCl, pH 7.0 was exposed to irradiation at 300 or 350 nm over 25 minutes. 20  $\mu$ L aliquots were withdrawn every 5 min, beginning at t=0, and added to the wells of a microtiter plate containing 180  $\mu$ L of 222.2  $\mu$ M 4-MUS in 0.1M Tris-HCl, pH 7.0. STS activity was determined as described previously. A control was performed where the enzyme was exposed to just room lighting.

#### **4.4.3 Spectrophotometric studies with compounds 4.1-4.8**

**4.1-4.6** and **4.8** were dissolved in a solution of 5% DMSO, 0.1M Tris-HCl, pH 7.0 0.01 % Triton X-100 to the desired concentration. Compound **4.7** was insoluble in buffer and so solutions of this compound were prepared in pure ethanol. 1 mL of these solutions were added to a 10mm Helma quartz cuvette, and their spectra were obtained. To determine the effect of 350 nm light on their absorbance spectra, 6 mL of these solutions were placed in a quartz test tube, and irradiated at 350 nm. 1 mL of sample was withdrawn at various time intervals and their spectra determined as described above. Controls were performed where the compound solutions were not irradiated at 350 nm but instead just subjected to room light.

#### **4.4.4 Photoaffinity labeling procedure**

Various solutions of **4.1**, and **4.2** with 30 nM of STS in buffer containing 2% DMSO, 0.1M Tris-HCl pH 7.0 in a 1 mL sample. This sample is pipetted into a quartz test tube, and irradiated at 350 nm UV irradiation for 20 minutes in a Rayonet Photochemical Reactor (Southern New England Ultraviolet). Simultaneously, a sample of STS in the same buffer is also pipetted into a quartz test tube. Every 5 minute beginning at time 0, a 20  $\mu$ L is withdrawn from each test tube and added to a well containing 180  $\mu$ L of 2mM 4-MUS 0.1M Tris-HCl pH 7.0; this is repeated in triplicates. The activity of STS determined as previously described above. The activity of STS in the presence of varying concentrations of photoaffinity label irradiated with UV light is compared to the activity of STS in the absence of photoaffinity label and UV irradiation. The results are averaged, analyzed and plotted as percent Activity using Excel 2007. Similar conditions with the omission of UV irradiation were used to determine if the photoaffinity label reacted with STS in the absence of UV irradiation.

1 mL solutions containing 50  $\mu$ M **4.1-4.8** and 55 nM STS in buffer containing 5 % DMSO, 0.1M Tris-HCl, pH 7.0, 0.01 %Triton X-100 were irradiated at 350 nm UV irradiation for 25minutes. Every 5 min starting at t = 0 a 20  $\mu$ L aliquot was withdrawn and added to a well of a 96-well microtiter plate containing 180  $\mu$ L of 2 mM 4-MUS in 0.1 M Tris-HCl pH 7.0, with the exception of compounds **4.6** and **4.7** where 4 mM 4-MUS was used. STS activity was determined as described previously. The following controls were performed: (A) the enzyme was incubated in the absence of compound and not irradiated at 350 nm; (B) the enzyme was incubated with 50  $\mu$ M of photoaffinity label but not irradiated at 350 nm; (C) the enzyme irradiated at 350 nm in the absence of compound. Any time-dependent inhibition over 25 minutes by the compound in the absence of UV irradiation was calculated as (STS activity in control B)/( STS activity in control A) $\times$  100%. The % activity remaining as a result of specific photoaffinity labeling of STS by the compounds was determined by [1- (STS activity in control C - STS incubated with 50  $\mu$ M of compound irradiated at 350nm UV irradiation) / (STS activity in control A)]  $\times$  100%.

#### **4.4.5 HPLC Studies with 4.1 and 4.2**

For standard studies of **4.1** and **4.2** elution off the HPLC, 20 $\mu$ L of 50  $\mu$ M **4.1** or **4.2** in 0.1 M Tris-HCl, 0.01 % Triton X-100 5% DMSO pH 7.0 are injected into a Phenomex Jupiter analytical reversed-phase C-18 column (Torrance, CA, USA) on a Waters 600 HPLC system (Milford, MA, USA). The Waters 2487 dual wavelength detector is set to 255 nm corresponding to the  $\lambda_{\text{maxima}}$  of these compounds. The elution is set to an isocratic elution of acetonitrile/0.1% trifluoroacetic Acid (TFA) water (5:5) for 45minutes.

For enzymatic studies with compounds **4.1** and **4.2**, 55nM STS is incubated with either 50  $\mu$ M **4.1** or **4.2** in buffer A containing 0.1 M Tris-HCl, 0.01 % Triton X-100, containing 5%

DMSO at pH 7.0 after 10 minutes. 20 $\mu$ L of this sample is injected into the HPLC and eluted off in the same conditions as stated above.

#### **4.4.6 IC<sub>50</sub> and K<sub>i</sub> determinations**

IC<sub>50</sub> and K<sub>i</sub> determinations were performed as described in section 3.4.2 and 3.4.3

#### **4.4.7 Deglycosylation of STS**

The deglycosylation of STS is followed according to the protocol provided by the PNGase F deglycosylation kit from New England Biolabs (Ipswich, MA). The procedure provided is based on the deglycosylation of 1-20  $\mu$ g glycoprotein, and we modified linearly it to accommodate a larger amount of protein. 137 $\mu$ g of STS, obtained by taking 0.9mL of the purified STS stock solution (0.152mg/ml) was added to 100 $\mu$ L of the provided 10X glycoprotein denaturing buffer. This solution was incubated for 100 $^{\circ}$ C for 10minutes. To this solution, 130 $\mu$ L of the provided 10X G7 reaction buffer, 130 $\mu$ L of 10% NP40, and 5 $\mu$ L of PNGase was added to make a total volume of 1265 $\mu$ L. The sample was incubated for 12 hours (instead of the recommended 1h), and results in complete deglycosylation of 137 $\mu$ g of STS.



## References

- Ahmed, V. F. Reversible and Mechanism-Based Irreversible Inhibitor Studies on Human Steroid Sulfatase and Protein Tyrosine Phosphatase 1B, (PhD). *University of Waterloo*, **2009**.
- Ahmed, V., Liu, Y., Silvestro, C., and Taylor, S. D. Boronic acids as inhibitors of steroid sulfatase. *Bioorganic and Medicinal Chemistry*, **2006**, 14, 8564-8573.
- Ahmed, V., Liu, Y., and Taylor, S. D. Multiple Pathways for the Irreversible Inhibition of Steroid Sulfatase with Quinone Methide-Generating Suicide Inhibitors. *ChemBioChem*, **2009**, 10, 1457-1461.
- Ahmed, S., James, K., Owen, C., Patel, C. K., and Patel, M. Novel Ihibitors of the Enzyme Estrone Sulfatase (ES). *Bioorg. Med. Chem. Lett.*, **2001**, 11, 841-844
- Ahmed, V., Ispahany, M., Ruttgaizer, S., Guillemette, G., and Taylor, S. D. A fluorogenic substrate for the continuous assaying of aryl sulfatases. *Analytical Biochem.*, **2005**, 340, 80-88.
- Anderson, J. C., Lucas, J. H. L., and Widlanski, T. S.. Molecular Recognition in Biological Systems: Phosphate Esters vs. Sulfate Esters and the Mechanism of Action of Steroid sulfatases. *J. Am. Chem. Soc.*, **1995**, 117, 3889-3890.
- Bojarova, P., and Williams, S. J. Aryl sulfamates are broad spectrum inactivators of sulfatases: Effects on sulfatases from various sources. *Bioorg. Med. Chem. Lett.*, **2009**, 19, 477-480.
- Bojarova, P., Denehy, E., Walker, I., Loft, K., Souza, P. D., Woo, L. W., Potter, L.V. B., McConville, J. M., and Williams, S. J. Direct Evidence for ArO-S Bond Cleavage upon Inactivation of *Pseudomonas aeruginosa* Arylsulfatase by Aryl Sulfamates. *ChembioChem.*, **2008**, 9, 613-623.
- Boivin. R. P., Luu-The, V., Cachance, R., Labrie, F., Poirier, D., Structure-activity relationships of 17alpha-derivatives of estradiol as inhibitors of steroid sulfatase. *J. Med. Chem.*, **2000**, 43, 4465-4478.
- Boltes, I., Czapinska, H., Kahnert, A., von Bulow, R., Dierks, T., Schmidt, B., von Figura, K., Kertesz, M. A., and Uson, I. A structure of Arylsulfatase from *Pseudomonas aeruginosa* Establishes the Catalytic Mechanism of Sulfate Ester Cleavage in the Sulfatase Family. *Structure*, **2001**, 9, 483-491.
- Bond C. S., Clements P. R., Ashby S. J., Collyer C. A., Harrop S. J., Hopwood J. J., and J. M. Guss. Structure of a human lysosomal sulfatase. *Structure*, **1997**, 5, 277-289.
- Briest, S. and Stearns, V. Tamoxifen metabolism and its effect on endocrine treatment of Breast Cancer. *Clin. Adv. Herm. and Onc.*, **2009**, 185-192.

Burns, G. R. J. Purification and partial characterization of arylsulfatase C from human placental microsomes. *Biochem. Biophys. Act.*, **1983**, 759, 199-204.

Ciobanu, C. L., and Poirier, D. Synthesis of Libraries of 16 $\beta$ -Aminopropyl Estradiol Derivatives for Targeting Two Key Steroidogenic Enzymes. *ChemMedChem*, **2006**, 1, 1249-1259.

Clemons, M. and Goss, P. Recent data on estrogen sulfatases and sulfotransferase activities in human breast cancer. *New Engl. J. Med.*, **2001**, 344, 276-285.

Conary, J. T., Lorkowski, G. Schmidt, B., Pohlmann, R., Nagel, G., Meyer, H. E., Krentler, C. Cully, J., Hasilik, A., and von Figura, K. Genetic Heterogeneity of Steroid Sulfatase Deficiency Revealed with cDNA for Human Steroid Sulfatase. *Biochem. and Biophys. Res. Commun.*, **1987**, 1010-1017.

Copeland, R. A. Enzymes: A practical Introduction to Structure, Mechanism, and Data Analysis. *VCH Publishers*, **1996**.

Dibbelt, L., Kuss, E. Human placental steryl-sulfatase: enzyme purification, production of antisera, and immunoblotting reactions with normal and sulfatase-deficient placentas. *Biol. Chem. Hoppe-Seyler*, **1986**, 367, 1223-1229.

Dibbelt, L., Kuss, E. Human placental sterylsulfatase. Interaction of the isolated enzyme with substrates, products, transition-state analogues, amino-acid modifiers and anion transport inhibitors. *Biol. Chem. Hoppe-Seyler*, **1991**, 372, 173.

Dibbelt, L., Li, P. K., Pillai, R., and Knuppen, R. Inhibition of Human Placental Sterylsulfatase by Synthetic Analogs of Estrone Sulfate. *J. Steroid Biochem. Molec. Biol.*, **1994**, 50, 261-266.

Elger, W., Schwarz, S., Hedden, A., Reddersen, G., Schneider, B. Sulphamates of various estrogens are prodrugs with increased systemic and reduced hepatic estrogenicity at oral applications. *J. Steroid Biochem. Molec. Biol.*, **1995**, 55, 395-403.

Elger, W., Bartha, A., Hedden, A., Reddersen, G., Ritter, P., Schneider, B., Zuchner, J., Krahl, E., Muller, K., Oettel, M., Schwarz, S. Estrogen sulfamates: a new approach to oral estrogen therapy. *Reprod. Fertil.-3097Dev.*, **2001**, 13, 297-305.

Folsom, B. R. Characterization of 2-nitrophenol uptake system of *Pseudomonas putida* B2. *J. Industrial Microbio. and Biotech.*, **1997**, 19, 123-129.

Foster, P. A., Chander, S. K., Newman, S. P., Woo, L. L., Sutcliffe, O. B., Bubert, C., Zhou, D., Chen, S., Potter, B. V. L., Reed, M. J., and Purohit, A. A New Therapeutic Strategy against Hormone-Dependent Breast Cancer: The Preclinical Development of a Dual Aromatase and Sulfatase Inhibitor. *Clin Cancer Res.*, **2008**, 14, 6469-6477.

Gamage, N. U., Duggleby, R. G., Barnett, A. C., Tresillian, M., Latham, C. F., Liyou, N. E., McManus, M. E. and Martin, J. L. Structure of a Human Carcinogen-converting Enzyme, SULT1A1. *J. Biol. Chem.*, **2003**, 278, 7655-7662.

Gnant, M., Mlineritsch, B., Schippinger, W., Luschin-Ebengreuth, G., Postlberger, S., Menzel, C., Jakesz, R., Seifert, M., Hubalek, M., Bjelic-Radisic, V., Samonigg, H., Tausch, C., Eidtmann, H., Steger, G., Kwasny, W., Dubsky, P., Fridrik, M., Fitzal, F., Stierer, M., Rucklinger, E., and Greil, R. Endocrine Therapy plus Zoledronic Acid in Premenopausal Breast Cancer. *New Engl. J. Med.*, **2009**, 360, 679-691.

Hankinson, S. E., Willett, W. C., Manson, J. E., Hunter, D. J., Colditz, G. A., Stampfer, M. J., and Longscope, C. Alcohol, Height, and Adiposity in Relation to Estrogen and Prolactin Levels in Postmenopausal Women. *J. of the Nat. Canc. Institute*, **1995**, 87, 1297-1302.

Hanon, S. R., Best, M.D., and Wong, C. Sulfatases: Structure, Mechanism, Biological Activity, Inhibition, and Synthetic Utility. *Angew. Chem. Intl. Ed. Eng.*, **2004**, 43, 5736.

Hejaz, H. A., Woo, L.W., Purohit, A., Reed, M.J., and Potter, B.V. Synthesis, in vitro and in vivo activity of benzophenone-based inhibitors of steroid sulfatase. *Bioorg. Med. Chem.*, **2004**, 12, 2759.

Hernandez-Guzman, G. F., Higashiyama, T., Osawa, Y., and Ghosh, D. Purification, characterization and crystallization of human placental estrone/dehydroepiandrosterone sulfatase, a membrane-bound enzyme of the endoplasmic reticulum. *J. Steroid Biochem. Molec. Biol.*, **2001**, 78, 441-50.

Hernandez-Guzman, G. F., Higashiyama, T., Pangborn, W., Osawa, Y., and Ghosh, D. Structure of Human Estrone Sulfatase Suggests Functional Role of Membrane Association. *J. Biol. Chem.*, **2003**, 278, 22989-22997.

Ho, Y. T., Purohit, A., Vicker, N., Newman, S. P., Robinson, J. J., Leese, M. P., Ganeshapillai, D., Woo, L. W. L., Potter, B. V. L. and Reed, M. J. Inhibition of carbonic anhydrase II by steroidal and non-steroidal sulphamates. *Biochem. and Biophys. Res. Commun.*, **2003**, 305, 909-914

Jekel, P.A., Weller, W. J., and Beintema, J.J. Use of Endoproteinase Lys-C from *Lysobacter* enzymogenes in Protein Sequence Analysis. *Anal Biochem.*, **1983**, 134, 347-354.

Jin, J., and Lin, S. Human Estrogenic 17 $\beta$ -Hydroxysteroid Dehydrogenase: predominance of Estrone Reduction and Its Induction by NADPH. *Biochem. and Biophys. Res. Commun.*, **1999**, 259, 489-493.

Jutten, P., Schumann, W., Hartl, A., Heinisch, L., Grafe, U., Werner, W., Ulbricht, H. A novel type of nonsteroidal estrone sulfatase inhibitor. *Bioorg. Med. Chem. Lett.*, **2002**, 12, 1339-1342.

Lapierre, J. Ph.D thesis. *University of Waterloo*, **2003**.

- Li, P.K., Pillai, R., Young, B.L., Bender, W.H., Martino, D.M., Lin, F.T. Synthesis and biochemical studies of estrone sulfatase inhibitors. *Steroids*, **1993**, 58, 106-111.
- Li, P. K., Pillai, R., and Dibbelt, L. Estrone sulfate analogs as estrone sulfatase inhibitors. *Steroids*, **1995**, 60, 299-306.
- Lin, Y., Lu, P., Tang, C., Mei, Q., Sandig, G., Rodrigues, D. A., Rushmore, T. H., and Shou, M. Substrate Inhibition Kinetics for Cytochrome P450-Catalyzed Reactions. *Drug Metabolism and Disposition*, **2001**, 29, 368-374.
- Loach, P. A., Sekura, D. L., Hadsell, R. M. and Stemer, A. Quantitative Dissolution of the Membrane and Preparation of Photoreceptor Subunits from *Rhodospseudomonas sepheroides*. *Biochemistry*, **1970**, 9, 724-733.
- Lukatela, G., Krauss, N., Theis, K., Selmer, T., Gieselmann, V., von Figura, K., and Saenger, W. Crystal Structure of Human Arylsulfatase A: The Aldehyde Function and the Metal Ion at the Active Site Suggests a Novel mechanism for Sulfate Ester Hydrolysis. *Biochem.*, **1998**, 37, 3654-3664.
- Miki, Y., Nakata, T., Suzuki, T., Darnel, A.D., Moriya, T., Kaneko, C., Hidaka, K., Shiotsu, Y., Kusaka, H., Sasano, H. Systemic distribution of steroid sulfatase and estrogen sulfotransferase in human adult and fetal tissues. *J. Clin. Endocrinol. Metab.*, **2002**, 87, 5760-5768.
- Masamura, S., Santner, S.J., Santen, R.J. Evidence of in situ estrogen synthesis in nitrosomethylurea-induced rat mammary tumors via the enzyme estrone sulfatase. *J. Steroid Biochem. Mol. Biol.*, **1996**, 58, 425-430.
- Mortaud, S., Donsez-Darcel, E., Roubertoux, P.L. and Degrelle H. Murine Steroid Sulfatase (mSTS) Purification, Characterization and Measurement by ELISA. *Molec. Biol.*, **1995**, 52, 81-96.
- Noel, H., Beauregard, G., Potier, M., Bleau, G., Chapdelaine, A., Roberts, K.D. The target sizes of the in situ and solubilized forms of human placental steroid sulfatase as measured by radiation inactivation. *Biochem. Biophys. Act.*, **1983**, 758, 88-90.
- Nomura, E., Katsuta, K., Ueda, T., Toriyama, M. Mori, T., and Inagaki, N. Acid-labile surfactant improves in-sodium dodecyl sulfate polyacrylamide gel protein digestion for matrix-assisted laser desorption/ionization mass spectrometric peptide mapping. *J. Mass Spectrom.*, **2004**, 39, 202-207.
- Nourescu, D., Caproiu, M. T., Luca, C., Pencu, G. I., and Constantinescu, T. The Behaviour of some estrogens in the nitration process. *Revue Roumaine de Chimie Eng.*, **1998**, 43, 1157-1164.
- Nussbaumer, P., and Billich, A. Steroid Sulfatase Inhibitors. *Med. Res. Rev.*, **2004**, 24, 529-576.

- O'Brien, J. P., and Herschlag, D. Sulfatase Activity of *E. Coli* Alkaline Phosphatase Demonstrates a Functional Link to Arylsulfatases, an Evolutionarily Related Enzyme Family. *J. Am. Chem. Soc.*, **1998**, 120, 12369-12370.
- Pasqualini, J. R., Schatz, B., Varin, C., and Nguyen, B.-L. Estrogen and the risk of breast cancer. *J. Steroid Biochem. Molec. Biol.*, **1992**, 41, 323-329.
- Payne, W. D., Katzenellenbogen, A. J., and Carlson, K. E. Photoaffinity labeling of Rat  $\alpha$ -Fetoprotein. *J. Biol. Chem.*, **1980**, 255, 10359-10367.
- Poirier, D., Boivin, R.P. 17-alpha-alkyl- or 17alpha-substituted-17beta-estradiols. A new family of estrone-sulfatase inhibitors. *Bioorg. Med. Chem. Lett.*, **1998**, 8, 1891-1896.
- Prost, O., Turrel, O. M., Dahan, N., Craveur, C., and Adessi, G. L. Estrone and Dehydroepiandrosterone Sulfatase Activities and Plasma and Estrone Sulfate Levels in Human Breast Carcinoma. *Canc. Res.*, **1984**, 44, 661-664.
- Purohit, A., Potter, B.V.L., Parker, M.G., Reed, M.J. Steroid sulphatase: expression, isolation and inhibition for active-site identification studies. *Chem-Biol. Interact.*, **1998**, 109, 183-192.
- Purohit, A., Williams, G.J., Howarth, N.M. Potter, B.V.L. Reed, M.J. Inactivation of steroid sulfatase by an active-site directed inhibitor, estrone-3-O-sulfamate. *Biochemistry*, **1995**, 34, 11508-11514.
- Robinette, D., Neamati, N., Tomer, B. K., and Borchers, C. H. Photoaffinity labeling combined with mass spectrometric approaches as a tool for structural proteomics. *Expert Rev. Proteomics*, **2006**, 3, 399-408.
- Santner, J., Feil, P.D., Santen, R.J. In situ estrogen production via estrone sulfatase pathway in breast tumors: relative importance versus aromatase pathway. *J. Clin. Endocrinol. Metab.*, **1984**, 59, 24-33.
- Schmidt, B., Selmer, T., Ingendoh, A., and von Figura, K. A Novel Amino Acid Modification in Sulfatases that is Defective in Multiple Sulfatase Deficiency. *Cell Press.*, **1995**, 82, 271-278.
- Schwarzenbach, P. R., Stierll, R., Folsom, R. B., and Zeyer, J. Compound Properties Relevant for Assessing the Environmental Partitioning of Nitrophenols. *Environ. Sci. Technol.*, **1988**, 22, 83-92.
- Sekulic, N., Konrad, M., and Lavie, A. Structural Mechanism for Substrate Inhibition of the Adenosine 5'-Phosphosulfate Kinase Domain of Human 3'-Phosphoadenosine 5'-Phosphosulfate Synthetase 1 and Its Ramifications for Enzyme Regulation. *J. Biol. Chem.*, **2007**, 282, 22112-22121.

- Selcer, K.W., Jagannathan, S., Rhodes, M.E., Li, P.K. Inhibition of placental estrone sulfatase activity and MCF-7 breast cancer cell proliferation by estrone-3-amino derivatives. *J Steroid Biochem. Mol. Biol.*, **1996**, 59, 83-91.
- Shankaran, R., Ameen, M., Daniel, W., Davidson, R.G., Chang, P.L. Characterization of arylsulfatase C isozymes from human liver and placenta. *Biochemica and Biophysica Acta.*, **1991**, 1078. 251-257.
- Stanway, S. J., Delavault, P., Purohit, A., Woo, L. L., Thurieau, C., Potter, B. V., and Reed, M. J.. Steroid Sulfatase: A new Target for the Endocrine Therapy of Breast Cancer. *The Oncologist*, **2007**, 12, 370-374.
- Stein, C., Hille, A., Seidel, J., Rihnbout, S., Waheed, A., Schmidt, B., Geuze, H., and von Figura, K. Cloning and Expression of Human Steroid-sulfatase. *J. Biol. Chem.*, **1989**, 264, 13 865.
- Stengel, C., Simon, P., Newman, J., Day, M., Tutill, H.J., Reed, M.J., Purohit, A. Effects of mutations and glycosylations on STS activity: A site directed mutagenesis study. *Molecular and Cellular Endocrinology*, **2008**, 283, 76-82.
- Sugawara, T., Nomura, E., and Hoshi, N. Both N-terminal and C-terminal regions of steroid sulfatase are important for enzyme activity. *Journal of Endocrinology*, **2006**, 188, 365-374.
- Suzuki, M., Ishida, H., Shiotsu, Y., Nakata, T., Akinaga, S., Takashima, S., Utsumi, T., Saeki, T., and Harada, N. Expression level of enzymes related to in situ estrogen synthesis and clinicopathological parameters in breast cancer patients. *J. Steroid Biochem. Molec. Biol.*, **2009**, 113, 195-201.
- Suzuki, T., Hirato, K., Yanaihara, T., Kodofuku, T., Sato, T., Hoshino, M., Yanaihara, N. Purification and properties of steroid sulfatase from human placenta. *Endocrinol. Jpn.*, **1992**, 39, 93-101.
- Suzuki, T., Nakata, T., Miki, Y., Kaneko, C., Moriya, T., Ishida, T., Akinaga, S., Hirakawa, H., Kimura, M., and Sasano, H. Estrogen sulfotransferase and steroid sulfatase in human breast carcinoma. *Cancer Res.*, **2003**, 63, 2762-2770.
- Tabatabai, A. M., and Bremner, J. M. Use of p-nitrophenyl phosphate for assay of soil phosphatase activity. *Soil Biol. Biochem.*, **1969**, 1, 301-307.
- Terentino, A.L., Gomez, C.M., and Plummer, T. H. Jr. Deglycosylation of Asparagine-Linked Glycans by peptide: N-Glycosidase F. *Biochem*, **1985**, 24, 4665-4671.
- Utsumi, T., Yoshimura, N., Takeuchi, S., Maruta, M., Maeda, K., and Harada, N. Elevated steroid sulfatase expression in breast cancers. *J. of Steroid Biochem. and Mol. Biol.*, **2000**, 73, 141-145.

Vaccaro, A. M., Salvioli, R., Muscillo, M., Renola, L. Purification and properties of arylsulfatase C from human placenta. *Enzyme*. **1987**, 37, 115-126.

Van der Loos, C. M., Van Breda, A. J., Van den Berg, F. M., Walboomers J. M. M., Jobsis, A. C. Human placental steroid sulfatase purification and monospecific antibody production in rabbits. *J. Inher. Metab.*, **1983**, 7, 97-103.

Woo, L. W. L., Purohit, A., Malini, B., Reed, M. J., Potter, B. V. L. Potent active site-directed inhibition of steroid sulphatase by tricyclic coumarin-based sulphamates. *Chem. Biol.*, **2000**, 7, 773-791.

Zeyer, J. Kocher, H. P., and Timmis, K. N. Influence of para-substituents on the Oxidative Metabolism of o-Nitrophenols by *Pseudomonas putida* B2. *Applied and Environmental Microbiology*, **1986**, 52, 33-339.

## Appendix A.

**IC<sub>50</sub> plots for compounds 3.3, 3.7-3.9, 3.11, 3.16-3.24, E1 and E2 and replots of the data in figures 3.10-3.12.**

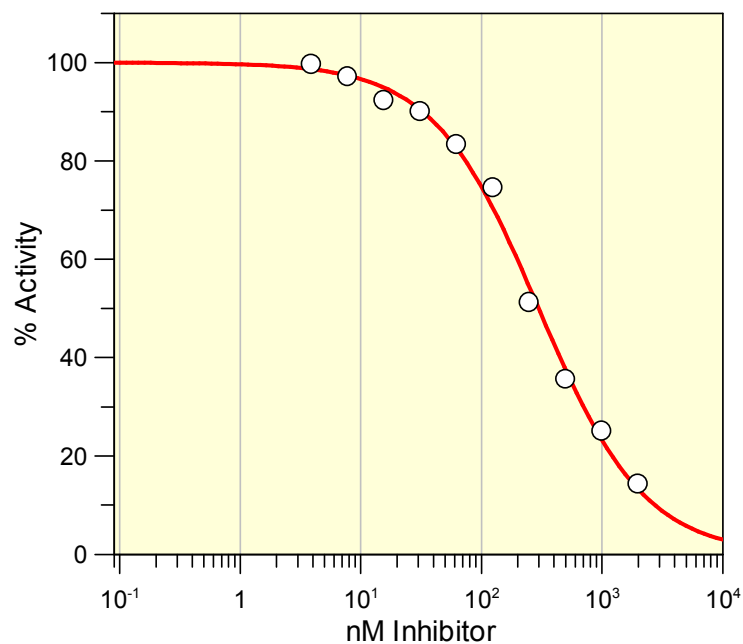


**Figure A.1** IC<sub>50</sub> for compounds **3.3** = 299 ± 14 nM

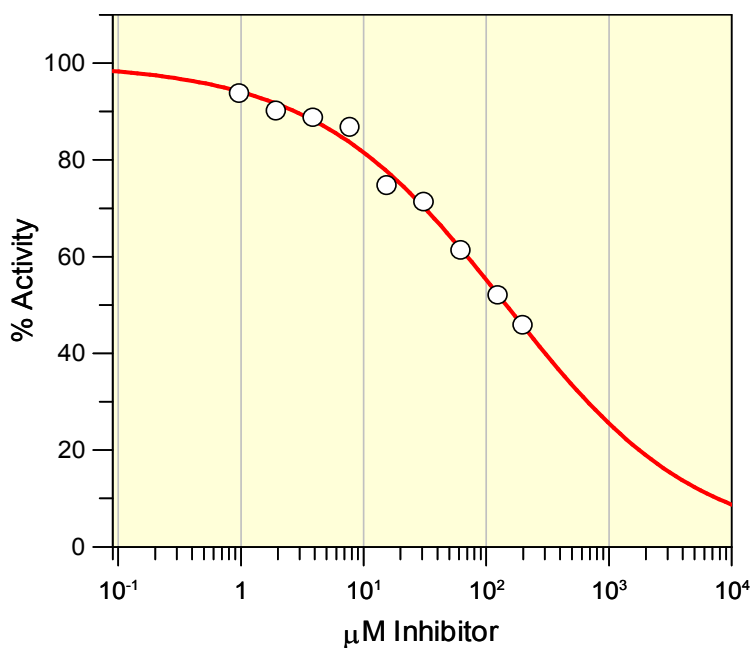


**Figure A.2** IC<sub>50</sub> for compounds **3.7** = 145 ± 11 μM



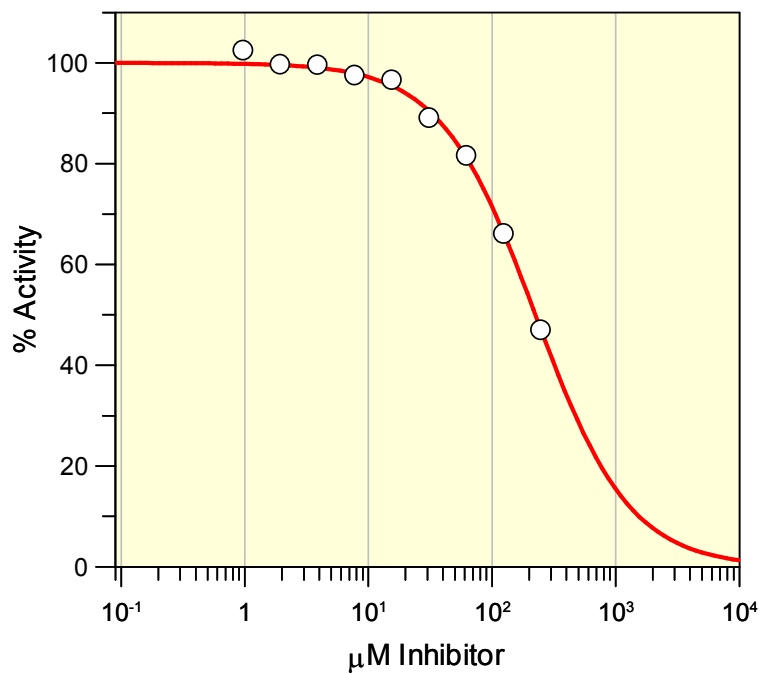


**Figure A.3** IC<sub>50</sub> for compounds **3.8** = 224 ± 7 μM

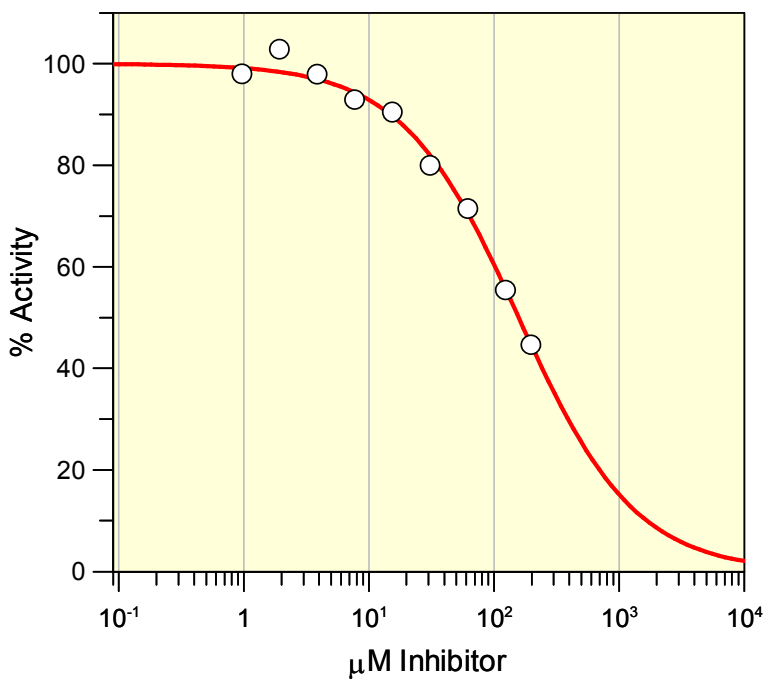


**Figure A.4** IC<sub>50</sub> for compounds **3.9** = 157 ± 9 μM

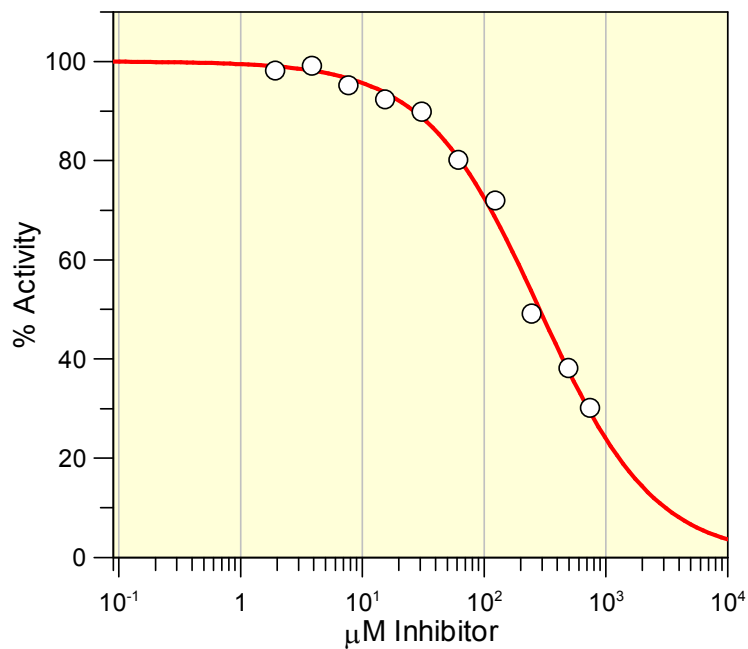


**Figure A.5** IC<sub>50</sub> for compounds **3.11** = 286 ± 13 μM

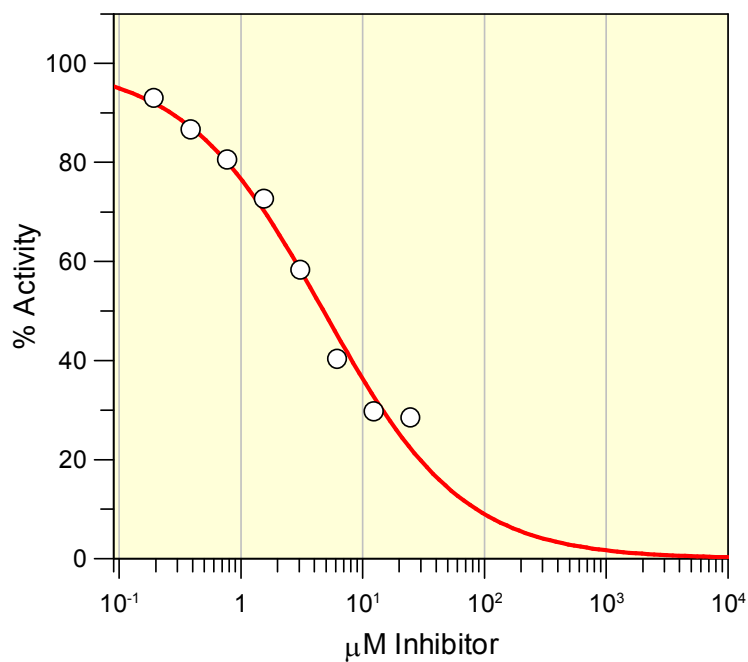


**Figure A.6** IC<sub>50</sub> for compounds **3.16** = 4.8 ± 0.4 μM

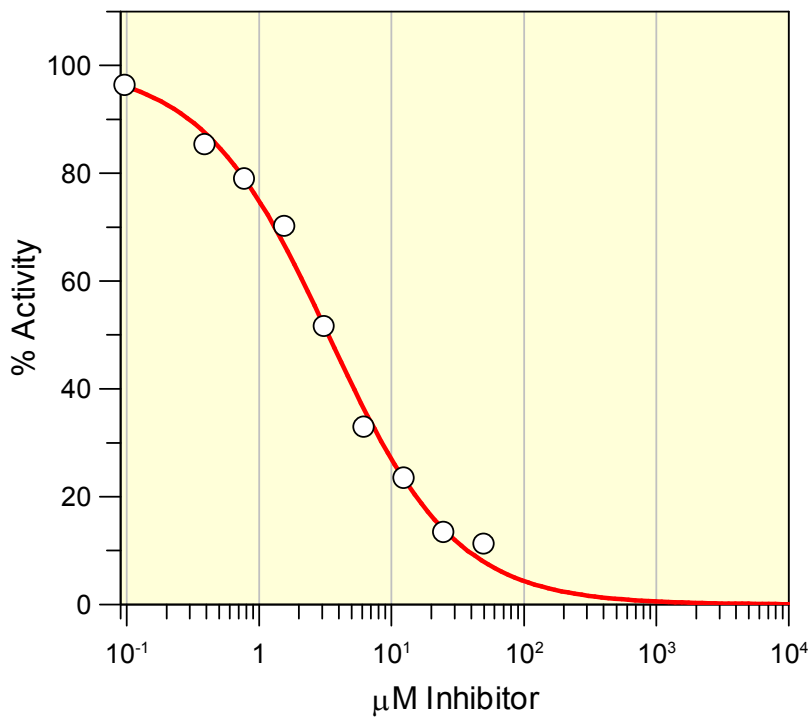


**Figure A.7**  $IC_{50}$  for compounds **3.17** =  $3.3 \pm 0.2 \mu\text{M}$

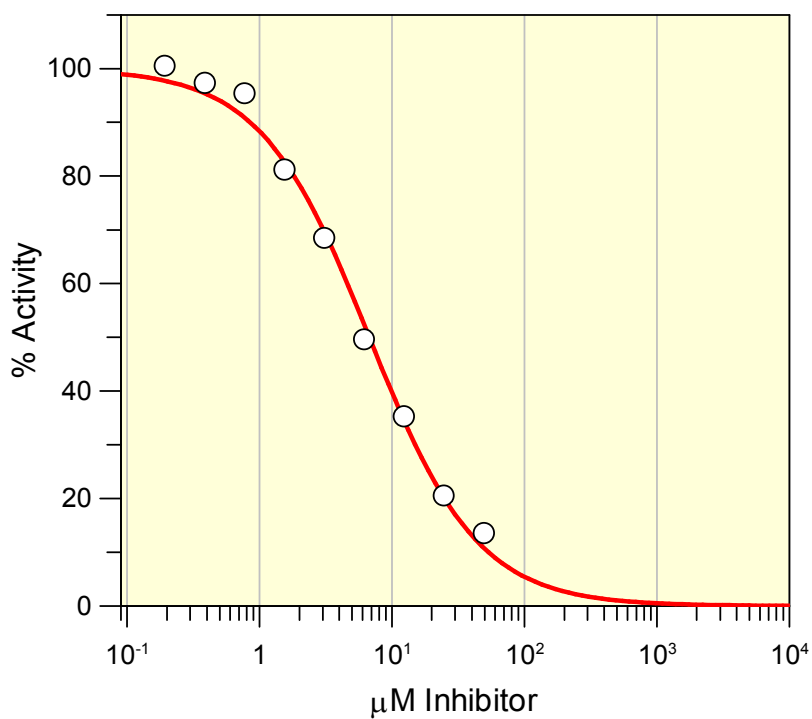


**Figure A.8**  $IC_{50}$  for compounds **3.18** =  $6.7 \pm 0.3 \mu\text{M}$

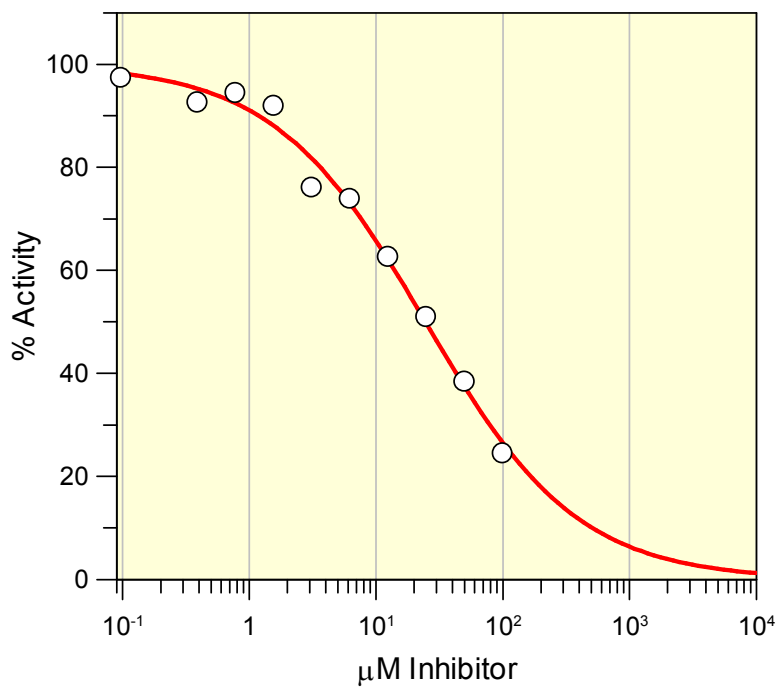


**Figure A.9** IC<sub>50</sub> for compounds **3.19** = 2.4 ± 0.1 μM

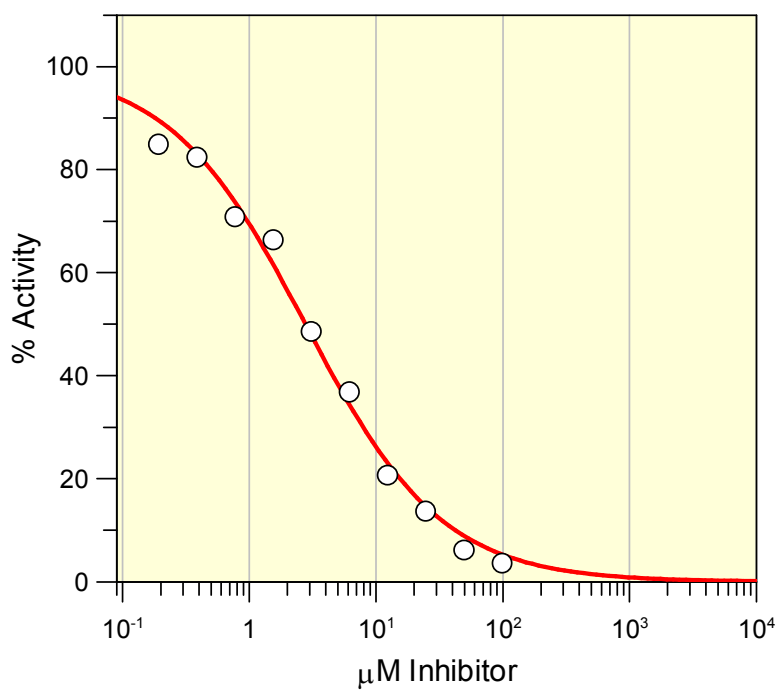


**Figure A.10** IC<sub>50</sub> for compounds **3.20** = 2.8 ± 0.2 μM

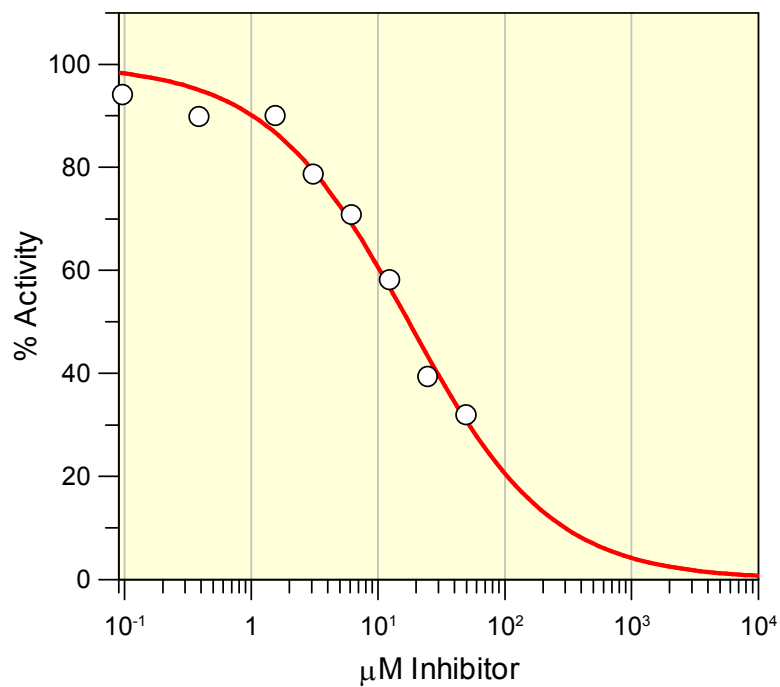


**Figure A.11** IC<sub>50</sub> for compounds **3.21** = 17 ± 1 μM

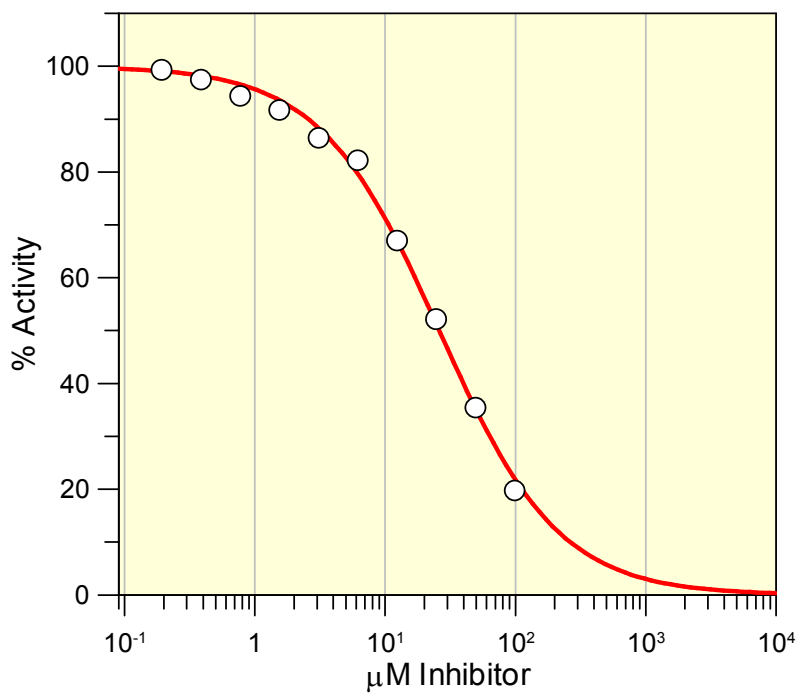


**Figure A.12** IC<sub>50</sub> for compounds **3.22** = 26 ± 1 μM

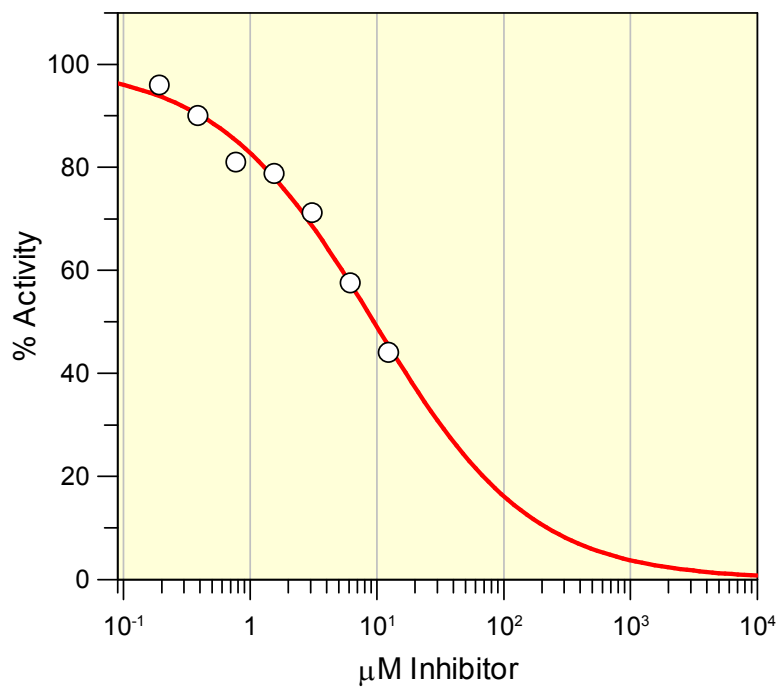


**Figure A.13** IC<sub>50</sub> for compounds **3.23** = 9.5 ± 0.9 μM

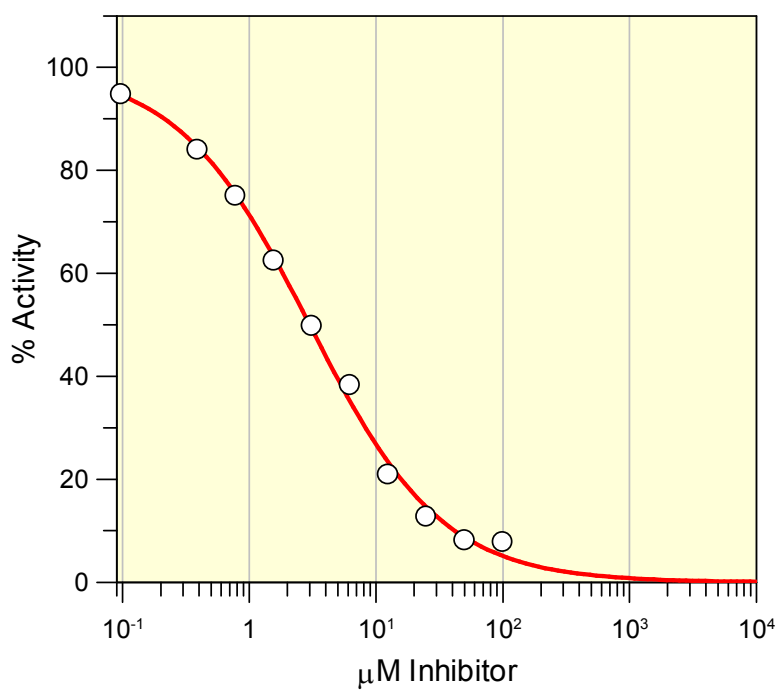


**Figure A.14** IC<sub>50</sub> for compounds **3.24** = 3.0 ± 0.1 μM

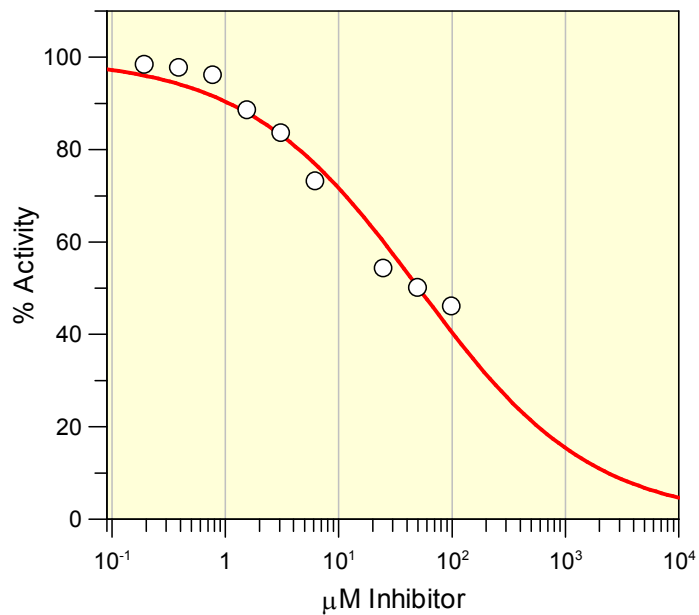


**Figure A.15** IC<sub>50</sub> for compounds **E1** = 51 ± 8 μM

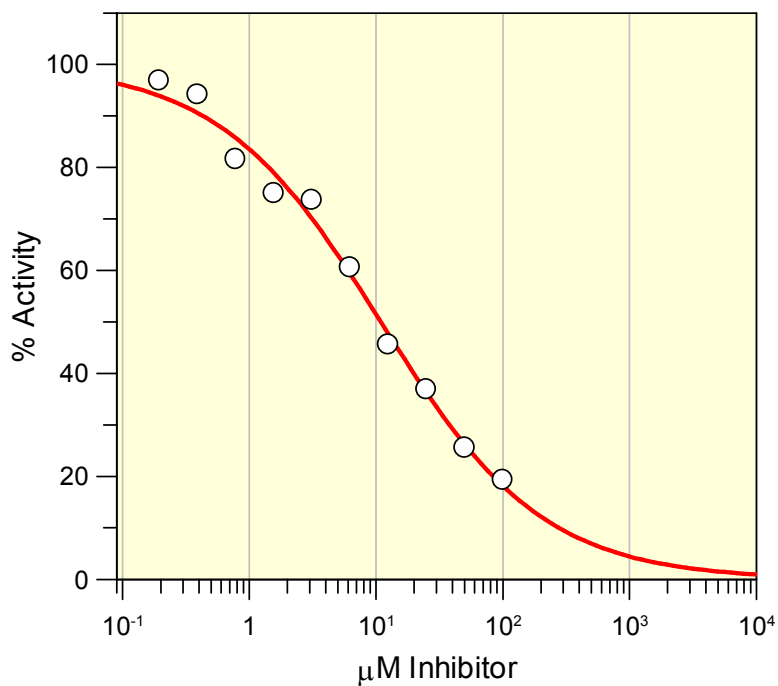


**Figure A.16** IC<sub>50</sub> for compounds **E2** = 11 ± 1 μM

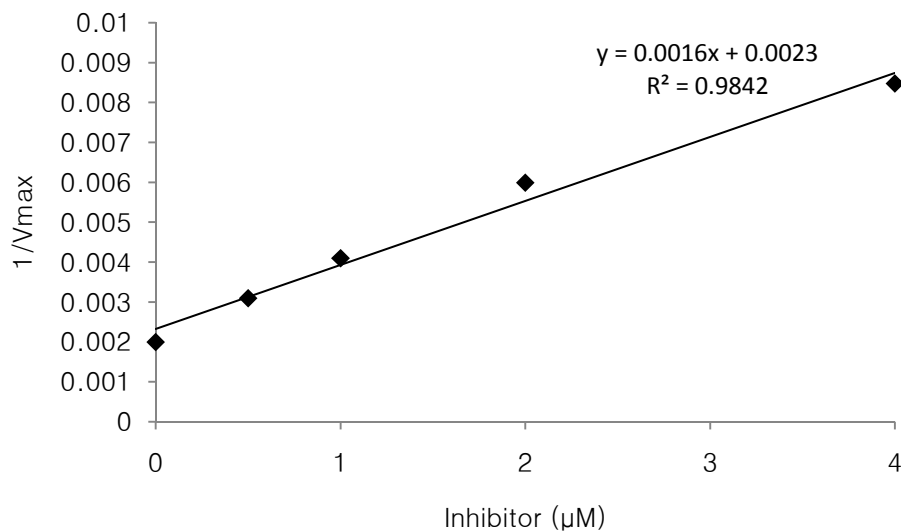


**Figure A.17** Replot of the data from **Figure 3.10** to determine  $K_i$  of inhibitor **3.19** ( $1.4\mu\text{M}$ )

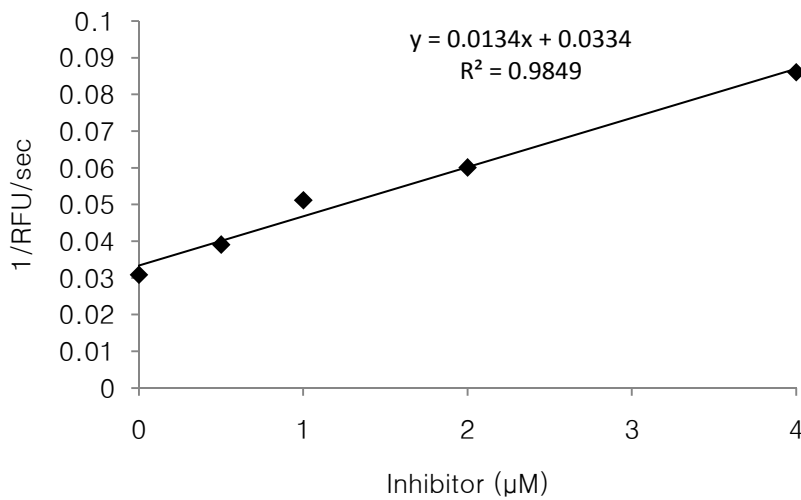


**Figure A.18** Replot of the data from **Figure 3.11** to determine  $K_i$  of inhibitor **3.20** ( $1.8\mu\text{M}$ )



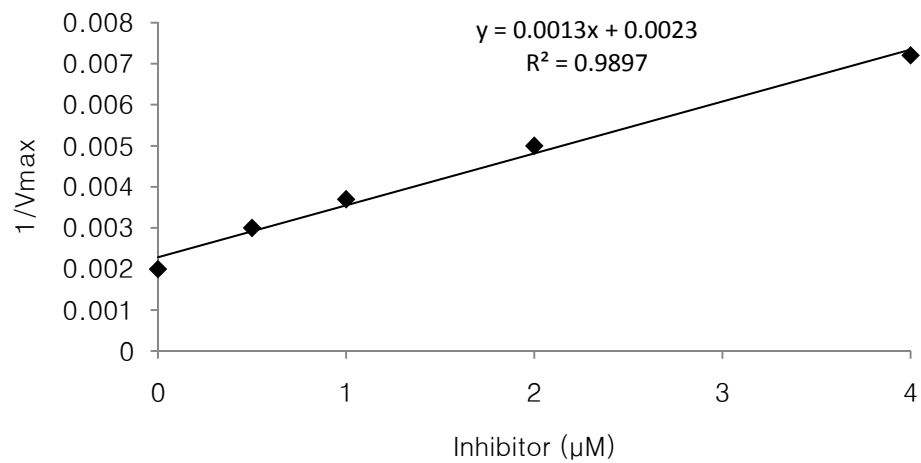


**Figure A.19** Replot of the data from **Figure 3.12** to determine  $K_i$  of inhibitor **3.16** ( $2.5\mu\text{M}$ )

## Appendix B.

**IC<sub>50</sub> plots for compounds 4.1-4.5, 4.8 and EP and replots of the data in figures 4.12, 4.13, 4.26, 4.27, 4.29**

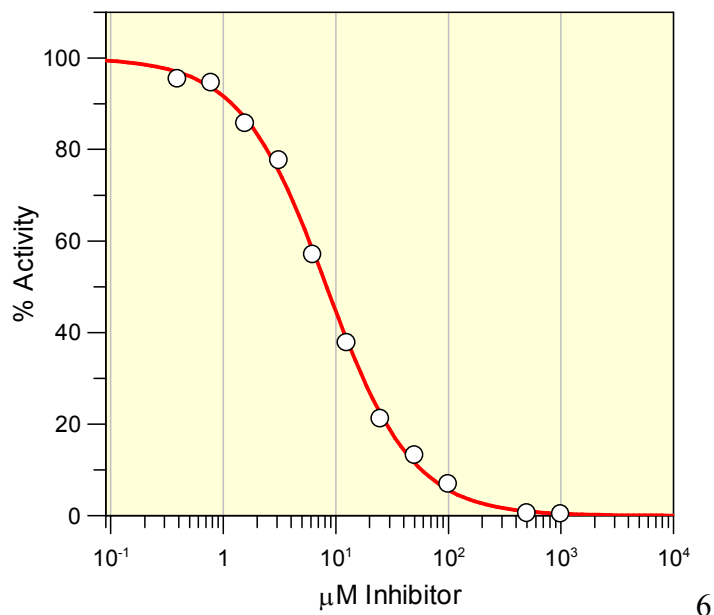


**Figure B.1** IC<sub>50</sub> for compounds **4.1** = 8.3 ± 0.2 μM

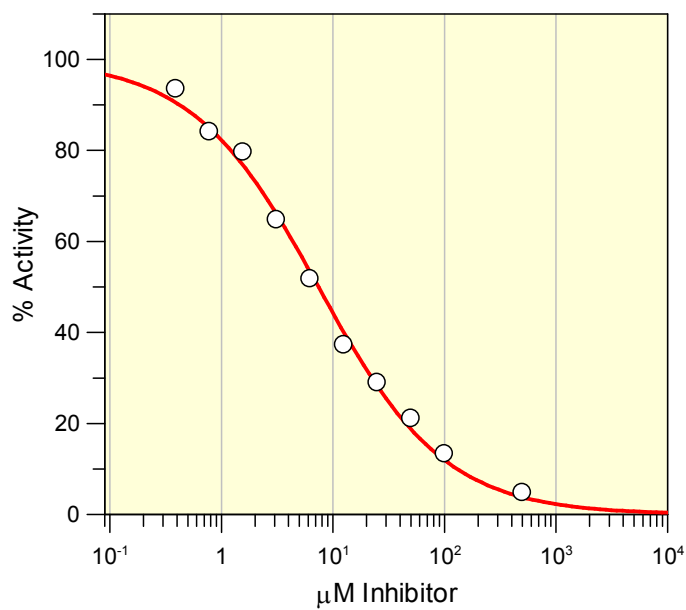


**Figure B.2** IC<sub>50</sub> for compounds **4.2** = 7.4 ± 0.4 μM

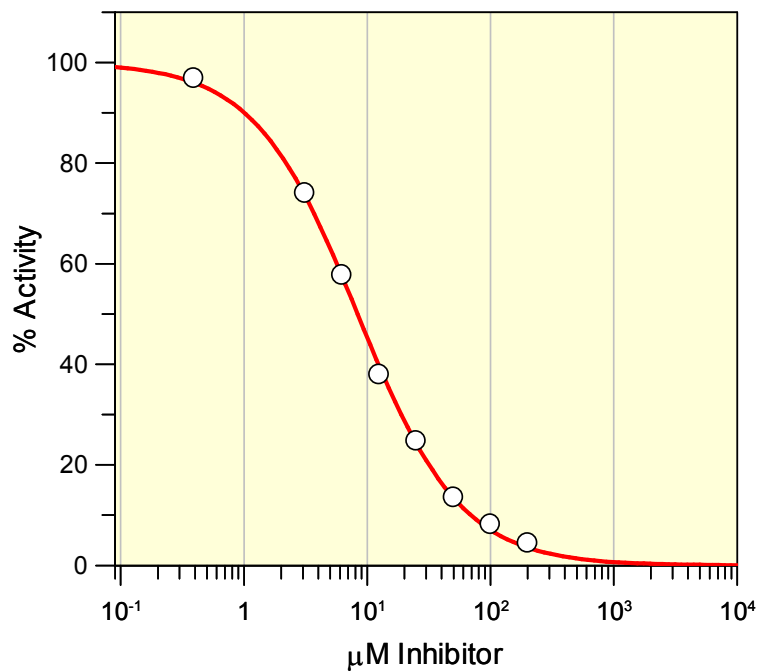


**Figure B.3** IC<sub>50</sub> for compounds **4.3** = 8.3 ± 0.2 μM

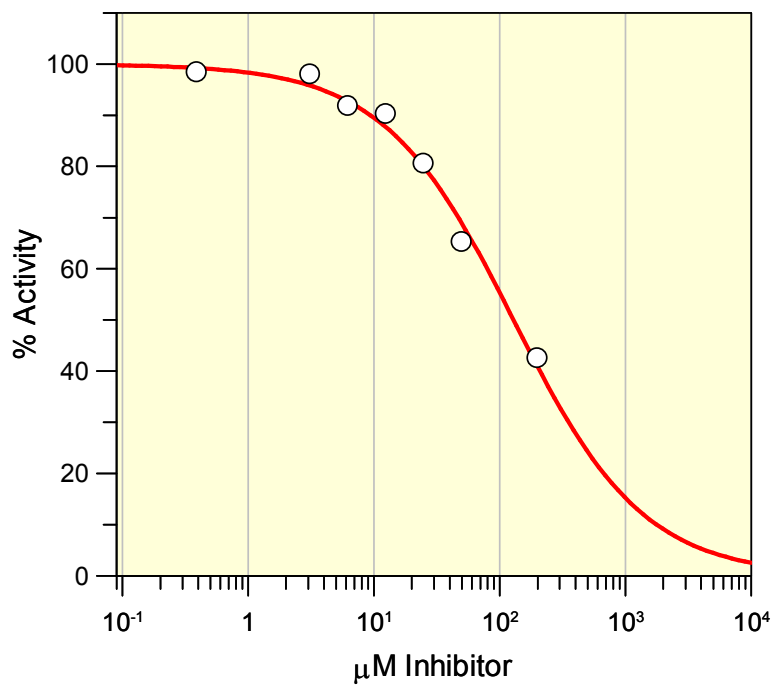


**Figure B.4** IC<sub>50</sub> for compounds **4.4** = 128.8 ± 10.6 μM

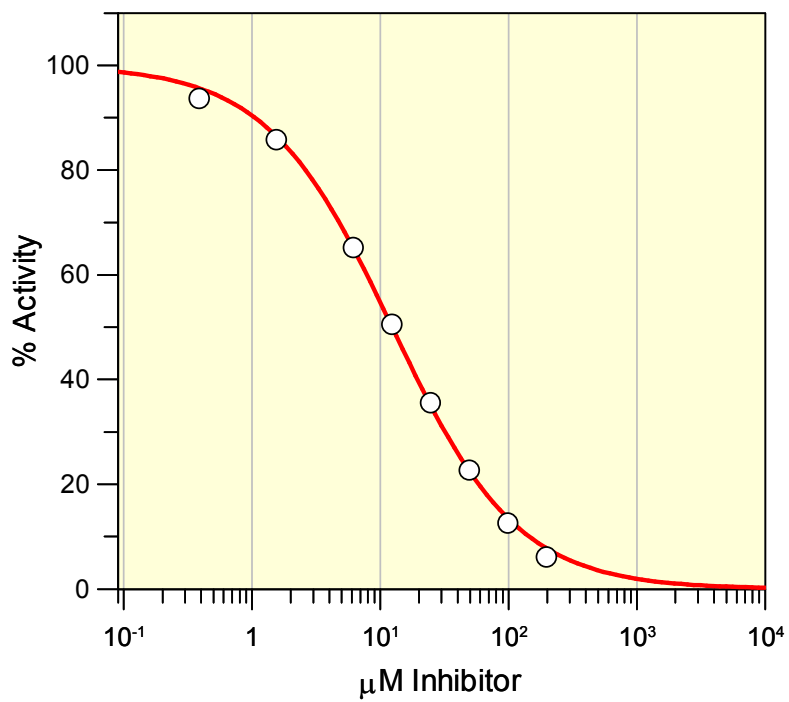


**Figure B.5** IC<sub>50</sub> for compounds 4.5 = 12.4 ± 0.3 μM

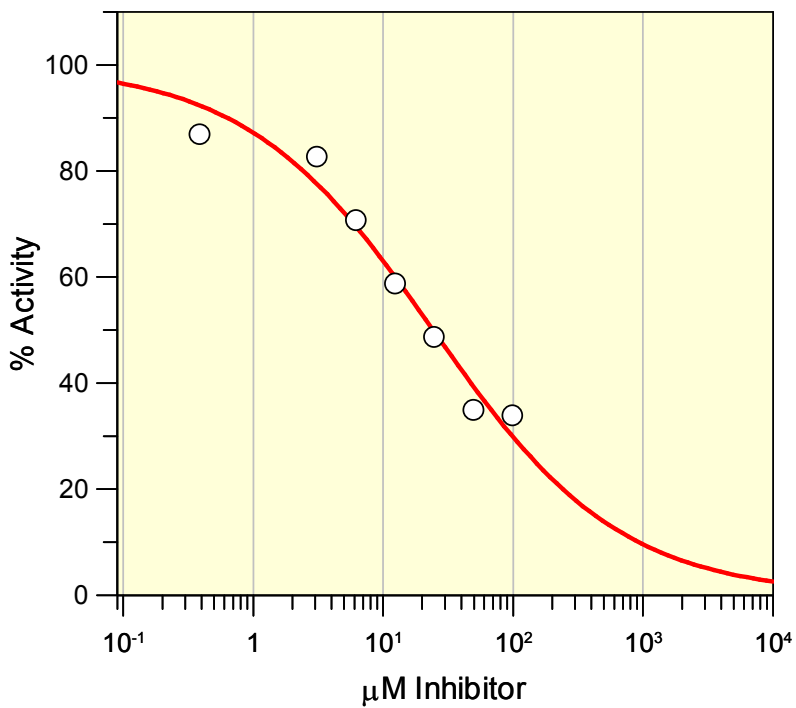


**Figure B.6** IC<sub>50</sub> for compounds 4.8 = 24.2 ± 3.0 μM

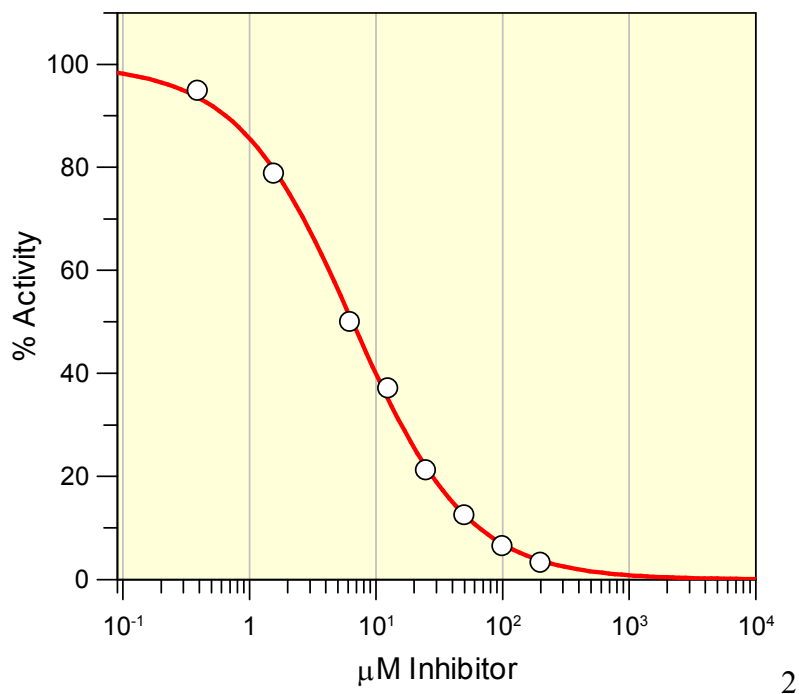


**Figure B.7.**  $\text{IC}_{50}$  for compounds EP =  $6.5 \pm 0.2 \mu\text{M}$

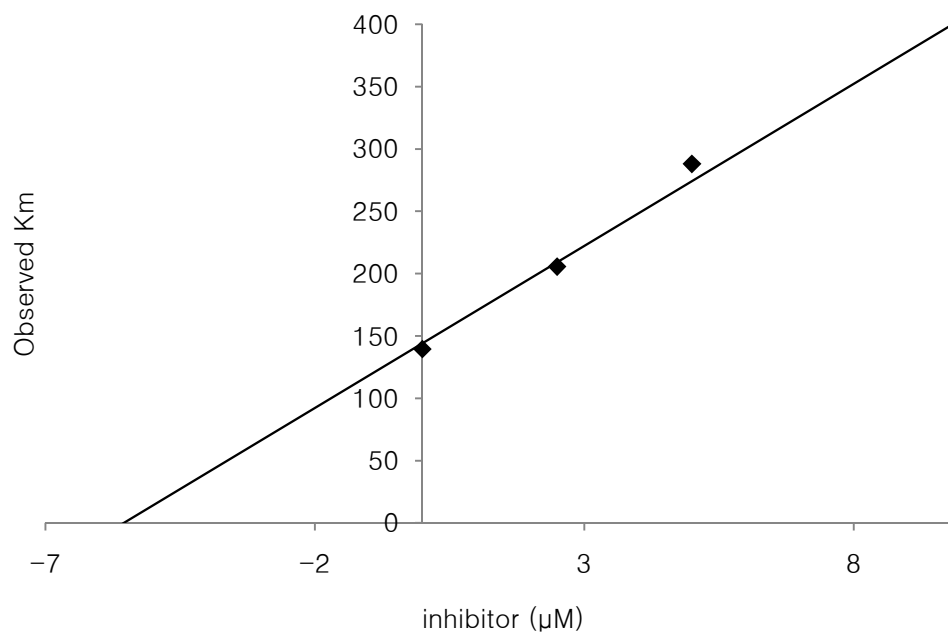


**Figure B.8** Replot of the data from **Figure 4.13** to determine  $K_i$  of inhibitor **4.1** ( $5.5 \mu\text{M}$ )

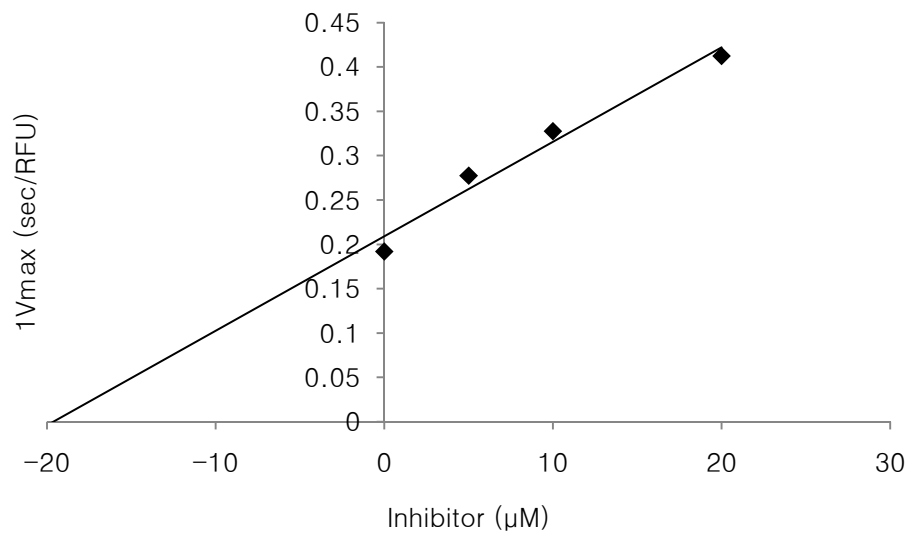


**Figure B.9** Replot of the data from **Figure 4.12** to determine  $\alpha K_i$  of inhibitor **4.2** ( $19.5\mu\text{M}$ )

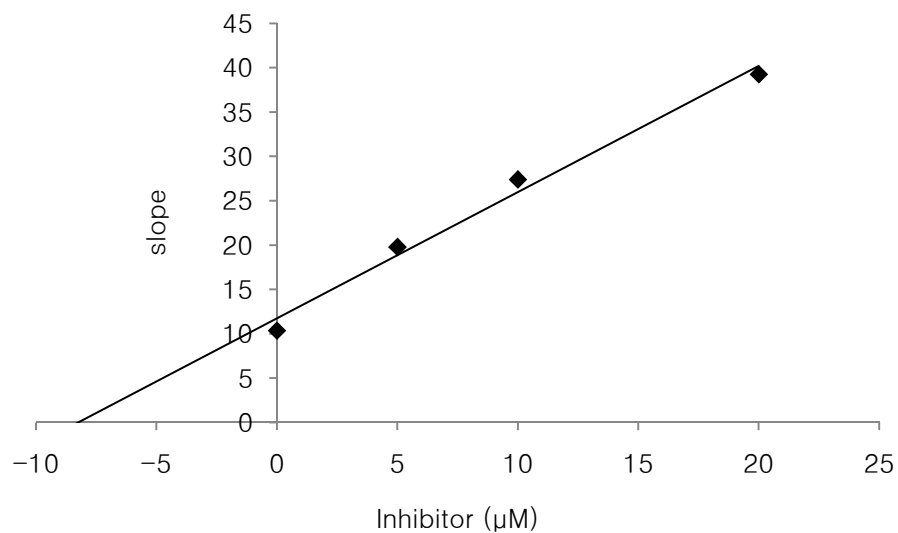


**Figure B.10** Replot of the data from **Figure 4.12** to determine  $K_i$  of inhibitor **4.2** ( $8.3\mu\text{M}$ )

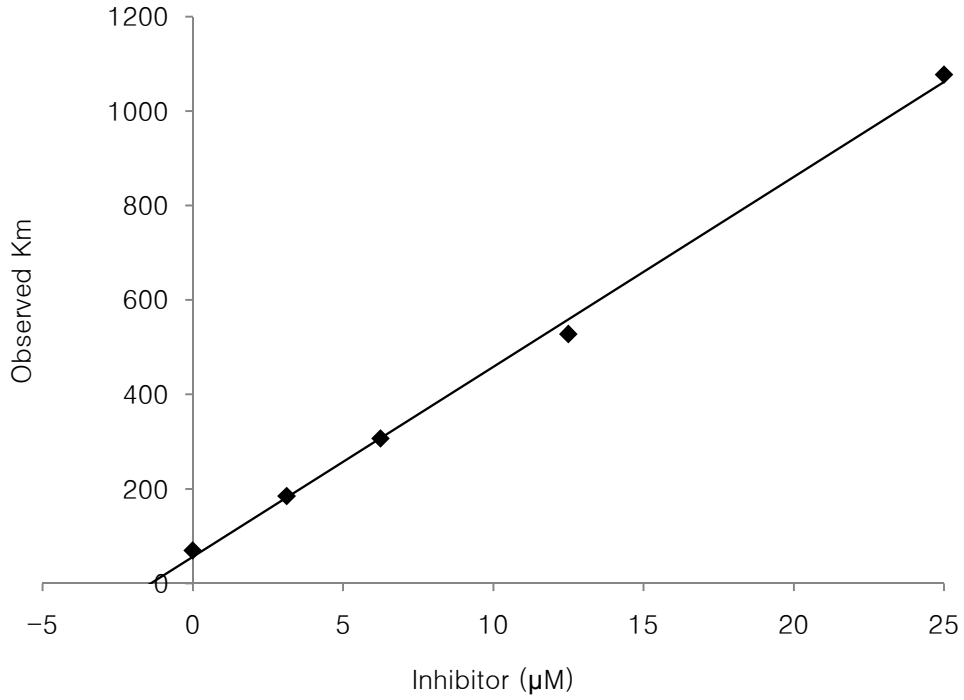


**Figure B.11** Replot of the data from **Figure 4.26** to determine  $K_i$  of inhibitor **4.5** ( $1.4\mu\text{M}$ )

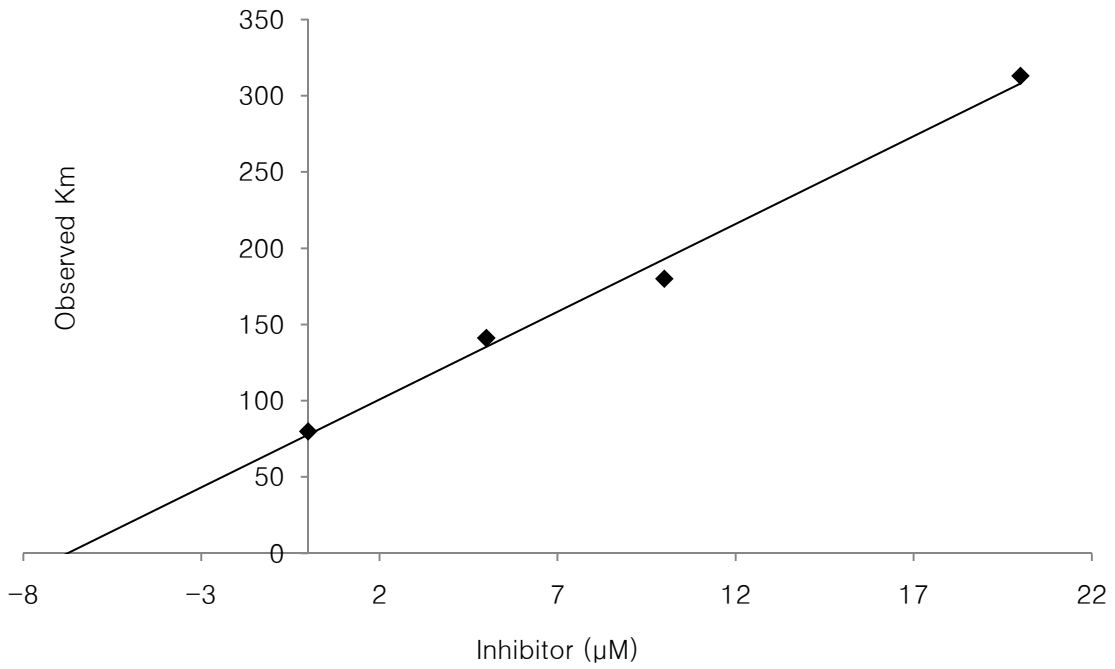


**Figure B.12** Replot of the data from **Figure 4.27** to determine  $K_i$  of inhibitor **4.3** ( $6.8\mu\text{M}$ )

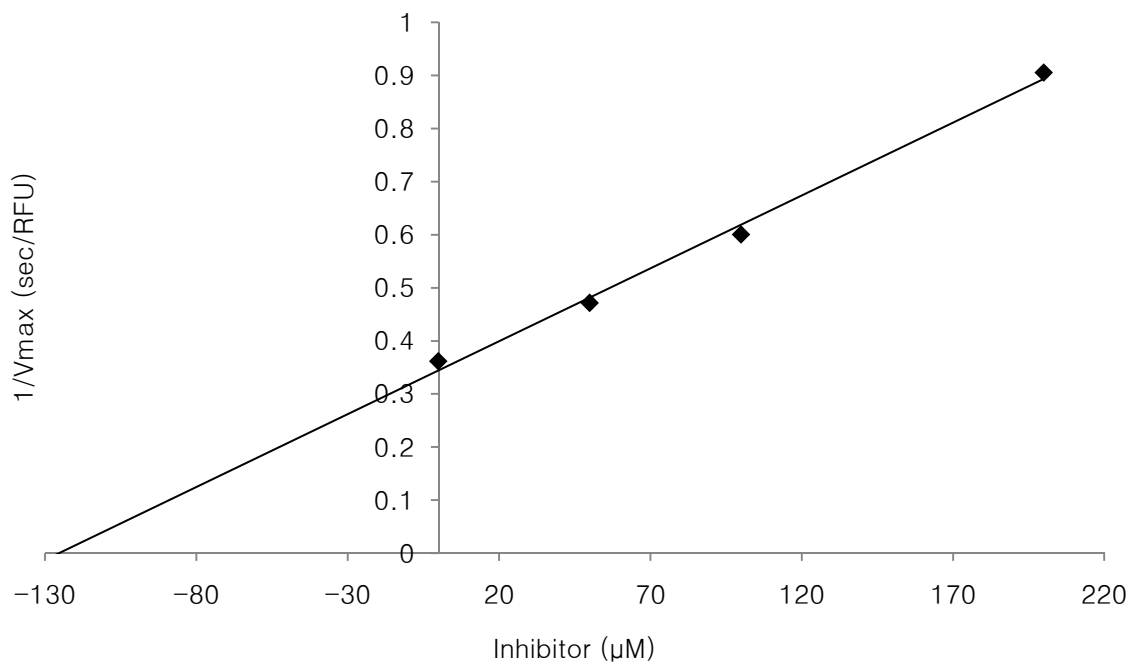


**Figure B.13** Replot of the data from **Figure 4.29** to determine  $\alpha K_i$  of inhibitor **4.4** ( $127 \mu\text{M}$ )

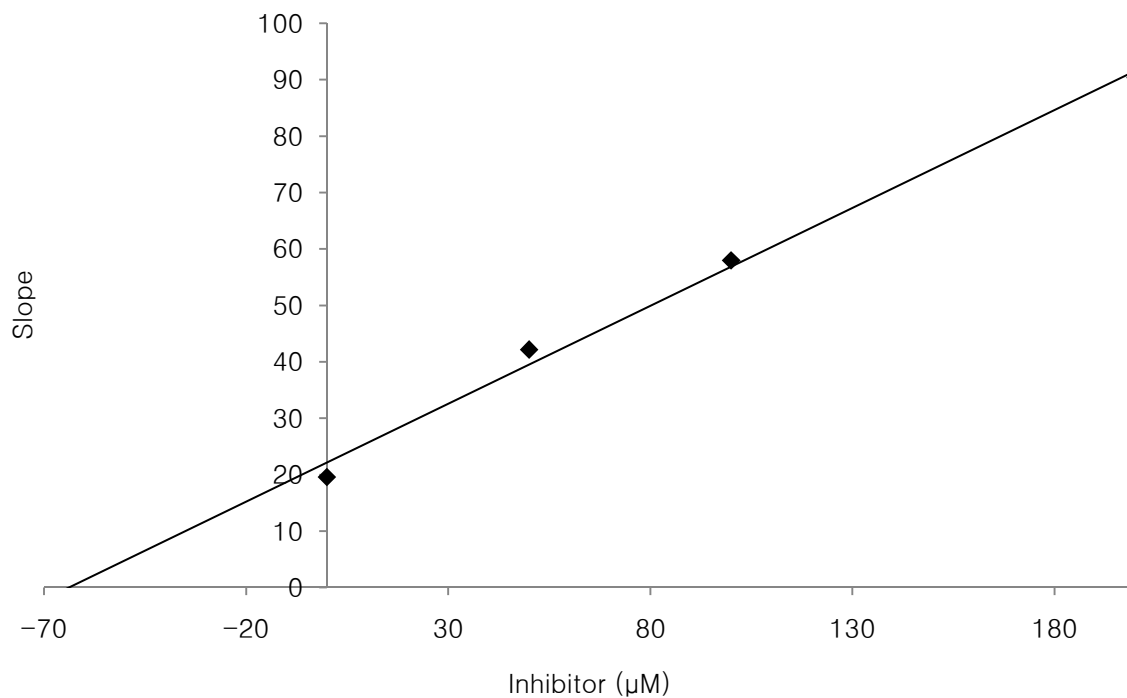


**Figure B.14** Replot of the data from **Figure 4.29** to determine  $K_i$  of inhibitor **4.4** ( $63.9 \mu\text{M}$ )